



ALGERIAN PEOPLE'S DEMOCRATIC REPUBLIC
MINISTRY OF HIGHER EDUCATION AND SCIENTIFIC
RESEARCH



UNIVERSITY OF KASDI MERBAH OUARGLA

Faculty of Faculty of Hydrocarbons and Renewable Energy and Sciences of
the Earth and the Universe

Memory

Submitted for graduation from

Master

Specialty: Mechanical Engineering

Option: Renewable Energies in Mechanics

Presented by:

Aimen-Arafat Zaboub

Nadjib-Allah Benabdelhafid

Theme

Establishment of a wind turbine field in various zones of Ouargla
with the establishment of small-power wind generators

Publicly supported the: 14 / 06 / 2023

In front of the jury composed of:

Dr. GHARBI Brahim

President UKM Ouargla

Dr. KHENTOUT Abdelkader

Supervisor /Reporter UK Ouargla

Dr.ROUAG Amar

Examiner UKM Ouargla

Dr.AMMARI Chouaib

Examiner UKM Ouargla

Academic year 2022/2023

اهداء

"ربي أوزعني أن أشكر نعمتك التي أنعمتها علي وعلى والدي وان أعمل صالحا ترضاه
ولئن شكرته لأزيدنكم" قال رسول الله صلى الله عليه وسلم " من لم يشكر الناس لا
يشكر الله " حديثه الشريف

الحمد لله والصلاة والسلام على الرسول الكريم

بعد هذه المدة الدراسية الحافلة بالعمل والجد نتقدم بالاهداءات التالية لمن يمثلون
أقرب الناس على قلوبنا

نهدى عملنا ونجاحنا هذا الى أغلب الناس الذين كانوا ينتظرون هذا اليوم بفارغ
الصبر الى كل من حثنا للوصول رغم كل الصعاب التي كانت تحول دون تحقيق ذلك

أود أن أذكر عن امتناني العميق لأمي وأبي وإخوتي الأغزاء على دعمهم اللامحدود
في مسيرتي الدراسية. لا يمكنني وصف مدى شكري وامتناني لكم على حبكم الذي
لا يعد وتشجيعكم الذي لا ينتهي. أنتم الدعامة التي تقف بجانبتي والقوة التي تدفعني
للأمام. أنا محظوظ بكوني جزءاً من عائلتكم الرائعة. شكراً لكم من أعماق قلبي

إلى العائلة والأساتذة وعلى رأسهم البروفيسور عبد القادر خنطوط والزلاء والطلبة
والأصدقاء وكل من ساهم من قريب أو بعيد حتى بدعوة أو كلمة في وصولنا

Thanks

I extend my thanks and gratitude to Allah Almighty first and to all the professors who helped me in the path of education and those who guided me to the right path and everyone who helped me in producing this research, led by Professor **Abdelkader Khentout**. I also extend my thanks to the administration of the College of Hydrocarbons and Renewable Energy for their good dealings and good care thanks.

Summaries

Chapter 01 Literature review on the development of low-altitude winds and methods of assessing wind potential.	
1. introduction	02
1.2. Statistic study :.....	02
1. 2.1. Methods for determining Weibull parameters:	04
1.2.1.2. Vertical extrapolation of wind speed :.....	07
1.2.1.3. Vertical extrapolation of Weibull parameters:	12
1.2.3. Definition of wind parameters:.....	14
1.2.3.1. Mean Velocity, Mean Cubic Velocity, and Variance:.....	14
1. 2.3.2. Power factor and variation index:.....	15
1.2.3.3. Most probable velocity and greatest energy velocity:.....	15
1. 2.3.4. Wind Turbulence Index:.....	16
1.2.3.5. Typical day (or composite day):.....	16
1.2.3.6. Turbulent Kinetic Energy Dissipation Rate:.....	16
1.2.4. Influence of Weibull parameters on potential quality wind:.....	17
1.2.4.1-Power density:.....	17
1.2.4.2-Turbine selection:.....	17
1.2.4.3-Capacity factor:.....	17
1.2.4.4-Energy yield:.....	18
1.2.5. Energy Evaluation and Wind Power Density Calculation:.....	18
1.2.6. Theoretical maximum recoverable power (Batez theorem) :.....	19
1.2.7. Useful power:.....	20
Conclusion:.....	21
Chapitre 02 : Estimation of wind energy potential and vertical extrapolation of the Weibull parameter	
2.1. Introduction.....	23
2.2. Geographical Location	23
2.3. Temporal Variation of Wind Speed:	23
2.3.1. Daily average variation of wind speed	24
2.3.2. Multi-year variation of wind speed:	29
2.3.3. Wind Roses:	29
2.4. Static Study:	30
2.4.1. Distributions	30
2.4.1.1. Histogram of occurrence frequency distributions:	30
2.4.1.2. Variation of Weibull parameters:	34
2.4.2. Wind parameter:	41
2.5. Wind energy potential	42
2.5.1. Wind power modeling:	42
2.5.2. Mean incident theoretical wind power	42
2.5.3. Theoretical maximum recoverable power (Betz limit):	44
2.5.4. Useful Power of a Wind Turbine:	50
conclusion:	51
Chapter03: Estimation of wind energy potential and vertical extrapolation of the Weibull parameter	
3.1 introduction:	53
3.2.The geographical location of the selected places.....	54
3.2.1. WIND ENERGY POTENTIAL: Modeling the power of the wind:	54
3.2.1.1 Theoretical mean incident wind power:	54

3.2.2 The theoretical maximum recoverable power (Betz limit):	56
3.2.3 Useful Power by a wind turbine:	61
3.3. Study of turbine surface change:	67
Conclusion :	76
General conclusion	77
Bibliographical references	78

Figures list

Figure 2.1: Schematic representation of successive degradations of wind energy before use.	23
Figure 2.2: The curve illustrates changes in wind speed in terms of days for the year 2012.	24
Figure 2.3: The curve illustrates changes in wind speed in terms of days for the year 2013.	24
Figure 2.4: The curve illustrates changes in wind speed for every day of the year 2014.	25
Figure 2.5: The curve represents the evolution of wind speed in terms of days for the year	25
Figure 2.6: The curve represents the evolution of wind speed in terms of days for the year	26
Figure 2.7: The graph illustrates the wind speed variation in terms of days for the year 2017.	26
Figure 2.8: The curve represents the changes in wind speed in terms of days for the year	27
Figure 2.9: The curve shows the variations in wind speed in terms of days for the year 2019.	27
Figure 2.10: The curve shows the changes in wind speed in terms of days for the year 2020.	28
Figure 2.11: The curve shows the changes in wind speed in terms of days for the year 2021.	28
Figure 2.12: The graph represents the evolution of wind speed in terms of days for a comparison between 2012 and 2021.	29
Figure 2.13: Histogram for the speed frequency ratio	33
Figure 2.14: Daily variation of the Weibull distribution for each year.	40
Figure 2.15: Daily variation of the Weibull distribution for 10 years (2012/2021)	41
Figure 2.16: Schematic representation of the successive degradations of wind energy before	42
Figure 2.17: Histogram of mean incident theoretical wind power for each year and for 10 years.	43
Figure 2.18: Representation of the current tube	44
Figure 2.19: Histogram of power absorbed by the rotor for each year and at 10 years.	45
Figure 2.20: Histogram of Maximum Recoverable Wind Power Average for Each Year and Over 10 Years.	46
Figure 2.21: Histogram of Average Recoverable Energy per Year over 10 Years	48
Figure 2.22: Variation in useful power.	49
Figure 3.1: picture showing the study areas in the state of Ouargla [24]	53
Figure 3.3 : theoretical mean incident wind power for each station [2012 to 2021]	54

Figure 3.4: The histogram of average energy power available at 10 years.	55
Figure 3.5: Representation of the current tube.[3]	55
Figure 3.6: power absorbed by the rotor per unit area for all stations [2012 to 2021].	56
Figure 3.7: The histogram of the power absorbed by the rotor per unit area (mean) a10 years.	57
Figure 3.8: average maximum recoverable power for all stations [2012 to 2021]	58
Figure 3.9: The histogram of the average maximum recoverable power at 10 years.	59
Figure 3.10: average recoverable energy over a year for all stations [2012 to 2021]	60
Figure 3.11: The average recoverable energy histogram over one year	60
Figure 3.12: Useful power curves P_{u1} , P_{u2} and the theoretical power at station ₁	66
Figure 3.13: Useful power curves P_{u1} , P_{u2} and the theoretical power at station ₂	67
Figure 3.14: Useful power curves P_{u1} , P_{u2} and the theoretical power at station ₃	67
Figure 3.15: Useful power curves P_{u1} , P_{u2} and the theoretical power at station ₄	68
Figure 3.16: Useful power curves P_{u1} , P_{u2} and the theoretical power at station ₁	68
Figure 3.17: Useful power curves P_{u1} , P_{u2} and the theoretical power at station ₂	
Figure 3.18: Useful power curves P_{u1} , P_{u2} and the theoretical power at station ₃	70
Figure 3.19: Useful power curves P_{u1} , P_{u2} and the theoretical power at station ₃	70
Figure 3.20: Mean incident theoretical wind power for 10 years	71
Figure 3.21: Histogram of mean incident theoretical wind power for each year and for 10 years.	71
Figure 3.22: Power absorbed by the rotor for each year and at 10 years.	72
Figure 3.23: Histogram of power absorbed by the rotor for each year and at 10 years.	72
Figure 3.24: Average maximum recoverable wind power for each year and over 10 years.	73
Figure3.25: Histogram of maximum recoverable wind power for each year and over 10 years.	73
Figure 3.26: Average recoverable energy for each year and over 10 years.	74
Figure 3.27: Histogram of Average Recoverable Energy per Year over 10 Years	74

Tables List

Table1.1: Arithmetic, Weibull, Hybrid-Weibull, Rayleigh equations for calculating average wind speed	14
Table 2.1: Frequency calculator each yea	30
Table 2.2: Find the word y, x and k	35
Table 2.3: Variation of Weibull parameters C and k."	39
Table 2.4: Wind parameters in Ouargla.	41
Table 2.5: The result of the values of V1, V2, V0, and Power absorbed .	44
Table 2.6: P_{the} and P_{the} results	46
Table 2.8: Nominal speed and useful power as a function of machine efficiency [0.3 to 0.5] for each year.	47
Table 3.1: Nominal velocities at all stations at 10 m height and machine performance interval [0.3 to 0.5], in each year	49
Table 3.2: this table gives the variations of the useful powers in the stations with a height of 10 m and at the efficiency interval of the machine [0.3 to 0.5], in each year.	62
Table 3.3: Rated speed at all stations at 10 m height and machine performance interval [0.3 to 0.5].	63
Table 3.4: variations of the useful power in the Stations with a height of 10 m and at the efficiency interval of the machine [0.3 to 0.5].	64
Table 3.5: Wind parameters at all stations at two altitudes.	65
Table 3.6: Variations of the useful powers in the stations with a height of 25 m-50 m and at the efficiency interval of the machine [0.3 to 0.5], in each year.	65

Nomenclature

$A, A1$: surface of the wheel	m^2
$A0$: the upstream surface (at the inlet of the current tube)	m^2
$A2$: the surface downstream of the rotor	m^2
$C, C1, C2$: weibull scale factor	$m s^{-1}$
$k, k1, k2$: weibull shape factor	
CP : Coefficient de puissance	
$P_{thé}$: average theoretical power	W
P_{abs} : the power absorbed by the rotor	W
P_{Max} : the maximum recoverable average power	W
P_r : the average recoverable power per unit area A equal to 1 m^2	W
P_u, P_{u1}, P_{u2} : power output	W
P_n : nominal power	W
E^- : average energy density recoverable over a year	KW/m^2
η : Overall system performance	
$V0$: wind speed upstream of the rotor (initial)	m/s
$V1$: wind speed in the plane of the rotor	m/s
$V2$: wind speed downstream of the rotor	m/s
V^- : estimated wind speed with Weibull model	$m s^{-1}$
V^-3 : average cubic wind speed estimated with Weibull model	$m^3 s^{-3}$
$VD, VN,;$ start, nominal and stop speed	$m s^{-1}$
$Vn1, Vn2$: rated speed	$m s^{-1}$
ρ : air density	kg/m^3
σ : Type of speed distribution	m/s
σ^2 : variance	
RP : Wind power factor	
IV : the index of change	
$Z1, Z2$: altitude	m
$Z0$: soil roughness	m
Zg : Geometric mean of altitude	m
Zr : the reference height equal to 10m	m
αe : Exposant de la loi de puissance	
n: Exponent of the law of power	
m: Scale factor extrapolation exponent	
α, β : Constants without dimension	
A, B: coefficients for the proposed model	
$f(V)$: frequency of occurrence of wind speeds	
$F(V)$: Cumulative frequency of weibull distribution	
$ff0$: the frequency of calm winds	
VPP : vitesse la plus probable	ms^{-1}
$VmaxE$: vitesse de plus grande énergie	ms^{-1}
r: indice de turbulence du vent	
ε : Taux de dissipation de l' énergie cinétique turbulente	

Summary:

Choosing different places to set up a wind farm and choosing the appropriate turbines in the Ouargla region and its environs, we must conduct a comprehensive study of wind speed over a period of 10 years, in order to obtain accurate results. In addition, we will classify the area according to productivity using a Weibull distribution and extract the parameters k and C , using several suitable models, such as the least squares method, standard deviation, mean velocity (MMV) method, wind variability and maximum likelihood method. This is done to calculate the Whipple V speed and the recovered power, with the aim of selecting the appropriate wind turbine for the project.

ملخص.

الاختيار اماكن مختلفه لإقامة مزرعة رياح واختيار التوربينات المناسبة في منطقة ورقلة وضواحيها، يتعين علينا إجراء دراسة شاملة لسرعة الرياح على مدى 10 سنوات، وذلك للحصول على نتائج دقيقة. بالإضافة إلى ذلك، سنقوم بتصنيف المنطقة وفقاً للإنتاجية باستخدام توزيع Weibull واستخراج المعلمات k و C ، وذلك باستخدام عدة نماذج مناسبة، مثل طريقة المربعات الصغرى والانحراف المعياري وطريقة متوسط السرعة (MMV) وتقلبات الرياح وطريقة الاحتمال الأقصى. يتم ذلك لحساب سرعة وييل V والاستطاعة المستردة، وذلك بهدف اختيار التوربينات الرياح المناسبة للمشروع

General introduction

Renewable energy sources play a pivotal role in mitigating climate change and reducing our dependence on fossil fuels. Among these sources, wind energy stands out as a promising and fast-growing sector. In the region of Ouargla, located in southern Algeria, wind power has emerged as a viable solution to harness the abundant natural resources and meet the energy needs of the region.

The Ouargla region has many favorable conditions for wind power. Because it has vast expanses of open land, strong and consistent winds, and relatively flat terrain. These factors make it an ideal location to set up a field for wind turbines, which can capture the kinetic energy of the wind and convert it into electricity. The strategic geographical location of the region provides an opportunity for transmission and distribution of electricity to neighboring regions.

Wind energy projects in the Ouargla region have the potential to bring multiple benefits. First, it contributes significantly to reducing greenhouse gas emissions, as wind energy is a clean and renewable energy source. By replacing traditional fossil fuel-based electricity generation, wind power helps mitigate climate change and improve air quality. Moreover, investment in wind energy promotes energy sufficiency and reduces dependence on fuel

The implementation of wind energy projects in the Ouargla region could stimulate economic growth and job creation. In addition, wind energy projects can attract investments and spur innovation to develop the field of renewable energies.

Therefore, in this research, we will study the best areas in which a wind farm can be established with the highest efficiency in the Ouargla region in terms of wind speed.

Chapter I:

Literature review on the development of low-altitude winds and methods of assessing wind potential.

1. introduction

In this chapter, we are discussing the movement of winds both horizontally and vertically within the boundary layer of the atmosphere. To support our analysis, we are referring to trusted bibliographic studies and focusing specifically on the WEIBULL distribution as a basis for our studies. We are examining wind variations and presenting our findings in the form of wind roses, and defining key wind parameters. Finally, we aim to provide a general overview or technique for the use of wind turbines based on our research.

2. Statistic study

The wind potential is calculated from the mean velocity Distributions. As the distributions are not always available, we got into the habit of model the distributions from the Following models:

- Weibull's law;
- Weibull's hybrid law;
- Rayleigh's law;

a- Weibull distribution:

In most places, surface wind speed distribution is well approximated by a Weibull distribution. The Weibull distribution fitting is therefore the method most commonly used in wind energy studies to obtain a smooth distribution despite under-sampling of wind speed due to limited observation periods. The Weibull distribution is a two-parameter function, mathematically represented by (u) while the cumulative distribution function is represented by $F(u)$:

$$f(u) = \frac{k}{c} \left(\frac{v}{c}\right)^{k-1} e^{-\left(\frac{v}{c}\right)^k} \dots\dots\dots(1)$$

$$f(u) = 1 - e^{-\left(\frac{v}{c}\right)^k} \dots\dots\dots(2)$$

where u is the reference wind speed at the height of measurement, k the non-dimensional shape parameter, and C the scale parameter whose dimensions coincides with that of u (m/s). $k, >0$. In the observed wind climate analysis of WASP, the Weibull distribution function of wind speed is represented with an estimated Weibull C parameter which indicates on average

how windy the site is, the Weibull shape parameter k which indicates how peaked the distribution is, Weibull mean U which indicates the long-term mean wind speed and P which indicates the available power density at the sites.

b- Rayleigh distribution:

The Rayleigh distribution is a special case of the Weibull distribution. If K and C are the parameters of the Weibull distribution, then the Rayleigh distribution with parameter b is equivalent to the Weibull distribution with parameters $K=\sqrt{2}b$ and $C = 2$.

If the component velocities of a particle in the x and y directions are two independent normal random variables with zero means and equal variances, then the distance the particle travels per unit time is distributed Rayleigh.

In communications theory, Nakagami distributions, Rician distributions, and Rayleigh distributions are used to model scattered signals that reach a receiver by multiple paths. Depending on the density of the scatter, the signal will display different fading characteristics. Rayleigh and Nakagami distributions are used to model dense scatters, while Rician distributions model fading with a stronger line-of-sight. Nakagami distributions can be reduced to Rayleigh distributions, but give more control over the extent of the fading.

$$f(v) = 2 \frac{v}{c^2} \exp\left(-\left(\frac{v}{c}\right)^2\right) \dots\dots\dots (3)$$

c) Hybrid Weibull distribution:

The hybrid Weibull distribution is used when the frequency of calm winds recorded, on a given site, is greater than or equal to 15%. In fact, this proportion cannot be overlooked and should be considered when characterizing a site from the wind potential point of view.

2.1. Methods for determining Weibull parameters:

The Weibull distribution function is commonly used to represent wind speed distribution. It can be described by the probability density function (PDF) and the cumulative distribution function (CDF). [1].

The PDF, $f(v)$, and the CDF, $F(v)$, are expressed thus

the relationship(1)(2)

where v is the wind speed, c is the scale parameter with the same wind speed unit (m/s), and k

is a unitless shape parameter. The scale parameter determines the abscissa scale on a plot of the distribution, while the shape parameter determines the shape of the distribution.

The wind speed data were analyzed using the six methods for estimating Weibull parameters, which are briefly explained below. [2]

A) Empirical Method

The empirical method has a practical and straightforward solution requiring only the average wind speed, v , and the standard deviation of the wind speed data, s . Weibull parameters are estimated

as:

$$k = \left(\frac{\sigma}{u}\right)^{-1.086} \dots\dots\dots(4)$$

$$c = \frac{u}{\Gamma\left(1+\frac{1}{k}\right)} \dots\dots\dots(5)$$

Where $G(x)$ is the Gamma function.

B) Moment Method

Using Equation (1), the average wind speed and the standard deviation of the wind speed data can be calculated in the equations:

$$u = c\Gamma\left(1 + \frac{1}{k}\right) \dots\dots\dots(6)$$

$$\sigma = c\left[\Gamma\left(1 + \frac{2}{k}\right) - \Gamma^2\left(1 + \frac{1}{k}\right)\right]^{\frac{1}{2}} \dots\dots\dots(7)$$

In Equation (1.4), the shape parameter, k , can be calculated by the numerical iteration method and the scale parameter, c , can be obtained from Equation (1.5).

C) Graphical Method

The graphical method is calculated using a linear least-squares regression. From a double logarithmic transformation in Equation (2), a new linear regression equation is derived as:

$$\ln\{-\ln[1 - F(u)]\} = k \ln(u) - k \ln(c) \dots\dots\dots(8)$$

Here, a straight line can be drawn through $\ln(v)$ on the x-axis and $\ln\{v\}\ln[1 - F(v)]$ on the y-axis. The shape parameter, k , is the slope of the straight line and the scale parameter, c , is obtained by the y-intercept of the straight line.

D) Power Density Method (PDM)

This method was suggested by Akdag et al (Akda & Dinler, 2009). The energy pattern factor is ratio of average of cube of velocity to cube of average velocity and k can be estimated using energy pattern factor. [31]

Value of c can be estimated using relationship of k and c in Equation 5

$$E_{pf} = \frac{\overline{v^3}}{\bar{v}^3} \dots \dots \dots (9)$$

where $\overline{v^3}$ is the average of wind speed cubed and \bar{v}^3 is the cube of the average wind speed. The shape parameter, k , can be estimated in the equation:

$$k = 1 + \frac{3.69}{E_{pf}^2} \dots \dots \dots (10)$$

The scale parameter is estimated using Equation (4).

E) Maximum Likelihood Method (MLM)

The maximum likelihood method uses time-series wind data for calculating Weibull parameters. [5].

Weibull parameters are estimated using the equations:

$$k = \left[\frac{\sum_{i=1}^n v_i^k \ln(v_i)}{\sum_{i=1}^n v_i^k} - \frac{\sum_{i=1}^n \ln(v_i)}{n} \right]^{-1} \dots \dots \dots (11)$$

$$c = \left(\frac{1}{n} \sum_{i=1}^n v_i^k \right)^{\frac{1}{k}} \dots \dots \dots (12)$$

Where v_i is the wind speed in timestep i and n is the number of nonzero wind speed data points.

Equation (1.11) should be calculated using numerical iteration, and then Equation (13) can be solved.

F) Modified Maximum Likelihood Method (MMLM)

This method uses the wind speed frequency, which is applied to the MLM. Weibull parameters are calculated as: [6].

$$k = \left[\frac{\sum_{i=1}^n v_i^k \ln(v_i) f(v_i)}{\sum_{i=1}^n v_i^k f(v_i)} - \frac{\sum_{i=1}^n \ln(v_i) f(v_i)}{f(v \geq 0)} \right]^{-1} \dots\dots\dots(13)$$

$$c = \left(\frac{1}{f(v \geq 0)} \sum_{i=1}^n v_i^k f(v_i) \right)^{\frac{1}{k}} \dots\dots\dots(14)$$

where v_i is the central value of wind speed in bin i , and n is the number of bins. $f(v_i)$ is the frequency that the wind speed falls within bin i , and $f(v \geq 0)$ is the probability that the wind speed equals or exceeds zero.

2.1.2. Vertical extrapolation of wind speed:

a) Log-linear distribution:

the log-linear law is a function of the friction velocity, the roughness length, and the Obukhov length. According to the studies of Monin and Obukhov [6], it is defined by the following expression:

$$V_h = \left(\frac{u_*}{\kappa} \right) \left[\ln \left(\frac{Z_h}{Z_0} \right) - \Psi_m \left(\frac{Z_h}{L} \right) \right] \dots\dots\dots(15)$$

where L is the Obukhov length, Z_0 the roughness length, u_* the friction velocity in $m \cdot s^{-1}$, $\Psi_m(Z_h/L)$ is the stability correction function, and κ the von Karman constant supposed to be equal to 0.4 and Z_h the height. According to the studies of Paulson [36, 37] reported by Businger [35], we have the following equation for an unstable atmospheric condition ($(Z_h/L) < 0$):

$$\Psi_m = \left(\frac{Z_h}{L} \right) = 2 \ln \left(\frac{1+x}{2} \right) + \ln \left(\frac{1+x^2}{2} \right) - 2 \tan^{-1}(x) + \frac{\pi}{2} \dots\dots\dots(16)$$

Where

$$x = \left(1 - 15 \frac{Z_h}{L} \right)^{1/4} \dots\dots\dots(17)$$

Two methods were exploited to determine the Obukhov length which characterizes the state of the surface layer stability. The first was based on the expression from the studies by Monin and Obukhov [6]:

b) Power law:

the information required by the log-linear law is not always available [19], and such a method is not always easy to use for general engineering studies [21]. This is why in the studies conducted by [10], the authors preferred likening the increase in the wind speed along with the height of the surface layer to a power law. This law was proposed by [22] and reported by [14, 44–46]

$$\frac{V_h}{V_1} = \left(\frac{Z_h}{Z_1}\right)^\alpha \dots\dots\dots(18)$$

where V_1 is the wind speed at 10 m.)is law depends only on a single parameter α which is the friction or Hellman exponent, also known as wind shear coefficient. Its value depends on several factors like the atmospheric stability, ground characteristics such as topography and the roughness Z_0 [7, 2] and gives information about the variations in wind intensity according to altitude. Considering the properties of logarithms, equation (14) becomes

$$\ln\left(\frac{V_h}{V_1}\right) = \alpha \ln\left(\frac{Z_h}{Z_1}\right) \dots\dots\dots(19)$$

Based on equation (15), the coefficient α can be determined through the equation below:

$$\alpha = \frac{\ln(V_h) - \ln(V_1)}{\ln(Z_h) - \ln(Z_1)} \dots\dots\dots(20)$$

From the studies of [23] and for an unstable atmosphere, α can be also compute by

$$\alpha = \frac{(1 - 16(Z/L))^{-1/4}}{\ln((\eta - 1)(\eta_0 + 1)(\eta_0 - 1)) + 2\text{Arctan}(\eta) - 2\text{Arctan}(\eta_0)} \dots\dots\dots(21)$$

c) Logarithmic law:

The logarithmic law origins lie in the boundary layer fluid mechanics and atmospheric research. To determine the horizontal velocity (v) at a height (z), it is commonly expressed as follows:

$$v(z) = \left(\frac{u_*}{\kappa}\right) \ln\left(\frac{z}{z_0}\right) \dots\dots\dots(22)$$

Where $\kappa = 0.4$ is von Karman constant. $u_* = \left(\frac{\tau}{\rho}\right)^{1/2}$ The roughness length (z_0) describes the roughness of the ground or terrain where the wind is blowing. There are cases where wind velocity v_1 is known and required at another height (Z_0) in a case that can be derived from Eq.1 [5]:

$$V_2 = V_1 \frac{\ln(z_2) - \ln(z_0)}{\ln(z_1) - \ln(z_0)} \dots\dots\dots(23)$$

Z_1 : measuring mast height

Z_2 : wind turbine height

V_1 : speed measured at the measuring mast

V_2 : speed we want to determine

d) Power Law 1/7:

The power law that allows the vertical extrapolation of the wind speed of a level

Z_1 at level Z_2 takes the form:

$$V(Z_2) = V(Z_1) \left(\frac{Z_2}{Z_1}\right)^\alpha \dots\dots\dots(24)$$

With :

$$\alpha = \frac{\psi_m\left(\frac{Z_g}{L}\right)}{\ln'\left(\frac{Z_g}{Z_a}\right) - \psi\left(\frac{Z_g}{L}\right)} \dots\dots\dots(25)$$

z_g Being the geometric mean of the height given by:

$$Z_g = (Z_1 * Z_2)^{1/2} \dots\dots\dots(26)$$

In order to eliminate the effect of atmospheric instability linked to the variation of the radiation between night and day, in the exponent of the power law, the author makes the Monin-Obukov length to infinity assuming neutral atmosphere. In this case, the exponent takes a logarithmic form and is then written:

$$\alpha_e = \frac{1}{\ln\left(\frac{Z_g}{Z_0}\right)} \dots\dots\dots(27)$$

Justus show graphically that for very high wind regimes and for high altitudes, the 1/7 power law is the limit of the similarity model hence the expression. [11]

$$V_2 = V_1 \left(\frac{Z_1}{Z_2}\right)^{1/7} \dots\dots\dots(28)$$

e) Modified power law

This model aims to combine theory and experimentation by introducing the parameter roughness in the power law. Indeed, in order to combine the precision of the model theory and the simplicity of the previous empirical model, the power model modified was proposed by Mikhail and Justus CG el all in 1981. [10] For an altitude equal to 10m, and for neutral stability conditions, the power law exponent takes the form:

$$n_m = \frac{1}{\ln\left(\frac{Z_g}{Z_0}\right)} - \left(\frac{0.0881}{1 - 0.0881 \ln\left(\frac{Z_1}{10}\right)} \right) \ln\left(\frac{V_1}{V_n}\right) \dots \dots \dots (29)$$

With:

V_n 6m/s for neutral stability conditions

Z_g the geometric mean of the two heights.

In 1985, Mikhail experimentally adjusted the previous model and proposed the following expression:

$$n = \frac{1}{\ln\left(\frac{Z_g}{Z_0}\right)} + \left(\frac{0.0881 - 0.0881 \ln V_1}{1 - 0.0881 \ln\left(\frac{Z_1}{10}\right)} \right) \dots \dots \dots (30)$$

f) Monin-Obukov similarity model:

The majority of works on the determination of the vertical profile of the wind in the layer surface limit is based on the Monin-Obukov similarity theory of 1954 and the [13] work by Businger 1955. [12] Established for flat and homogeneous terrain, it connects the turbulent heat flow H as the product of the quantities u^* and θ^* called respectively friction velocity and temperature scale. The similarity theory specifies that the respective equations of the wind speed and temperature gradient in the layer atmospheric limit are related to the flux via the universal functions Φ_M and Φ_H These equations take the following form:

$$\frac{\partial V}{\partial Z} = \frac{u^*}{KZ} \Phi_M\left(\frac{Z}{L}\right) \dots \dots \dots (31)$$

$$\frac{\partial \theta}{\partial Z} = - \frac{H}{\rho c_p K V Z} \Phi_H\left(\frac{Z}{L}\right) \dots \dots \dots (32)$$

With:

- H: sensible heat flux (W/m^2)
- ρ : the density of the air (kg/m^3)
- κ : Von-Karman constant = 0.41
- u^* : friction speed (m/s)
- CP: Specific heat at constant pressure (kJ/kg)
- L: Monin-Obukov length (m)

z: Altitude (m).

These universal functions depend on dimensionless parameters, a function of the vertical stability of the atmosphere, namely Z/L and Ri (Richardson number representing the ratio between the heat flux and the turbulent moment squared).

The Monin-Obukov length is given by:

$$L = \frac{\rho C_p u^{*3} T}{K_g H} = \frac{u^*}{K_g \theta^*} \dots \dots \dots (33)$$

g) Power law Justus CG and Mikhail 1976:

Equation (1.31) was taken up by Justus et al. proposing an expression allowing The estimation of the coefficient of friction in order to draw the vertical profile thus allowing Instantaneous extrapolation of wind speeds. It is written in the following form: [13]

$$\alpha = a + b \ln V_1$$

Where a and b are constants whose values depend on the height of the anemometer, given by:

$$a = \frac{0.37}{1 - 0.088 \ln(\frac{Z_1}{10})} \dots \dots \dots (34)$$

And

$$b = \frac{-0.088}{1 - 0.088 \ln(\frac{Z_1}{10})} \dots \dots \dots (35)$$

With:

$$\alpha = \frac{0.37 - 0.088 \ln(V_1)}{1 - 0.088 \ln(\frac{Z_1}{10})} \dots \dots \dots (36)$$

2.1.3. Vertical extrapolation of Weibull parameters:

a) Justus and Mikhail extrapolation model:

In 1976, Justus and Mikhail proposed, for an initial altitude reference equal to 10m, the following extrapolation formulas

$$\frac{k_2}{k_1} = \frac{1 - 0.0881 * \ln(\frac{Z_1}{10})}{1 - 0.088 \ln(\frac{Z_2}{10})} \dots \dots \dots (37)$$

And:

$$\frac{C_1}{C_2} = \left(\frac{Z_2}{Z_1}\right)^m \dots\dots\dots(38)$$

With :

$$m = \left(\frac{0.37 - 0.0881 \ln(C_1)}{1 - 0.0881 \ln\left(\frac{Z_1}{10}\right)}\right) \dots\dots\dots(39)$$

b) Justus extrapolation model modified by Poje:

Taken over by Poje, Justus modified in 1978, the extrapolation expression of the parameters of Weibull by introducing the roughness of the ground, such as[28]:

$$\frac{k_2}{k_1} = \frac{1}{1 - 0.0881 \ln\left(\frac{Z_2}{Z_1}\right)} \dots\dots\dots(40)$$

And

$$\left(\frac{C_2}{C_1}\right) = \left(\frac{Z_2}{Z_1}\right)^{m_1} \dots\dots\dots(41)$$

With

$$m_1 = \frac{1}{\ln\left(\frac{Z_g}{Z_0}\right)} - 0.0881 \ln\left(\frac{C_1}{6}\right) \dots\dots\dots(42)$$

2.3. Definition of wind parameters:

2.3.1. Mean Velocity, Mean Cubic Velocity, and Variance:

Starting from the wind measurements (speed and direction), the weighted average speed is written[14]:

$$\bar{V} = \int_0^\infty f(V) dV \dots\dots\dots(43)$$

While the mean cubic velocity is determined by:

$$\bar{V}^3 = \int_0^{\infty} V^3 f(V) dV \dots\dots\dots(44)$$

The standard deviation of the speed variations (V) characterizes the global turbulence of the wind horizontal over the entire frequency range (full spectrum). It is given by:

$$\sigma(V) = \sqrt{Var(V)} \dots\dots\dots(45)$$

The variance is given by:

$$\sigma^2 = Var(V) = \int_0^{\infty} (V - \bar{V})^2 f(V) dV \text{ ou } Var(V) = \frac{1}{n-1} \sum_{i=1}^n (V_i - \bar{V})^2 \dots (1.46)$$

The expressions relating to the different models are shown in table 2.1 'being the gamma function given by:

$$\Gamma(X) = \int_0^{\infty} \exp(-t)t^{x-1} dt \dots\dots\dots(47)$$

Table1.1: Arithmetic, Weibull, Hybrid-Weibull, Rayleigh equations for calculating average wind speed

Distributions	\bar{V}	\bar{V}^3	σ	σ^2
Arithmetic	$\sum_{i=1}^n f_i v_i$	$\sum_{i=1}^n f_i V_i^3$	$\frac{1}{n} \sum_{i=1}^n f_i (V_i - \bar{V}_i)$	$\frac{1}{n} \sum_{i=1}^n f_i (V_i - \bar{V}_i)^2$
Weibull	$c\Gamma(1 + \frac{1}{k})$	$c^3\Gamma(1 + \frac{3}{k})$	$\sqrt{c^2[\Gamma(1 + \frac{2}{k}) - \Gamma^2(1 + \frac{1}{k})]}$	$c^2[\Gamma(1 + \frac{2}{k}) - \Gamma^2(1 + \frac{1}{k})]$
Hybrid Weibull	$(1 - ff_0)c\Gamma(1 + \frac{1}{k})$	$(1 - ff_0)c^3\Gamma(1 + \frac{3}{k})$	$\sqrt{(1 - ff_0)c^2[\Gamma - \Gamma^2(1 + \frac{1}{k})]}$	$(1 - ff_0)c^2[\Gamma - \Gamma^2(1 + \frac{1}{k})]$
Rayleigh	0.886 C	1.32C ³	0.4632 C	0.2146 C ²

2.3.2. Power factor and variation index:

Furthermore, other parameters useful for the characterization of a site, from the point of viewwind, must be calculated, namely:

- The wind power factor, given by (according to the Weibull distribution):

$$R_p = \frac{\langle V^3 \rangle}{\langle V \rangle} = \frac{\Gamma(1+\frac{3}{k})}{\Gamma^3(1+\frac{1}{k})} \dots\dots\dots(48)$$

- The index of variation given by (according to the Weibull distribution):

$$I_V = \frac{\sigma}{\langle V \rangle} = \left(\frac{\Gamma(1+\frac{2}{k})}{\Gamma^2(1+\frac{1}{k})} - 1 \right)^{1/2} \dots\dots\dots(49)$$

2.3.3. Most probable velocity and greatest energy velocity:

The most frequent speed in the distribution of frequencies of occurrence of speeds the wind. The speed of greater energy corresponds to the speed of the wind, which contains the maximum possible energy.

They are calculated from the speed probability density function as well than values of mean velocity and mean velocity and cubic velocity medium (Jamil et al ,1995). They are expressed by [16]:

$$V_{pp} = c(1 + \frac{1}{k})^{1/k} \dots\dots\dots(50)$$

$$V_{maxE} = c(1 + \frac{2}{k})^{1/k} \dots\dots\dots(51)$$

2.3.4. Wind Turbulence Index:

The turbulence index characterizes the degree of turbulence (turbulence intensity) of the wind for a fixed period. It influences the service life of the wind turbine through the fluctuations it induces on the blades and rotor of the aero generator.

The index of turbulence is calculated over a period of 10 minutes, in order to be in the 'gap' spectral of the wind spectrum. The turbulence index is the ratio between the standard deviation of the speed fluctuation (V) [16]

The average magnitude of speed V:

$$\tau = \frac{\sigma(V)}{\bar{V}} \dots \dots \dots (52)$$

2.3.5. Typical day (or composite day):

The composite day of wind speed (or direction) of a month or a year is determined by calculating the weighted average of the wind speeds of the month (or affected by the angular variations of their directions).

2.3.6. Turbulent Kinetic Energy Dissipation Rate:

The rate of dissipation of turbulent kinetic energy also characterizes turbulence, but in the high frequency part of the wind speed spectrum. This parameter corresponds to the dissipation of the energy of all the three components of the wind speed unlike the standard deviation used previously, which only characterizes that of horizontal [16].

It therefore includes the fluctuations of the vertical speed which are related to convection and friction. Indeed, in the absence of advection and mesoscale vertical velocity, the expression for the rate of dissipation of the turbulent kinetic energy is given by:

$$\varepsilon = \frac{g}{\theta_v} \overline{W\theta v} - \overline{WU} \frac{\partial \bar{U}}{\partial Z} \dots \dots \dots (53)$$

2.4. Influence of Weibull parameters on potential quality wind:

The Weibull parameters are used to model the wind speed distribution at a given location, and they can have a significant influence on the quality and potential of a wind resource.

The shape parameter of the Weibull distribution (k) determines the shape of the distribution curve, while the scale parameter (c) determines the average wind speed. Here are some ways in which the Weibull parameters can affect the quality of a wind resource:

2.4.1-Power density:

The power density of a wind turbine is proportional to the cube of the wind speed. Therefore, small changes in the average wind speed can have a significant impact on the power output of a wind turbine. The scale parameter (c) of the Weibull

distribution can thus have a major impact on the potential power output of a wind turbine.

2.4.2-Turbine selection:

The Weibull parameters can be used to select the most suitable type of wind turbine for a given location. For instance, if the Weibull shape parameter (k) is high, it means that the wind resource is more variable, and a turbine with a high rotor inertia may be needed to maintain stable power output. On the other hand, if the Weibull shape parameter is low, a turbine with a lower rotor inertia may be more appropriate.

2.4.3-Capacity factor:

The capacity factor of a wind turbine is the ratio of its actual power output to its maximum potential power output over a given period. The Weibull parameters can have a major impact on the capacity factor, as they determine the frequency and duration of high wind speeds. A Weibull distribution with a high scale parameter and low shape parameter will result in a high capacity factor, as there will be more frequent and longer periods of high wind speeds.

2.4.4-Energy yield:

The energy yield of a wind turbine is the total amount of energy that it produces over a given period of time. The Weibull parameters can affect the energy yield by influencing the frequency and duration of high wind speeds. A wind resource with a high scale parameter and low shape parameter will generally produce a higher energy yield, as there will be more frequent and longer periods of high wind speeds.

In summary, the Weibull parameters can have a significant influence on the quality and potential of a wind resource, and they are important considerations in wind resource assessment and wind turbine design.

$$E_{cin} = \frac{1}{2} mV^2 \dots\dots\dots(54)$$

2.5. Energy Evaluation and Wind Power Density Calculation:

To analyze the wind-based energy production, the distribution of the energy produced by a wind turbine differs in wind speed per unit time and rotor area, which is called the power Density distribution $e(v)$ in W/m^2 [3] and is explained as :

$$e(v) = \frac{1}{A} f(v)p(v) \dots\dots\dots(55)$$

By considering the equation , the following equation can be calculated as below:

$$e(v) = \frac{1}{2} \rho C_{p,eq} \begin{cases} 0v < v_{ci} \text{ or } v > v_{\infty} \\ v^3 f(v) v_{ci} \leq v \leq v_r \dots\dots\dots(53) \\ v_r^3 f(v) v_r < v \leq v_{\infty} \end{cases}$$

The total power density E at a specific wind site can be calculated as below:

$$E = \int_{ci}^{co} e(v)dv = \frac{1}{2} \rho C_{p,eq} (\int_{v_{ci}}^{v_r} v^3 f(dv) + \int_{v_r}^{v_{co}} v_r^3 f(v)dv) \dots\dots(56)$$

as a special case, a power density of E can be received analytic which the wind is showed by a Weibull probability distribution function [26]–[27]. The case can be determined as follows

$$P(v) = \frac{1}{2} \rho V^2 \dots\dots\dots(57)$$

A. average theoretical power, available on a given site per unit of time, and per unit area $A = 1 m^2$, is a relation that writes before (1.66), but we are in a relation this subject writes velocity V as general, but now rewrite the average speed equation extracted from the WEIBULL distribution, while the relationship[4] :

$$P = \frac{1}{2} \rho \overline{V^3} \dots\dots\dots(58)$$

$\overline{V^3}$ is the mean cubic wind speed, derived from the weibull distribution.

2.6. Theoretical maximum recoverable power (Batez theorem) :

- Baetz formula:

Whatever the type of wind turbine, not all the kinetic energy of the wind exploited by wind turbines, and is converted into mechanical energy, but part of the wind flow arriving on the rotor propellers will pass through the blades and part deflected to the sides,

- Betz, a German exploration, this law bears his name, applying the Froude's theory (and the

associated hypotheses), we obtain:

-For the power absorbed by rotor:

$$P = \rho A_1 V_1^2 (V_0 - V_2) \dots\dots\dots(59)$$

With (kg/m^3) density of air

-For the variation of the kinetic energy per second:

$$\Delta E_c = \frac{1}{2} \rho A_1 V_1^2 (V_0^2 - V_2^2) \dots\dots\dots(60)$$

And because the study in most cases study in unit area $A = 1m^2$, therefore:

$$\Delta E_c = \frac{1}{2} \rho V_1^2 (V_0^2 - V_2^2) \dots\dots\dots(61)$$

As $P = \Delta$ gives:

$$V_1 = \left(\frac{V_0 + V_2}{2}\right) \dots\dots\dots(62)$$

$$P = \frac{1}{2} \rho \left(\frac{V_0 + V_2}{2}\right) (V_0^2 - V_2^2) \dots\dots\dots(63)$$

When studying the change in power, depending on the downstream speed provides a

Only physically acceptable root:

Correspond to the maximum power, and by this change V_2 in relation (63), giving us an equation of the derived maximum power, namely:

$$P_{max} = \frac{1}{2} \rho \left(\frac{2V_0}{3}\right) \left(\frac{8}{9} V_0^2\right) \dots\dots\dots(64)$$

As V_0 is the upstream velocity ($V_0^3 = \bar{V}_3$), and through determining the power coefficient

$C_P = P \frac{1}{\rho A_1 V_0^3}$, we have arrived at the Betz limit C_P Or in other words ($V_{03} = \bar{V}_3$) and referring to equation (61)

The equation becomes $P = \frac{1}{2} \rho V_0^3$

From equation (64) which is:

$$\begin{aligned} P_{max} &= \frac{1}{2} \rho \left(\frac{2v_0}{3}\right) \left(\frac{8}{9} V_0^2\right) \\ \Rightarrow P_{max} &= \frac{1}{2} \rho \left(\left(\frac{2}{3}\right) X \left(\frac{8}{9}\right)\right) (V_0^3) \\ \Rightarrow P_{max} &= \frac{1}{2} \rho \left(\frac{16}{26}\right) (V_0^3) \\ &= \frac{1}{2} \rho V_0^3 \left(\frac{16}{26}\right) \\ &= P \left(\frac{16}{26}\right) = P C_{p max} \dots\dots\dots(65) \end{aligned}$$

Then $C_{p\ max} = \frac{P_{max}}{P} = \left(\frac{16}{27}\right) \approx 0.593$ is a Betz limit

C. recoverable power among its technical parameters three essential speed data for its operation.

It is about:

- **The starting speed V_D :** this is the speed from which the wind turbine starts to produce energy.

Below this threshold, the wind turbine produces no energy.

- **The nominal speed V_N :** The wind turbine reaches its maximum energy production threshold from this speed. This threshold remains constant up to the cut-off speed.

- **The cut-off speed V_C :** The wind turbine stops producing energy due to automatic stopping of the blades for safety from this speed.

Velocities beyond V_C have no effect in the energy calculation. [23]

- The curve shows that the energy power recoverable by a wind turbine varies very quickly with the wind speed. In fact, a wind turbine only delivers its rated power within a restricted range of wind speeds.

- For wind speeds around V_D ($mais > V_d$), the blades start their

Rotation: this is said to be the attachment fork.

- In the neighborhood of, the power delivered increases very quickly. This is the exponential power growth range.

- Between , the rotation of the blades is slowed down by inclination of the blades at the level of the hub. This allows the machine to avoid excessive mechanical stress due to very high speeds. In this speed range, the energy delivered is constant.

- Beyond, the wind turbine is stopped, this is the cut-off speed.

Thus, the ideal power $P_{Récupérable}$ (en W) by a wind turbine is given by:

$$P_{annealing} = \frac{1}{2} \rho A \int_0^{\infty} V^3 f(V) dV = \frac{1}{2} \rho A \int_{V_D}^{V_N} V^3 f(V) dV + \frac{1}{2} \rho A \int_{V_N}^{V_C} V^3 f(V) dV \dots \dots (66)$$

Where A is the area swept by the rotor ($A = \pi D^2/4$, with D the diameter of the rotor).

Since the nominal power density is equal to:

$$P_n = \frac{1}{2} \rho A V_n^3 \dots \dots (67)$$

This recoverable power can be written in the form (Tsang-Jung Chang et al, 2003).

2.7. Useful power:

The wind turbine, like all real systems, does not fully transform the energy kinetics of wind into electricity. It has an efficiency (or power coefficient) in because of the irreversibility's involved in the transformations. The power coefficient indicates how efficiently the wind turbine converts wind energy into electricity.

There value of the power coefficient (η) of the wind turbine is obtained by taking the ratio between the nominal power given by the manufacturer and the calculated theoretical electrical power for a constant wind speed equal to its nominal speed. This value of the coefficient power is always less than or equal to the Betz limit (0.59). A coefficient of correct performance is between 0.3 and 0.5

$$\eta = \frac{P_n}{P_{the}} \dots\dots (68)$$

The useful power of a wind turbine is equal to the product of the power coefficient of the wind turbine (η) by the recoverable power (Recoverable P) by the same wind turbine in operation between its start speed and its cut-off speed.

$$P_{output} = \eta P_{annealing} \dots\dots (69)$$

CONCLUSION:

This chapter provided a comprehensive guide on the steps required to achieve the research objective. The bibliographical study conducted included an in-depth examination of statistical models used for analyzing random wind speeds, as well as models for extracting Weibull parameters. These models will enable us to calculate the average wind speed and the average usable power.

Additionally, the chapter briefly discussed wind turbine technology, types, and components, as well as the principle of operation and the research site.

Chapter II:

Estimation of wind energy potential and
vertical extrapolation of the Weibul
parameter

2.1. Introduction

In this chapter, we will study the possibility of winds in the Ouargla area, the dynamic energy power of winds with the transformation of wind dynamic energy into rotational wind energy of a wind turbine. It identifies a range of losses in the latter and calculates the maximum useful power, even in one form.

2.2. Geographical Location:

The Wilayat of Ouargla is located in the southeast of the Algerian state and is part of the great desert depression whose width varies between 12-18 km and is thirty kilometers long. Its altitude varies between one hundred and three hundred and fifty meters, and the basin of the city extends between two plateaus, the first of which is tilted to the west and is about 230 meters high, while the second is bordered to the east and is 160 meters high, connected to the large sands of the Erg. The state of Ouargla is approximately eight hundred and twenty kilometers from the Algerian capital.

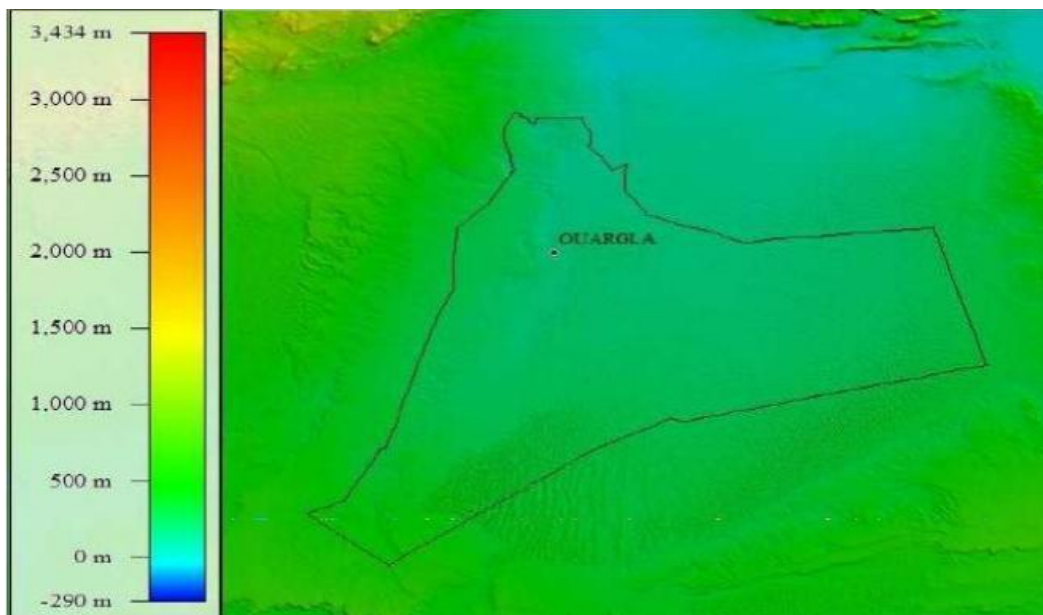


Figure 2.1: Schematic representation of successive degradations of wind energy before use.

2.3. Temporal Variation of Wind Speed:

To determine the importance of wind at a given point, it is sufficient to determine the weighted annual arithmetic average speed calculated over a minimum period of 10 years. This gives an estimate of the wind speed at a given site. Furthermore, winds vary differently depending on the day, season, and year. This variation must be determined as it allows the sizing of wind

systems to adapt to energy needs that may vary depending on the days or years. The daily variation is established on an hourly scale. The annual variation is determined by Daily-scale studies establishment. Multi-year variation requires long-term series processed on an annual scale.

2.3.1. Daily average variation of wind speed

The daily variation in wind speed is due to thermal phenomena related to solar radiation. The average wind speed varies little at night and increases during the day from sunrise. In the wind rose, it is noticed that the speed and direction of the wind vary randomly.

2012

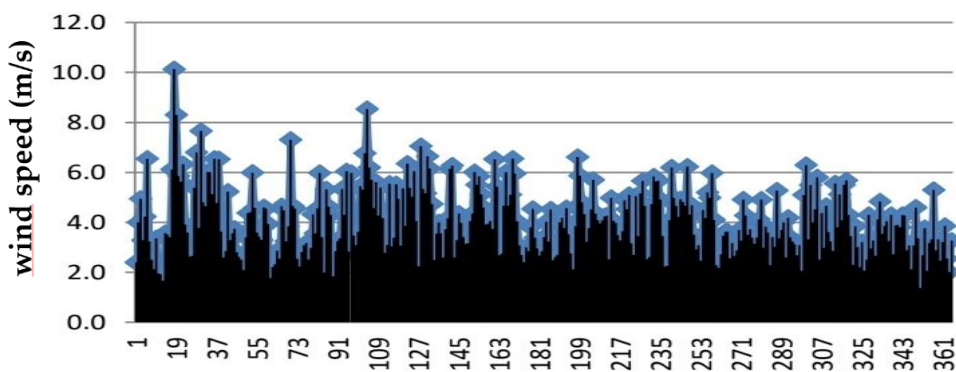


Figure 2.2: The curve illustrates changes in wind speed in terms of days for the year 2012.

The curve depicts variations in wind speed across days for 2012. The highest wind speed recorded was 10 m/s, while the lowest was 2.0 m/s, with speeds ranging from 2m/s to 7m/s throughout the year.

2013

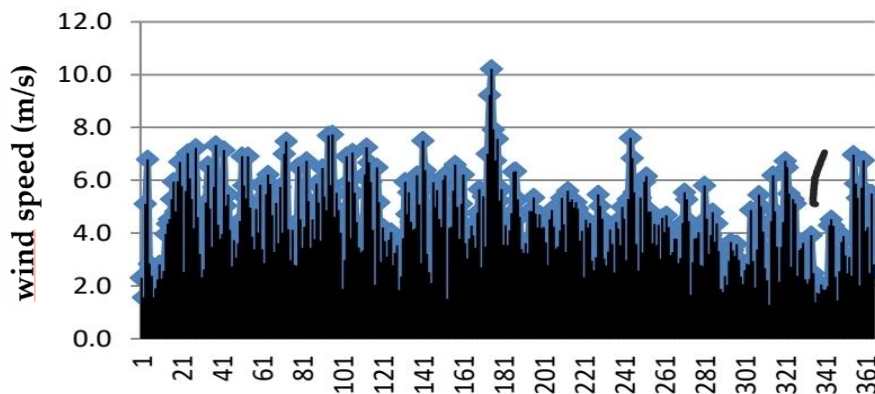


Figure 2.3: The curve illustrates changes in wind speed in terms of days for the year 2013.

The curve shows changes in wind speed for every day of the year 2013, where the highest wind speed value was 10.1m/s and the lowest wind speed value was 1.9m/s, with most wind speed values ranging between 2.0m/s and 8m/s.

2014

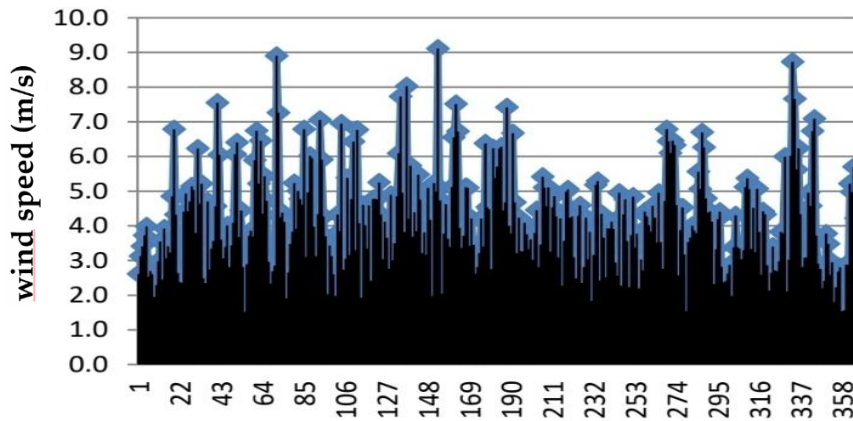


Figure 2.4: The curve illustrates changes in wind speed for every day of the year 2014. The curve displays changes in wind speed for every day of the year 2014, where the highest estimated wind speed value was 9.1m/s and the lowest estimated wind speed value was 1.5m/s, with most wind speed values varying between 2m/s and 5m/s.

2015

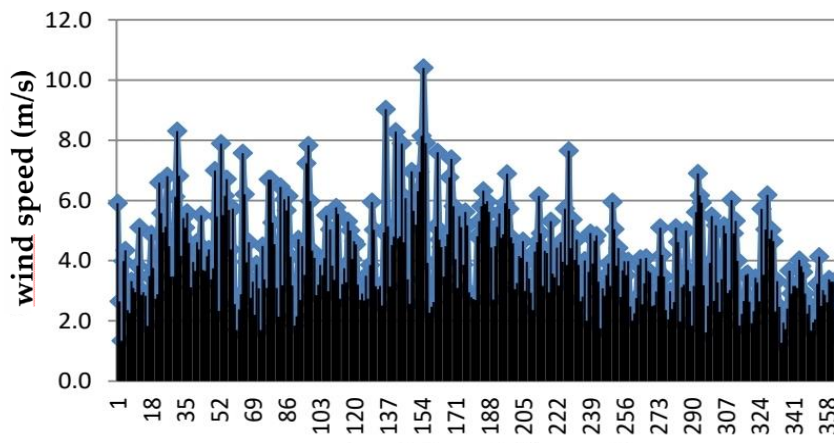


Figure 2.5: The curve represents the evolution of wind speed in terms of days for the year 2015.

The curve shows the wind speed's variation in days for the year 2015, where the maximum speed value is estimated to be 10.1m/s, and the minimum speed value is estimated to be 1.5m/s. The majority of wind speeds for this year fall between 2.0m/s and

2016

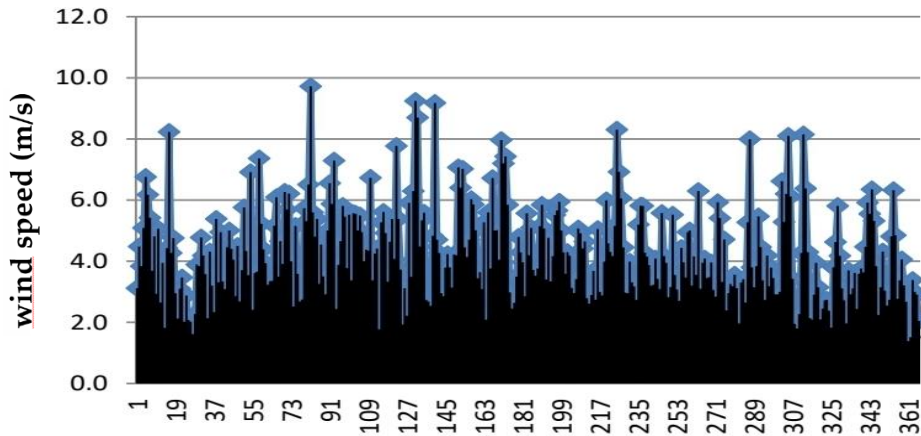


Figure 2.6: The curve represents the evolution of wind speed in terms of days for the year 2016.

The curve represents the variation of wind speed in days for the year 2016, where the highest speed value is estimated at 9.1m/s and the lowest speed value is estimated at 1.7m/s. The majority of wind speeds throughout the year fall between 2.0m/s and 6.0m/s.

2017

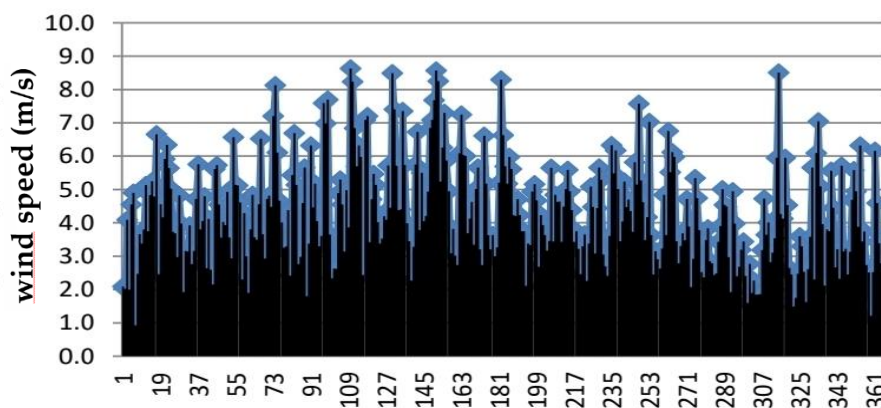


Figure 2.7: The graph illustrates the wind speed variation in terms of days for the year 2017.

The curve shows the change in wind speed throughout the days of the year 2017. It can be observed that the highest wind speed value throughout the year is estimated to be 8.9m/s, while the lowest wind speed is estimated to be 1.0m/s. Additionally, it is worth noting that the majority of wind speeds fall between 2.0m/s and 5.7m/s.

2018 :

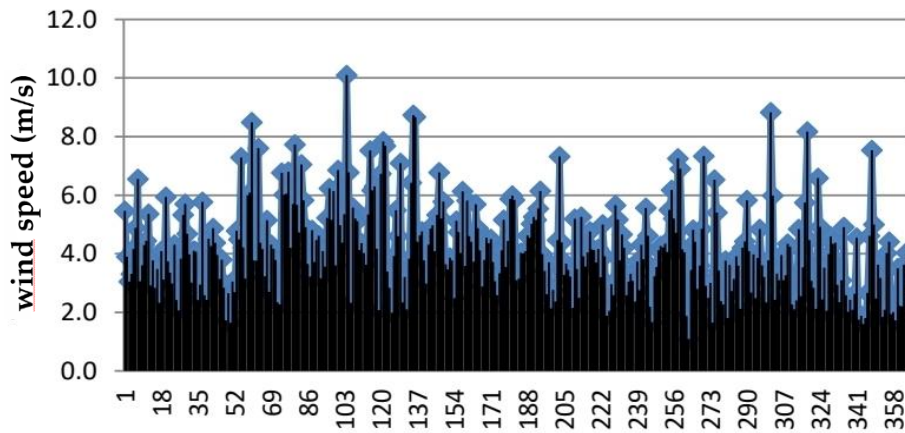


Figure 2.8: The curve represents the changes in wind speed in terms of days for the year 2018.

The graph shows the variations in wind speed for each day of the year 2018. It can be seen that the highest wind speed value is estimated to be 10.1m/s, and the lowest value is estimated to be 1.1m/s. Furthermore, most of the wind speeds range between 2.0m/s and 6.0m/s.

2019

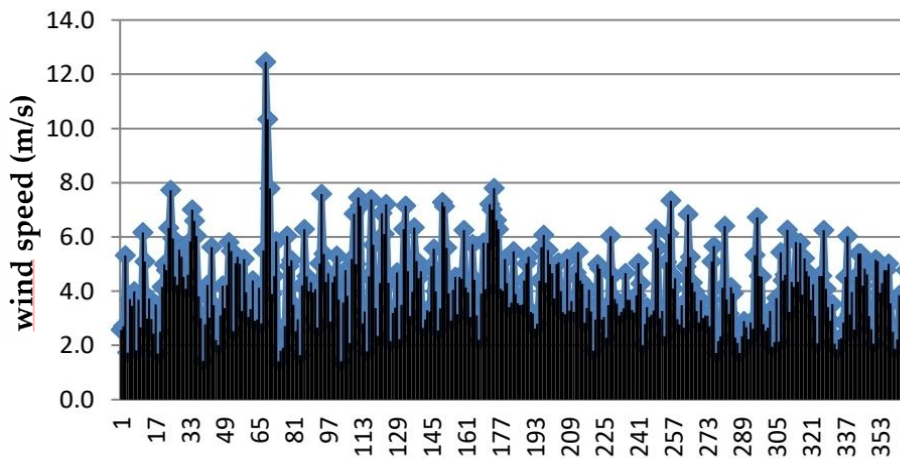


Figure 2.9: The curve shows the variations in wind speed in terms of days for the year 2019.

The graph depicts the changes in wind speed for each day of the year 2019. It can be observed that the highest wind speed value is estimated to be 12.0m/s, while the lowest value is estimated to be 1.8m/s. Additionally, it is worth noting that the majority of wind speeds oscillate between 2.0m/s and 6.0m/s.

2020

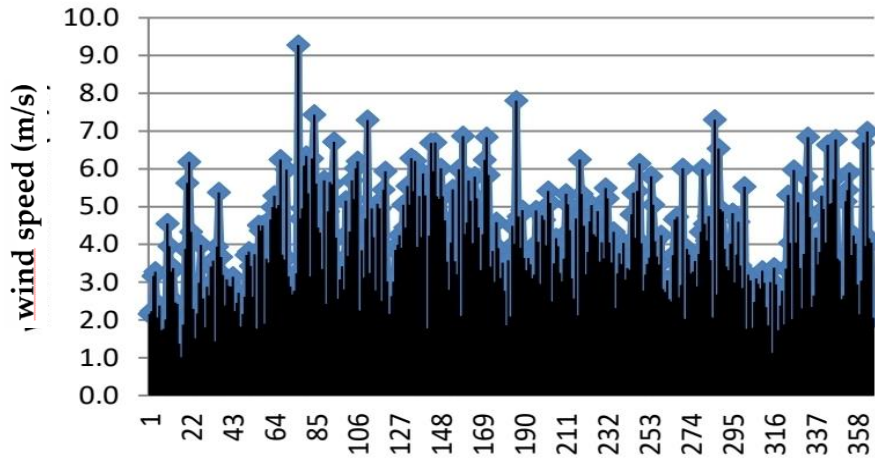


Figure 2.10: The curve shows the changes in wind speed in terms of days for the year 2020.

The graph represents the variations in wind speed for each day of the year 2020. It can be observed that the highest wind speed value is 9.3m/s, while the lowest value is estimated to be 1.0m/s. The majority of wind speeds fall within the range of 2.0m/s to 6.0m/s.

2021

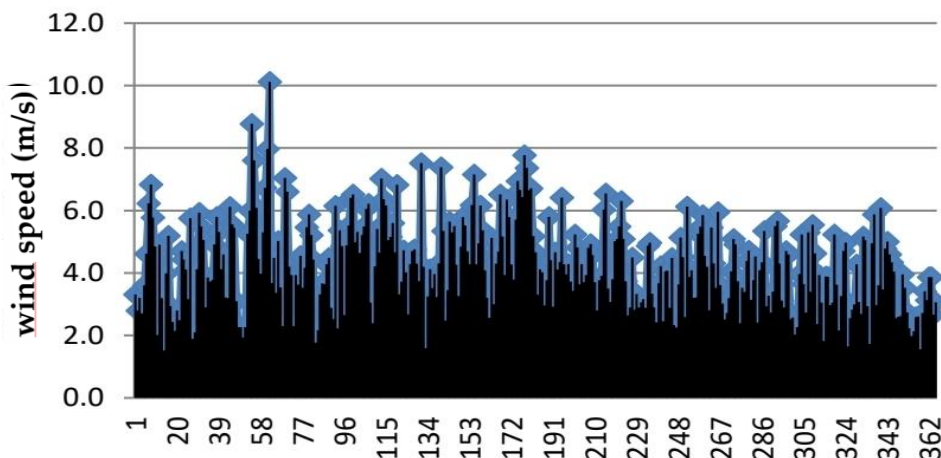


Figure 2.11: The curve shows the changes in wind speed in terms of days for the year 2021.

The graph depicts the changes in wind speed for each day of the year 2021. It is noteworthy that the highest wind speed

value is 9.3m/s, and the lowest value is estimated to be 1.0m/s. The majority of wind speeds fall within the range of 2.0m/s to 6.0m/s.

2.3.2. Multi-year variation of wind speed:

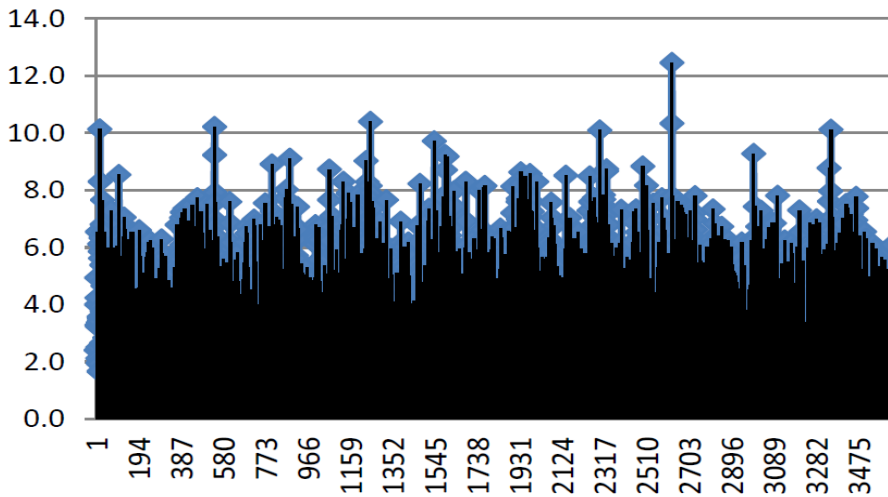
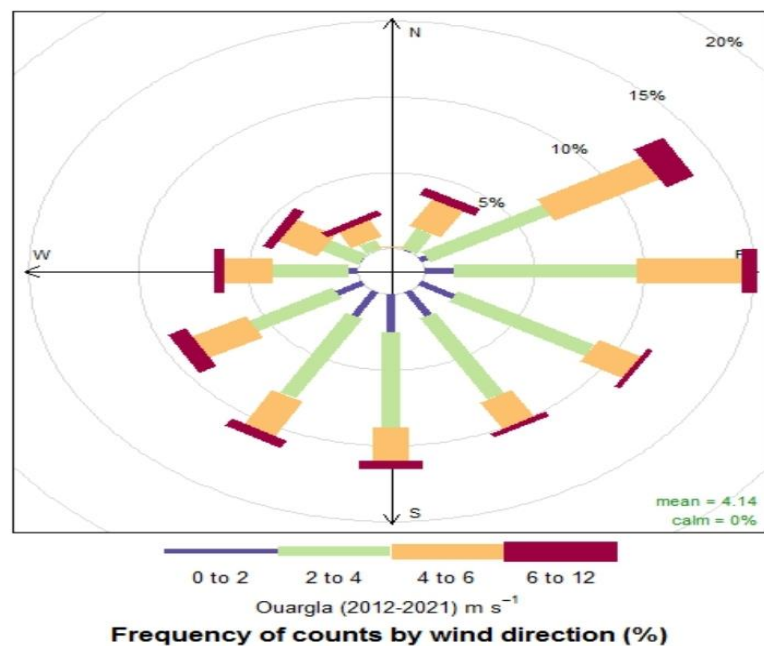


Figure 2.12: The graph represents the evolution of wind speed in terms of days for a comparison between 2012 and 2021.

It is noted that the highest wind speed of the two years was estimated at 10.1 m/s, and the lowest wind speed was estimated at 1.4 m/s. Most of the wind speeds ranged between 2.0 m/s and 7.0 m/s.

2.3.3. Wind Roses:

In the wind rose, it can be observed that the speed and direction of the wind vary randomly.



2.4. Static Study:

2.4.1. Distributions

2.4.1.1. Histogram of occurrence frequency distributions:

Number of classes N_c :

$$N_c = 3.33 \log N + 1 \dots\dots\dots(70)$$

$$\Rightarrow N_c = \sqrt{N} \dots\dots\dots(71)$$

N: Number of observations

Class interval:

$$h = \frac{V_{max} - V_{min}}{N_c} \dots\dots\dots(72)$$

Relative frequency:

$$f_r = \frac{n_i}{N} \dots\dots\dots(73)$$

n_i : Number of observations in the class.

N: Total number.

Table 2.1: Frequency calculator

2012	Class	f_a	Fr	$f_{ré}$	$fr\%$	2013	Class	f_a	fr	$f_{ré}$	$fr\%$
1	1.4-1.83	2	0.005	0.005	0.5	1	1.3-1.74	6	0.016	0.016	1.6
2	1.83-2.26	13	0.035	0.04	3.5	2	1.74-2.18	15	0.041	0.057	4.1
3	2.26-2.69	26	0.071	0.111	7.1	3	2.18-2.62	26	0.071	0.128	7.1
4	2.69-3.12	49	0.133	0.244	13.3	4	2.62-3.06	29	0.079	0.207	7.9
5	3.12-3.55	54	0.147	0.391	14.7	5	3.06-3.50	41	0.112	0.319	11.2
6	3.55-3.98	42	0.114	0.505	11.4	6	3.50-3.94	39	0.106	0.425	10.6
7	3.98-4.41	52	0.142	0.647	14.2	7	3.94-4.38	39	0.106	0.531	10.6
8	4.41-4.84	35	0.095	0.742	9.5	8	4.38-4.82	38	0.104	0.635	10.4
9	4.84-5.27	23	0.062	0.804	6.2	9	4.82-5.26	29	0.079	0.714	7.9
10	5.27-5.70	25	0.068	0.872	6.8	10	5.26-5.70	36	0.098	0.812	9.8
11	5.70-6.13	20	0.054	0.926	5.4	11	5.70-6.14	21	0.057	0.869	5.7
12	6.13-6.56	11	0.03	0.956	3	12	6.14-6.58	11	0.03	0.899	3
13	6.56-6.99	9	0.024	0.98	2.4	13	6.58-7.02	17	0.046	0.945	4.6
14	6.99-7.42	2	0.005	0.985	0.5	14	7.02-7.46	9	0.024	0.969	2.4
15	7.42-7.85	0	0	0.985	0	15	7.46-7.90	6	0.016	0.985	1.6
16	7.85-8.28	1	0.002	0.987	0.2	16	7.90-8.34	1	0.002	0.987	0.2
17	8.28-8.71	1	0.002	0.989	0.2	17	8.34-8.78	0	0	0.987	0
18	8.71-9.14	0	0	0.989	0	18	8.78-9.22	0	0	0.987	0
19	9.14-9.57	0	0	0.989	0	19	9.22-9.66	1	0.002	0.989	0.2

2014	Class	fa	Fr	f ré	fr%
1	1.5-1.88	4	0.01	0.01	1
2	1.88-2.26	12	0.032	0.042	3.2
3	2.26-2.64	23	0.063	0.105	6.3
4	2.64-3.02	40	0.109	0.214	10.9
5	3.02-3.4	42	0.115	0.329	11.5
6	3.4-3.78	28	0.076	0.405	7.6
7	3.78-4.16	46	0.126	0.531	12.6
8	4.16-4.54	45	0.123	0.654	12.3
9	4.54-4.92	33	0.09	0.744	9
10	4.92-5.30	33	0.09	0.834	9
11	5.30-5.68	8	0.021	0.855	2.1
12	5.68-6.06	7	0.019	0.874	1.9
13	6.06-6.44	15	0.041	0.915	4.1
14	6.44-6.82	12	0.032	0.947	3.2
15	6.82-7.2	7	0.019	0.966	1.9
16	7.2-7.58	2	0.005	0.971	0.5
17	7.58-7.96	4	0.01	0.981	1
18	7.96-8.34	1	0.002	0.983	0.2
19	8.34-8.72	0	0	0.983	0
20	8.72-9.1	3	0.008	0.991	0.8

2015	Class	fa	fr	f ré	fr%
1	1.3-1.75	4	0.01	0.01	1
2	1.75-2.2	18	0.049	0.059	4.9
3	2.2-2.65	29	0.079	0.138	7.9
4	2.65-3.1	49	0.134	0.272	13.4
5	3.1-3.55	47	0.128	0.4	12.8
6	3.55-4	45	0.123	0.523	12.3
7	4-4.45	28	0.076	0.599	7.6
8	4.45-4.9	39	0.106	0.705	10.6
9	4.9-5.35	29	0.079	0.784	7.9
10	5.35-5.80	27	0.073	0.857	7.3
11	5.80-6.25	16	0.043	0.9	4.3
12	6.25-6.70	9	0.024	0.924	2.4
13	6.70-7.15	11	0.03	0.954	3
14	7.15-7.60	2	0.005	0.959	0.5
15	7.60-8.05	7	0.019	0.978	1.9
16	8.05-8.50	3	0.008	0.986	0.8
17	8.50-8.95	0	0	0.986	0
18	8.95-9.4	1	0.002	0.988	0.2
19	9.4-9.85	0	0	0.988	0
20	9.85-10.3	0	0	0.988	0
21	10.3-10.75	1	0.002	0.99	0.2

2016	Class	fa	Fr	f ré	fr%
1	1.4-1.81	3	0.008	0.008	0.8
2	1.81-2.22	18	0.049	0.057	4.9
3	2.22-2.63	14	0.038	0.095	3.8
4	2.63-3.04	36	0.098	0.193	9.8
5	3.04-3.45	47	0.128	0.321	12.8
6	3.45-3.86	42	0.114	0.435	11.4
7	3.86-4.27	36	0.098	0.533	9.8
8	4.27-4.68	42	0.114	0.647	11.4
9	4.68-5.09	21	0.057	0.704	5.7
10	5.09-5.50	36	0.098	0.802	9.8
11	5.50-5.91	25	0.068	0.87	6.8
12	5.91-6.32	14	0.038	0.908	3.8
13	6.32-6.73	10	0.027	0.935	2.7
14	6.73-7.14	6	0.016	0.951	1.6
15	7.14-7.55	5	0.013	0.964	1.3
16	7.55-7.96	1	0.002	0.966	0.2
17	7.96-8.37	5	0.013	0.979	1.3
18	8.37-8.78	1	0.002	0.981	0.2
19	8.78-9.19	1	0.002	0.983	0.2
20	9.19-9.60	2	0.005	0.988	0.5
21	9.60-10.01	1	0.002	0.99	0.2

2017	Class	fa	fr	f ré	fr%
1	0.9-1.28	1	0.002	0.002	0.2
2	1.28-1.66	2	0.005	0.007	0.5
3	1.66-2.04	11	0.03	0.037	3
4	2.04-2.42	14	0.038	0.075	3.8
5	2.42-2.8	33	0.09	0.165	9
6	2.8-3.18	18	0.049	0.214	4.9
7	3.18-3.56	43	0.117	0.331	11.7
8	3.56-3.94	47	0.128	0.459	12.8
9	3.94-4.32	32	0.087	0.546	8.7
10	4.32-4.70	30	0.081	0.627	8.1
11	4.70-5.08	25	0.068	0.695	6.8
12	5.08-5.46	30	0.081	0.776	8.1
13	5.46-5.84	23	0.062	0.838	6.2
14	5.84-6.22	16	0.043	0.881	4.3
15	6.22-6.60	9	0.024	0.905	2.4
16	6.60-6.98	9	0.024	0.929	2.4
17	6.98-7.36	7	0.019	0.948	1.9
18	7.36-7.74	6	0.016	0.964	1.6
19	7.74-8.12	2	0.005	0.969	0.5
20	8.12-8.5	4	0.01	0.979	1
21	8.5-8.88	4	0.01	0.989	1

2018	Class	fa	Fr	f ré	fr%
1	1.1-1.55	1	0.002	0.002	0.2
2	1.55-2	14	0.038	0.04	3.8
3	2-2.45	26	0.07	0.11	7
4	2.45-2.9	37	0.101	0.211	10.1
5	2.9-3.35	36	0.098	0.309	9.8
6	3.35-3.80	42	0.115	0.424	11.5
7	3.80-4.25	48	0.131	0.555	13.1
8	4.25-4.70	54	0.147	0.702	14.7
9	4.70-5.15	25	0.068	0.77	6.8
10	5.15-5.60	24	0.065	0.835	6.5
11	5.60-6.05	16	0.043	0.878	4.3
12	6.05-6.50	14	0.038	0.916	3.8
13	6.50-6.95	8	0.021	0.937	2.1
14	6.95-7.40	8	0.021	0.958	2.1
15	7.40-7.85	5	0.013	0.971	1.3
16	7.85-8.30	2	0.005	0.976	0.5
17	8.30-8.75	1	0.002	0.978	0.2
18	8.75-9.20	3	0.008	0.986	0.8
19	9.20-9.65	0	0	0.986	0
20	9.65-10.1	1	0.002	0.988	0.2

2019	Class	fa	fr 0	f ré	fr%
1	1.4-1.95	12	0.032	0.032	3.2
2	1.95-2.5	29	0.079	0.111	7.9
3	2.5-3.05	37	0.101	0.212	10.1
4	3.05-3.6	70	0.191	0.403	19.1
5	3.6-4.15	40	0.109	0.512	10.9
6	4.15-4.70	62	0.169	0.681	16.9
7	4.70-5.25	36	0.098	0.779	9.8
8	5.25-5.80	31	0.084	0.863	8.4
9	5.80-6.35	16	0.043	0.906	4.3
10	6.35-6.90	14	0.038	0.944	3.8
11	6.90-7.45	11	0.03	0.974	3
12	7.45-8	6	0.016	0.99	1.6
13	8-8.55	0	0	0.99	0
14	8.55-9.1	0	0	0.99	0
15	9.1-9.65	0	0	0.99	0
16	9.65-10.2	0	0	0.99	0
17	10.2-10.75	1	0.002	0.992	0.2
18	10.75-11.3	0	0	0.992	0
19	11.3-11.85	0	0	0.992	0
20	11.85-12.4	0	0	0.992	0

2020	Class	fa	Fr	f ré	fr%
1	1-1.41	2	0.005	0.005	0.5
2	1.41-1.82	5	0.013	0.018	1.3
3	1.82-2.23	22	0.06	0.078	6
4	2.23-2.64	23	0.062	0.14	6.2
5	2.64-3.05	34	0.092	0.232	9.2
6	3.05-3.46	45	0.122	0.354	12.2
7	3.46-3.87	47	0.128	0.482	12.8
8	3.87-4.28	39	0.106	0.588	10.6
9	4.28-4.69	30	0.081	0.669	8.1
10	4.69-5.1	34	0.092	0.761	9.2
11	5.1-5.51	32	0.087	0.848	8.7
12	5.51-5.92	16	0.043	0.891	4.3
13	5.92-6.33	16	0.043	0.934	4.3
14	6.33-6.74	7	0.019	0.953	1.9
15	6.74-7.15	9	0.024	0.977	2.4
16	7.15-7.56	3	0.008	0.985	0.8
17	7.56-7.97	1	0.002	0.987	0.2
18	7.97-8.38	0	0	0.987	0
19	8.38-8.79	0	0	0.987	0
20	8.79-9.2	0	0	0.987	0
21	9.2-9.61	1	0.002	0.989	0.2

2021	Class	fa	fr	f ré	fr%
1	1.5-1.93	7	0.019	0.019	1.9
2	1.93-2.36	12	0.032	0.051	3.2
3	2.36-2.79	30	0.082	0.133	8.2
4	2.79-3.22	45	0.123	0.256	12.3
5	3.22-3.65	36	0.098	0.354	9.8
6	3.65-4.08	39	0.106	0.46	10.6
7	4.08-4.51	49	0.134	0.594	13.4
8	4.51-4.94	33	0.09	0.684	9
9	4.94-5.37	34	0.093	0.777	9.3
10	5.37-5.80	29	0.079	0.856	7.9
11	5.80-6.23	17	0.046	0.902	4.6
12	6.23-6.66	14	0.038	0.94	3.8
13	6.66-7.09	8	0.021	0.961	2.1
14	7.09-7.52	6	0.016	0.977	1.6
15	7.52-7.95	3	0.008	0.985	0.8
16	7.95-8.38	1	0.002	0.987	0.2
17	8.38-8.81	0	0	0.987	0
18	8.81-9.24	1	0.002	0.989	0.2
19	9.24-9.67	0	0	0.989	0
20	9.67-10.1	1	0.002	0.991	0.2

A. Daily variation: We performed a statistical analysis on the available data, which consisted of the monthly average speeds for each year at the study station. Using the example we saw earlier, we obtained the fol

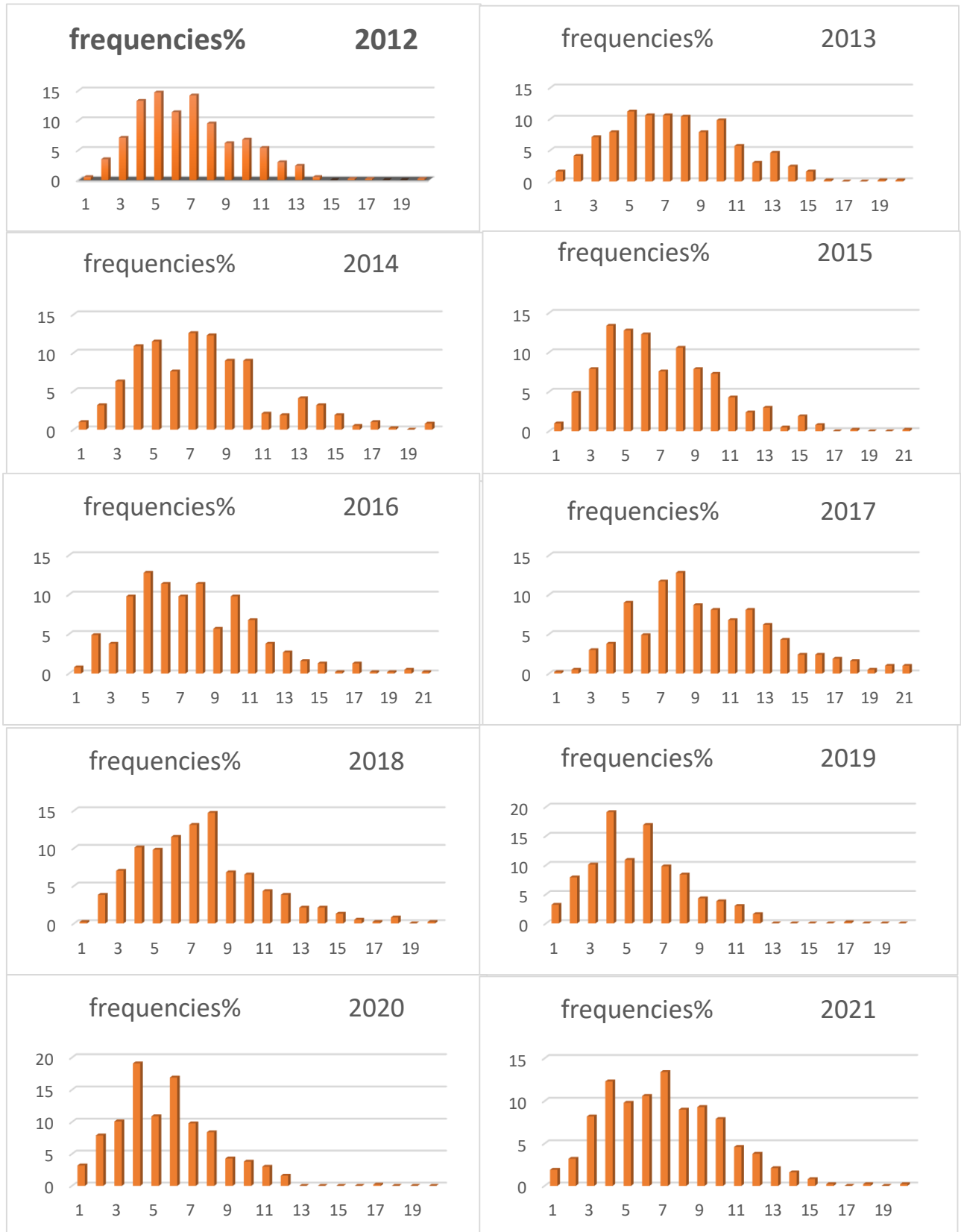


Figure 2.13: Histogram for the speed frequency ratio

In Ouargla, the figure shows us that the distribution of wind frequencies for daily average speeds for each year is different due to the variation in years. The figure displays multiple classes with their respective relative frequencies. For example, in the year 2015, the class with an interval of [1.3 m/s - 10.75 m/s] had a percentage of 1%, while the simultaneous classes had percentages of 4.9% and 7.8%. The highest percentage of a class was 13.4%, followed by 12.8%, 12.3%, 7.6%, 10.6%, 7.9%, 7.3%, 4.3%, 2.4%, 3%, 0.7%, 1.9%, and 0.8%, which were divided among the other years. In the Ouargla station, the relative frequencies were generally almost equal in all years. This means that there was no majority global interval for all years [2012-2021]. However, in 2019, the interval [3.05-3.60] had a significant percentage of 19.1%. In the following years [2014-2016-2017-2020], the class with the value of 12.8% was found.

2.4.1.2. Variation of Weibull parameters:

In addition to the weighted arithmetic mean method, three statistical methods are used to model the wind speed distribution presented in chapter 2:

- The Weibull distribution;
- The hybrid Weibull distribution;
- The Rayleigh distribution.

These distributions are used to determine wind factors characterizing a site, including:

- The mean wind speed;
- The average cube of wind speed;
- The variance of the speed distribution;
- The power factor;
- The variation index.

Several methods are used to fit statistical data (determine Weibull coefficients k and C). The most commonly used methods are the graphical method of least squares to calculate the shape coefficient and the graphical method to calculate the scale parameter.

$$F(v) = 1 - \exp \left[- \left(\frac{v}{C} \right)^K \right]$$

Convert this exponential equation into a linear equation like this:

$$\text{Ln} [-\text{Ln}(1-F(V))] = k \text{Ln}(V) - k \text{Ln}(C)$$

Let:

$$X_i = \text{Ln}(V_i) \qquad Y_i = \text{Ln} \left[\text{Ln} \left(\frac{1}{1-F(V)} \right) \right]$$

Where $i=1, 2, 3, \dots, n$

The linear approximation of these data is obtained by the method of least squares, under

the form

$$Y = a + bX$$

$$\text{Ln} \left[\text{Ln} \left(\frac{1}{1-F(V)} \right) \right] = k \text{Ln}(V_i)$$

Table 2.2: Find the word y, x and k

2012

bin	NO V	frq	frq %	f(V)	1-f(V)	Ln(1-f(V))	Ln(-Ln(1-f(V)))	Ln(V)
0	0	0	0	0	1	0		
1	0	0	0	0	1	0		0
2	27	0.0787	7.8717	0.07871	0.9212	-0.0819	-2.5011	0.6931
3	112	0.3265	32.6530	0.4052	0.5947	-0.5196	-0.6546	1.0986
4	91	0.2653	26.5306	0.6705	0.3294	-1.1103	0.1046	1.3862
5	61	0.1778	17.7842	0.8483	0.1516	-1.8864	0.6347	1.6094
6	40	0.1166	11.6618	0.9650	0.0349	-3.3528	1.2098	1.7917
7	10	0.0291	2.9154	0.9941	0.0058	-5.1445	1.6379	1.9459
8	2	0.0058	0.5831	1	0			

2013

bin	NO V	frq	frq %	f(V)	1-f(V)	Ln(1-f(V))	Ln(-Ln(1-f(V)))	Ln(V)
0	0	0	0	0	1	0		
1	2	0.0053	0.5347	0.0053	0.9946	-0.0053	-5.2284	0
2	39	0.1042	10.4278	0.1096	0.8903	-0.1161	-2.1531	0.6931
3	73	0.1951	19.5187	0.3048	0.6951	-0.3635	-1.0117	1.0986
4	100	0.2673	26.7379	0.5721	0.4278	-0.8490	-0.1635	1.3862
5	74	0.1978	19.7860	0.7700	0.2299	-1.4699	0.3852	1.6094
6	50	0.1336	13.3689	0.9037	0.0962	-2.3407	0.8504	1.7917
7	27	0.0721	7.2192	0.9759	0.0240	-3.7270	1.3156	1.9459
8	7	0.0187	1.8716	0.9946	0.0053	-5.2311	1.6546	2.0794
9	1	0.0026	0.2673	0.9973	0.0026	-5.9242	1.7790	2.1972
10	1	0.0026	0.2673	1	0			2.3025

2014

bin	NO V	frq	frq %	f(V)	1-f(V)	Ln(1-f(V))	Ln(-Ln(1-f(V)))	Ln(V)
0	0	0	0	0	1	0		
1	0	0	0	0	1	0		0
2	34	0.0934	9.3406	0.0934	0.9065	-0.0980	-2.3221	0.6931
3	100	0.2747	27.4725	0.3681	0.6318	-0.4590	-0.7785	1.0986
4	105	0.2884	28.8461	0.6565	0.3434	-1.0688	0.0665	1.3862
5	73	0.2005	20.0549	0.8571	0.1428	-1.9459	0.6657	1.6094
6	28	0.0769	7.6923	0.9340	0.0659	-2.7191	1.0003	1.7917
7	16	0.0439	4.3956	0.9780	0.0219	-3.8177	1.3396	1.9459
8	5	0.0137	1.3736	0.9917	0.0082	-4.7985	1.5683	2.0794
9	3	0.0082	0.8241	1	0			

2015

bin	NO V	frq	frq %	f(V)	1-f(V)	Ln(1-f(V))	Ln(-Ln(1-f(V)))	Ln(V)
0	0	0	0	0	1	0		
1	2	0.0054	0.5479	0.0054	0.9945	-0.0054	-5.2040	0
2	41	0.1123	11.2328	0.1178	0.8821	-0.1253	-2.0766	0.6931
3	105	0.2876	28.7671	0.4054	0.5945	-0.52	-0.6539	1.0986
4	79	0.2164	21.6438	0.6219	0.3780	-0.9726	-0.0277	1.3862
5	70	0.1917	19.1780	0.8136	0.1863	-1.6803	0.5190	1.6094
6	43	0.1178	11.7808	0.9315	0.0684	-2.6810	0.9861	1.7917
7	13	0.0356	3.5616	0.9671	0.0328	-3.4149	1.2281	1.9459
8	10	0.0273	2.7397	0.9945	0.0054	-5.2067	1.6499	2.0794
9	1	0.0027	0.2739	0.9972	0.0027	-5.8998	1.7749	2.1972
10	1	0.0027	0.2739	1	0			

2016

bin	NO V	frq	frq %	f(V)	1-f(V)	Ln(1-f(V))	Ln(-Ln(1-f(V)))	Ln(V)
0	0	0	0	0	1	0		
1	1	0.0027	0.2732	0.0027	0.9972	-0.0027	-5.9012	0
2	31	0.0846	8.4699	0.0874	0.9125	-0.0914	-2.3915	0.6931
3	100	0.2732	27.3224	0.3606	0.6393	-0.4473	-0.8044	1.0986
4	98	0.2677	26.7759	0.6284	0.3715	-0.9899	-0.0100	1.3862
5	66	0.1803	18.0327	0.8087	0.1912	-1.6541	0.5032	1.6094
6	45	0.1229	12.2950	0.9316	0.0683	-2.6837	0.9872	1.7917
7	14	0.0382	3.8251	0.9699	0.0300	-3.5047	1.2541	1.9459
8	7	0.0191	1.9125	0.9890	0.0109	-4.5163	1.5077	2.0794
9	3	0.0081	0.8196	0.9972	0.0027	-5.9026	1.7753	2.1972
10	1	0.0027	0.2732	1	0			

2017

bin	NO V	frq	frq %	f(V)	1-f(V)	Ln(1-f(V))	Ln(-Ln(1-f(V)))	Ln(V)
0	0	0	0	0	1	0		
1	2	0.0059	0.5952	0.0059	0.9940	-0.0059	-5.1209	0
2	32	0.0952	9.5238	0.1011	0.8988	-0.1066	-2.2378	0.6931
3	77	0.2291	22.9166	0.3303	0.6696	-0.4010	-0.9137	1.0986
4	82	0.2440	24.4047	0.5744	0.4255	-0.8542	-0.1575	1.3862
5	70	0.2083	20.8333	0.7827	0.2172	-1.5266	0.4230	1.6094
6	43	0.1279	12.7976	0.9107	0.0892	-2.4159	0.8820	1.7917
7	19	0.0565	5.6547	0.9672	0.0327	-3.4192	1.2294	1.9459
8	8	0.0238	2.3809	0.9910	0.0089	-4.7184	1.5514	2.0794
9	3	0.0089	0.8928	1	0			

2018

bin	NO V	frq	frq %	f(V)	1-f(V)	Ln(1-f(V))	Ln(-Ln(1-f(V)))	Ln(V)
0	0	0	0	0	1	0	#NOMBRE!	
1	1	0.0027	0.2747	0.0027	0.9972	-0.0027	-5.895	0
2	50	0.1373	13.7362	0.1401	0.8598	-0.1509	-1.8908	0.6931
3	72	0.1978	19.7802	0.3379	0.6620	-0.4123	-0.8858	1.0986
4	118	0.3241	32.4175	0.6620	0.3379	-1.0849	0.0815	1.3862
5	62	0.1703	17.0329	0.8324	0.1675	-1.7862	0.5801	1.6094
6	34	0.0934	9.3406	0.9258	0.0741	-2.6013	0.9560	1.7917
7	15	0.0412	4.1208	0.9670	0.0329	-3.4122	1.2273	1.9459
8	7	0.0192	1.9230	0.9862	0.0137	-4.2877	1.4557	2.0794
9	4	0.0109	1.0989	0.9972	0.0027	-5.8971	1.7744	2.1972
10	1	0.0027	0.2747	1	0			

2019

bin	NO V	frq	frq %	f(V)	1-f(V)	Ln(1-f(V))	Ln(-Ln(1-f(V)))	Ln(V)
0	0	0	0	0	1	0		
1	3	0.0084	0.8474	0.0084	0.9915	-0.0085	-4.7664	0
2	37	0.1045	10.4519	0.1129	0.8870	-0.1199	-2.1210	0.6931
3	95	0.2683	26.8361	0.3813	0.6186	-0.4802	-0.7335	1.0986
4	87	0.2457	24.5762	0.6271	0.3728	-0.9864	-0.0135	1.3862
5	72	0.2033	20.3389	0.8305	0.1694	-1.7749	0.5737	1.6094
6	37	0.1045	10.4519	0.9350	0.0649	-2.7338	1.0056	1.7917
7	16	0.0451	4.5197	0.9802	0.0197	-3.9233	1.3669	1.9459
8	5	0.0141	1.4124	0.9943	0.0056	-5.1761	1.6440	2.0794
10	1	0.0028	0.2824	0.9971	0.0028	-5.8692	1.7697	2.3025
13	1	0.0028	0.2824	1	0			

2020

bin	NO V	frq	frq %	f(V)	1-f(V)	Ln(1-f(V))	Ln(-Ln(1-f(V)))	Ln(V)
0	0	0	0	0	1	0		
1	4	0.0113	1.1363	0.0113	0.9886	-0.011	-4.4716	0
2	41	0.1164	11.647	0.1278	0.8721	-0.1367	-1.9893	0.6931
3	95	0.2698	26.988	0.3977	0.6022	-0.5070	-0.6791	1.0986
4	86	0.2443	24.431	0.6420	0.3579	-1.0273	0.0269	1.3862
5	72	0.2045	20.454	0.8465	0.1534	-1.8746	0.6284	1.6094
6	39	0.1107	11.079	0.9573	0.0426	-3.1555	1.1491	1.7917
7	13	0.0369	3.6931	0.9943	0.0056	-5.1704	1.6429	1.9459
8	1	0.0028	0.2840	0.9971	0.0028	-5.8636	1.7687	2.0794
9	1	0.0028	0.2840	1	0			

2021

bin	NO V	frq	frq %	f(V)	1-f(V)	Ln(1-f(V))	Ln(-Ln(1-f(V)))	Ln(V)
0	0	0	0	0	1	0		
1	1	0.0027	0.2777	0.0027	0.9972	-0.0027	-5.8847	0
2	29	0.0805	8.0555	0.0833	0.9166	-0.0870	-2.4417	0.6931
3	86	0.2388	23.8888	0.3222	0.6777	-0.3889	-0.9443	1.0986
4	104	0.2888	28.8888	0.6111	0.3888	-0.9444	-0.0571	1.3862
5	75	0.2083	20.8333	0.8194	0.1805	-1.7117	0.5374	1.6094
6	46	0.1277	12.7777	0.9472	0.0527	-2.9416	1.0789	1.7917
7	13	0.0361	3.6111	0.9833	0.0166	-4.0943	1.4096	1.9459
8	4	0.0111	1.1111	0.9944	0.0055	-5.1929	1.6473	2.0794
9	1	0.0027	0.2777	0.9972	0.0027	-5.8861	1.7725	2.1972
10	1	0.0027	0.2777	1	0			

2012/2021

bin	NO V	frq	frq %	f(V)	1-f(V)	Ln(1-f(V))	Ln(-Ln(1-f(V)))	Ln(V)
0	0	0	0	0	1	0		
1	16	0.0044	0.4471	0.0044	0.9955	-0.0044	-5.4077	0
2	361	0.1008	10.0894	0.1053	0.8946	-0.1113	-2.1951	0.6931
3	915	0.2557	25.5729	0.3610	0.6389	-0.4480	-0.8029	1.0986
4	950	0.2655	26.5511	0.6266	0.3733	-0.9851	-0.0149	1.3862
5	695	0.1942	19.4242	0.8208	0.1791	-1.7195	0.5420	1.6094
6	405	0.1131	11.3191	0.9340	0.0659	-2.7187	1.0001	1.7917
7	156	0.0435	4.3599	0.9776	0.0223	-3.8005	1.3351	1.9459
8	56	0.0156	1.5651	0.9932	0.0067	-5.0045	1.6103	2.0794
9	17	0.0047	0.4751	0.9980	0.0019	-6.2366	1.8304	2.1972
10	6	0.0016	0.1676	0.9997	0.0002	-8.1825	2.1020	2.3025
13	1	0.0002	0.0279	1	0			

Let:

$$X_i = \text{Ln}(V_i)$$

$$Y_i = \text{Ln} \left[\text{Ln} \left(\frac{1}{1 - F(V)} \right) \right]$$

Or

$$Y = a + bX$$

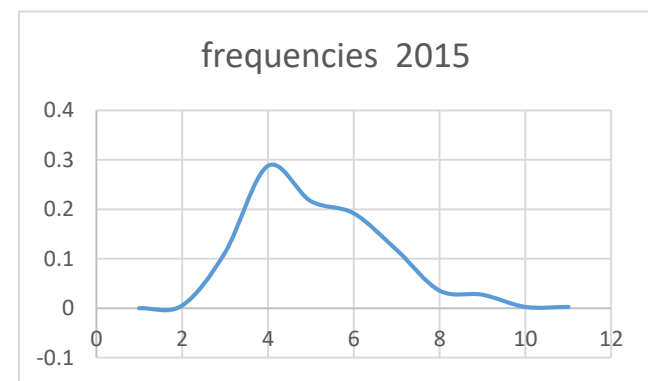
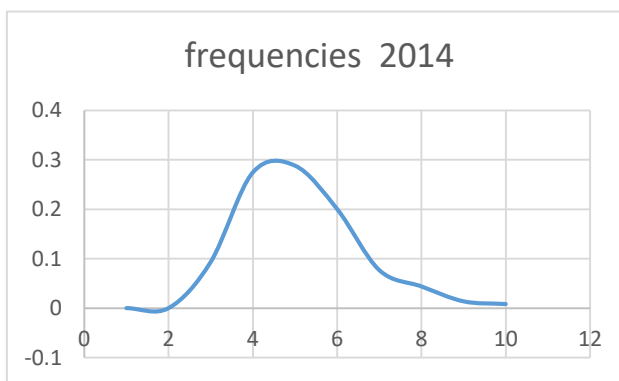
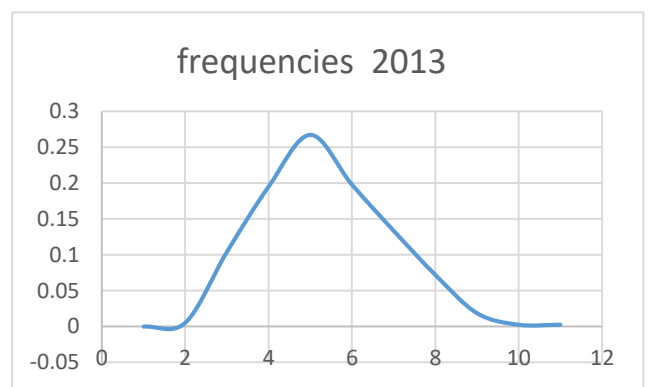
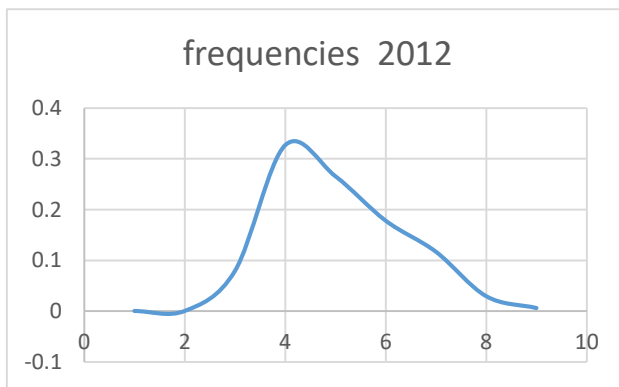
"Thus, the Weibull parameters are obtained as follows: $k = b$,

and the scale parameters are $C = e^{-\frac{a}{b}}$

"Table 2.3: Variation of Weibull parameters C and k."

year	a (intercept)	K = b	C = e ^(-a/b)
2012	-4.460433665	3.189837421	4.048418589
2013	-3.93969883	2.669461577	4.374710062
2014	-3.971759554	2.766928604	4.201492587
2015	-3.601320703	2.516087022	4.184210445
2016	-3.93002597	2.676325021	4.342460908
2017	-3.979983498	2.700410323	4.365985688
2018	-3.46407575	2.422407117	4.178757105
2019	-3.560719344	2.477519646	4.208942153
2020	-3.798386618	2.747533769	3.984737002
2021	-4.133033106	2.81733558	4.336209776
2012/2021	-3.756547422	2.596324755	4.249796779

A) Daily variation of the Weibull distribution for each year:



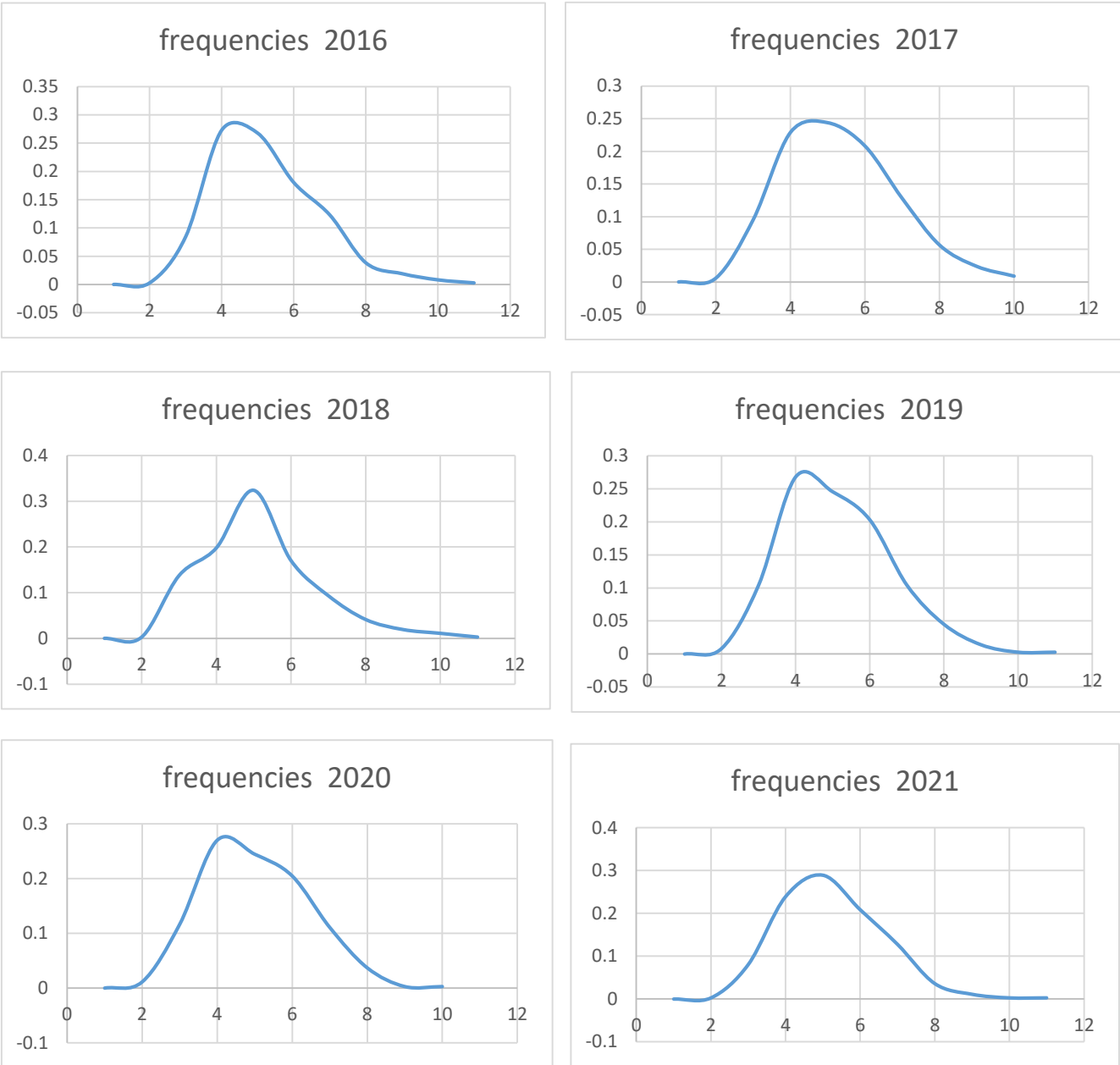


Figure 2.14: Daily variation of the Weibull distribution for each year.

The figures above clearly show that as the shape parameter k increases, the distribution becomes narrower, with winds centered around a specific value (a special interval). Conversely, when k is low, the winds are distributed over a very wide range. The scale factor C has a significant impact as well, with high values indicating strong winds and low values indicating weak winds in the area or at that time.

All of these trends are illustrated in the figures

B) Daily variation of the Weibull distribution for 10 y ears (2012/2021):

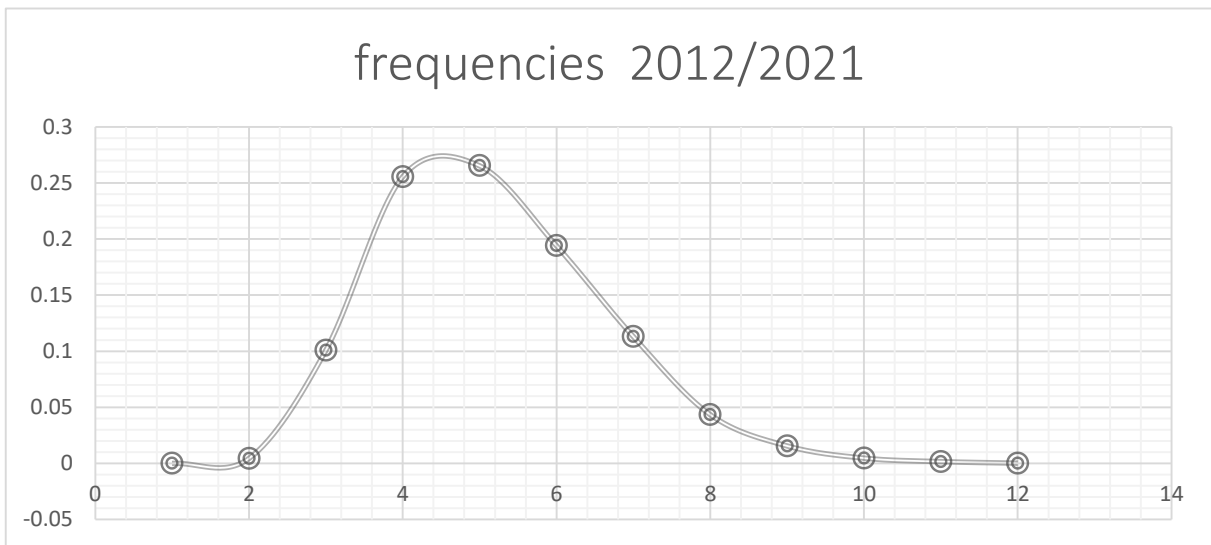


Figure 2.15: Daily variation of the Weibull distribution for 10 years (2012/2021)

2.4.2. Wind parameter:

Among the laws presented in the second chapter and Table 2.4, we have calculated the wind parameters, which are listed in the following table:

Table 2.4: Wind parameters in Ouargla.

Ouargla station				
year	V	V^3	σ	σ^2
2012	3.5868	87.5850	1.8752	3.5172
2013	3.8759	110.5151	2.0263	4.1070
2014	3.72252	97.9004	1.9461	3.7882
2015	3.70721	96.6973	1.9381	3.7571
2016	3.84742	108.0890	2.0114	4.0467
2017	3.8682	109.8552	2.0223	4.0906
2018	3.7023	96.3197	1.9356	3.74734
2019	3.7291	98.4221	1.94958	3.8016
2020	3.5304	83.5166	1.8457	3.4074
2021	3.8418	107.6229	2.0085	4.0350
2012/2021	3.7653	101.3160	1.9685	3.8758

2.5. Wind energy potential

2.5.1. Wind power modeling:

In wind turbines, it is necessary to convert the dynamic energy of the wind into a rotational energy of the blades. This is achieved by pushing the wind onto the blades, which results in energy losses due to the Betz limit, machine thresholds, and conversion losses [1].

The figure presented below shows the available power versus the useful power, along with the losses encountered.

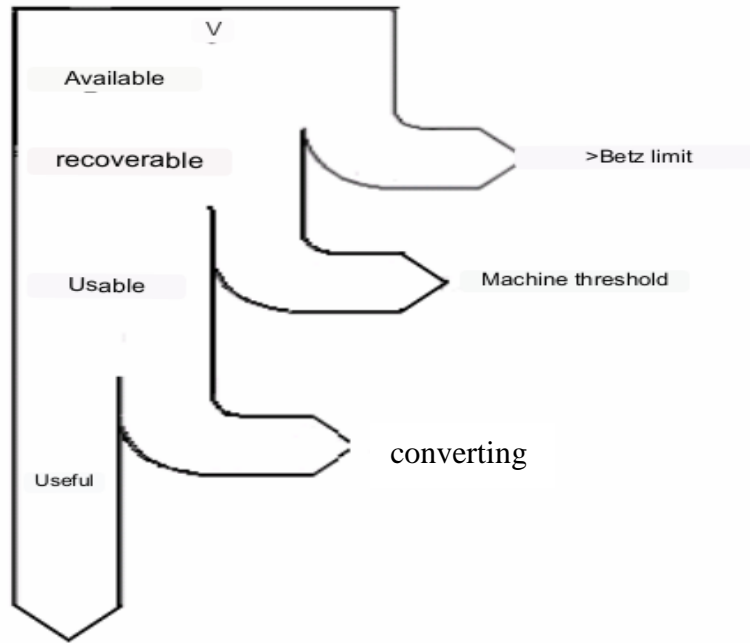


Figure 2.16: Schematic representation of the successive degradations of wind energy before use. [29]

2.5.2. Mean incident theoretical wind power

This is what we are looking for, the available energy power. We calculate the mean kinetic energy at Ouargla, during a unit of time and unit of surface, based on the wind speed according to the following law (58):

$$P = \frac{1}{2} \rho \bar{V}^3$$

A savoir que $\rho = 1.25 \text{ m}^3\text{kg}$

Anne	2012	2013	2014	2015	2016	2017	2018	2019	2020	2021	2012/2021
$P_{\text{thé}}$	54.74	69.07	61.18	60.43	67.55	68.65	60.19	61.513	52.19	67.26	63.32

These results have been converted into graphs which are shown in Figure (2.18), and in Histogram (2.19).

Table 2.4: theoretical wind power for 10 years

year	$P_{thé}$
2012	54.74
2013	69.07
2014	61.18
2015	60.43
2016	67.55
2017	68.65
2018	60.19
2019	61.51
2020	52.19
2021	67.26
2012/2021	63.32

The mean theoretical power of a 10-year wind is estimated at 63.3225 W.

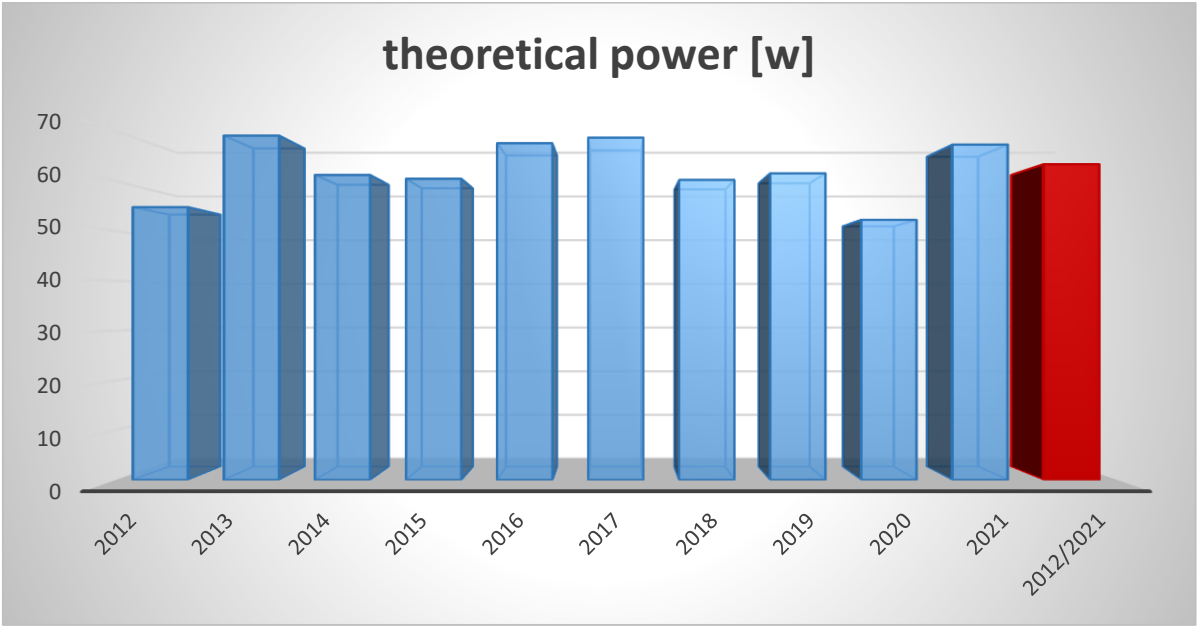


Figure 2.17: Histogram of mean incident theoretical wind power for each year and for 10 years. In the histogram of the theoretical average power, we notice that each year the power differs from another, as it reached its lowest value in 2012 estimated at 54.74 W.

2.5.3. Theoretical maximum recoverable power (Betz limit):

The figure below gives us an idea about the Betz theorem that we discussed in the 2nd chapter:

Figure 2.20: Representation of the current tube

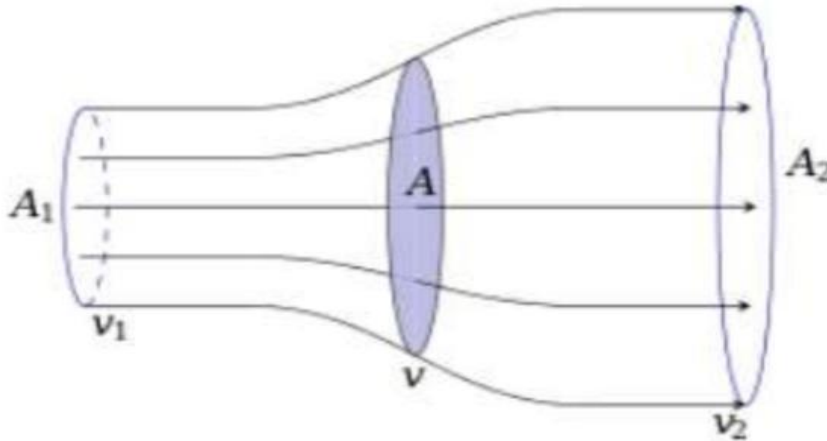


Figure 2.18: Representation of the current tube

A) The power absorbed by the rotor per unit of surface:

Here, the surface A is assumed to be equal to 1 m^2 , while the relationship will be:

$$P_{abs} = V_1^2(V_0 - V_2)$$

Table 2.5: The result of the values of V_1 , V_2 , V_0 , and Power absorbed .

Anne	V_0	V_1	V_2	Pabs
2012	3.5864	2.3673	1.1836	16.83565
2013	3.8759	2.5581	1.2790	21.2432
2014	3.72252	2.4568	1.2284	18.8184
2015	3.70721	2.4467	1.22337	18.5872
2016	3.84742	2.5392	1.2696	20.7769
2017	3.8682	2.5530	1.2765	21.1164
2018	3.7023	2.4435	1.2217	18.51463
2019	3.72912	2.4612	1.23061	18.91876
2020	3.53047	2.3301	1.1650	16.05361
2021	3.84188	2.5356	1.26782	20.68734
2012/2021	3.76531	2.4851	1.24255	19.4750

These results were converted into graphical curves, which are shown in Figure (2.21), and a Histogram (2.22).

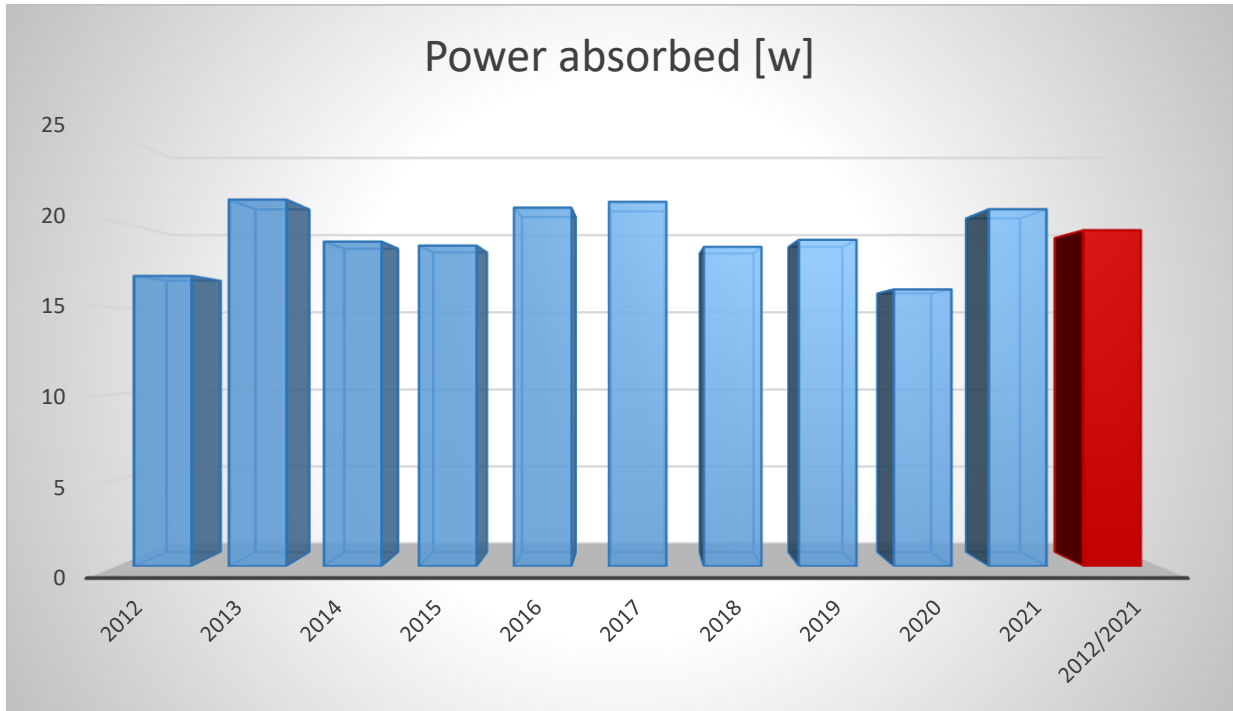


Figure 2.19: Histogram of power absorbed by the rotor for each year and at 10 years.

Histogram shows that the value of absorbed power for a period of 10 years with some years is not lower than other years, it reached an estimated value of 19.475 W.

B) Average maximum recoverable power:

The average power during a unit of time and in surface area A, depends on the velocities V_0 , V_1 , V_2 , and can be found with Betz's theorem using the following formula:

$$P = \frac{1}{2} \rho A V_1 (V_0^2 - V_2^2)$$

$$P_{max} = \frac{16}{27} P_{the}$$

Table 2.6: $P_{thé}$ and $P_{thé}$ results

<i>year</i>	<i>P_{thé}</i>	<i>P_{max}</i>
2012	54.74	32.29
2013	69.07	40.75
2014	61.18	36.10
2015	60.43	35.65
2016	67.55	39.85
2017	68.65	40.50
2018	60.19	35.51
2019	61.51	36.29
2020	52.19	30.79
2021	67.26	39.68
2012/2021	63.32	37.36

And we explain the results on this graph for the years:

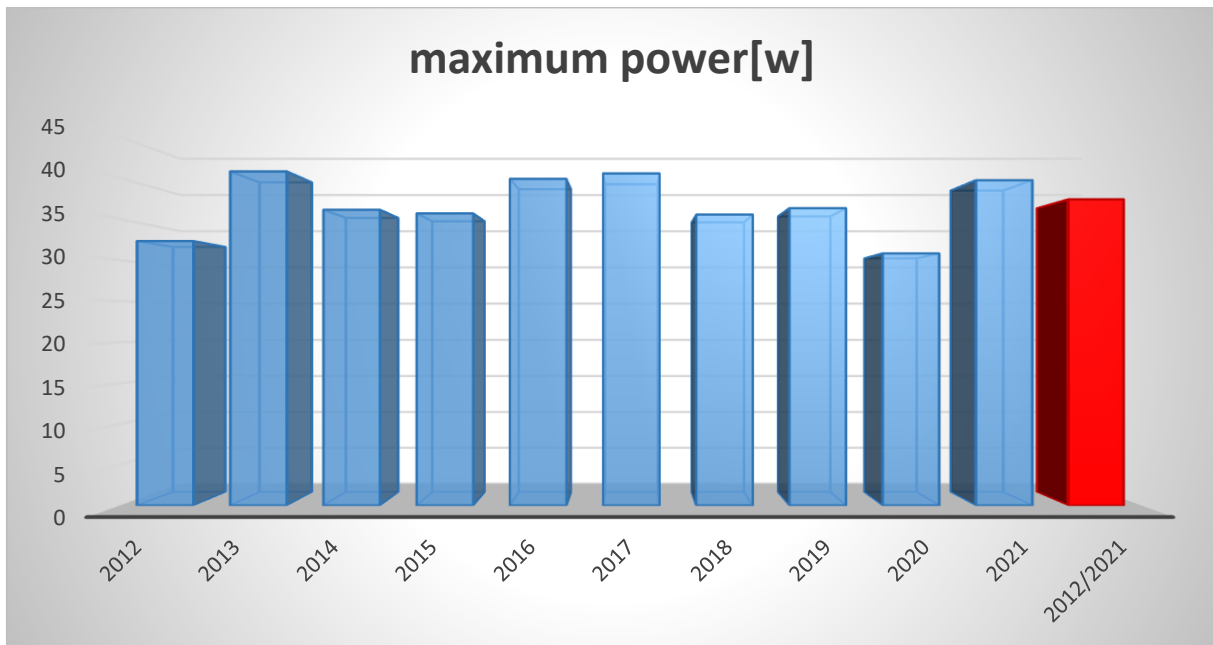


Figure 2.20: Histogram of Maximum Recoverable Wind Power Average for Each Year and Over 10 Years.

Histogram shows more of the maximum power value and theoretical power over 10 years, as it is noted that the theoretical value was higher than the maximum value.

C)Average recoverable energy over one year:

The average power recoverable per unit surface area A equal to 1 m² is given by:

$$Pr = 0.37 \bar{V}_3$$

However, the average recoverable energy density, symbolized by \bar{E} , expressed as the relation over one year is equal to:

$$\bar{E} = Pr \Delta t = 0.37 \times 24 \times 365 \times \bar{V}^3 \text{ [KWh]}$$

Table 2.7: Average cubic hour of wind,Average recoverable capacity,recoverable energy

Anne	\bar{V}^3	P_r	E
2012	87.585	32.40	283880.78
2013	110.515	40.89	358201.65
2014	97.9	36.22	317314.97
2015	96.697	35.77	313415.39
2016	108.089	39.99	350338.21
2017	109.855	40.64	356062.86
2018	96.319	35.63	312191.55
2019	98.422	36.41	319005.83
2020	83.516	30.90	270694.07
2021	107.622	39.82	348827.41
2012/2021	101.316	37.48	328385.71

Translate the obtained results in the two following forms:

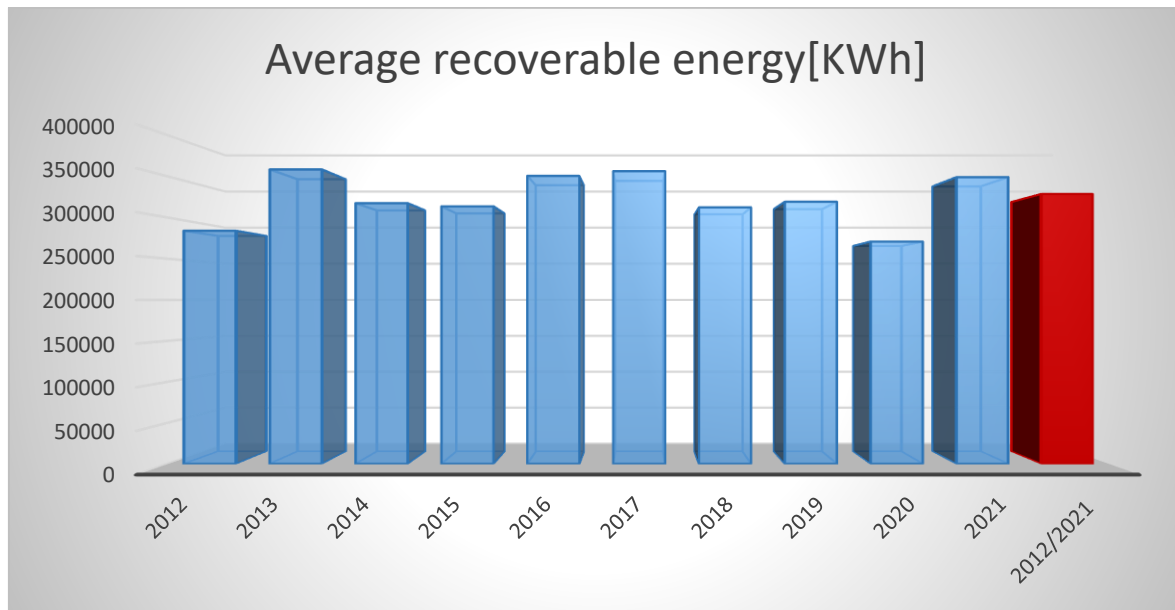


Figure 2.21: Histogram of Average Recoverable Energy per Year over 10 Years

The histogram displays the average recoverable energy for each year over a 10-year period, with some reaching 328385.71 W.

2.5.4. Useful Power of a Wind Turbine:

For each wind turbine unit, the factory provides us with three technical parameters of speed required for it to operate, which are:

The start-up speed V_D : this is the speed at which the wind turbine begins to produce energy. Below this threshold, the wind turbine produces no energy.

The nominal speed V_n : this is the speed at which the wind turbine reaches its maximum energy production threshold. This threshold remains constant until the cut-off speed.

The cut-off speed V_C : this is the speed at which the wind turbine stops producing energy due to automatic blade stop for safety. Speeds beyond V_C have no effect on the energy calculation.

$$P_n = \frac{1}{2} \rho A V_n^3 \quad V_n = \begin{cases} 0.67 \bar{V} \\ 0.79 \bar{V} \end{cases}$$

Using this data, we can create a table that shows the nominal speeds at the station, as well as the efficiency [0.3 to 0.5] for each year. With this information, we can calculate the average useful wind power: $P_u = 1/2 \rho V_n^3$

Table 2.8: Nominal speed and useful power as a function of machine efficiency [0.3 to 0.5] for each year.

year	V	V _n	P _u
2012	3.58689887	[2.4032 - 2.8336]	[8.67484697 - 14.2206251]
2013	3.875993115	[2.5969 - 3.0620]	[10.9459489 - 17.943629]
2014	3.722522432	[2.4940 - 2.9407]	[9.69653113 - 15.8954659]
2015	3.707210454	[2.4838 - 2.9286]	[9.57736742 - 15.7001215]
2016	3.847420364	[2.5777 - 3.0394]	[10.7056575 - 17.5497207]
2017	3.86826332	[2.5917 - 3.0559]	[10.8805917 - 17.8364894]
2018	3.702378795	[2.4805 - 2.9248]	[9.53996926 - 15.638815]
2019	3.729122748	[2.4985 - 2.9460]	[9.7482007 - 15.9801675]
2020	3.530476984	[2.3654 - 2.7890]	[8.27188674 - 13.5600548]
2021	3.841881862	[2.5740 - 3.0350]	[10.6594904 - 17.4740394]
2012/2021	3.76531995	[2.5227 - 2.9746]	[10.0348314 - 16.4500395]

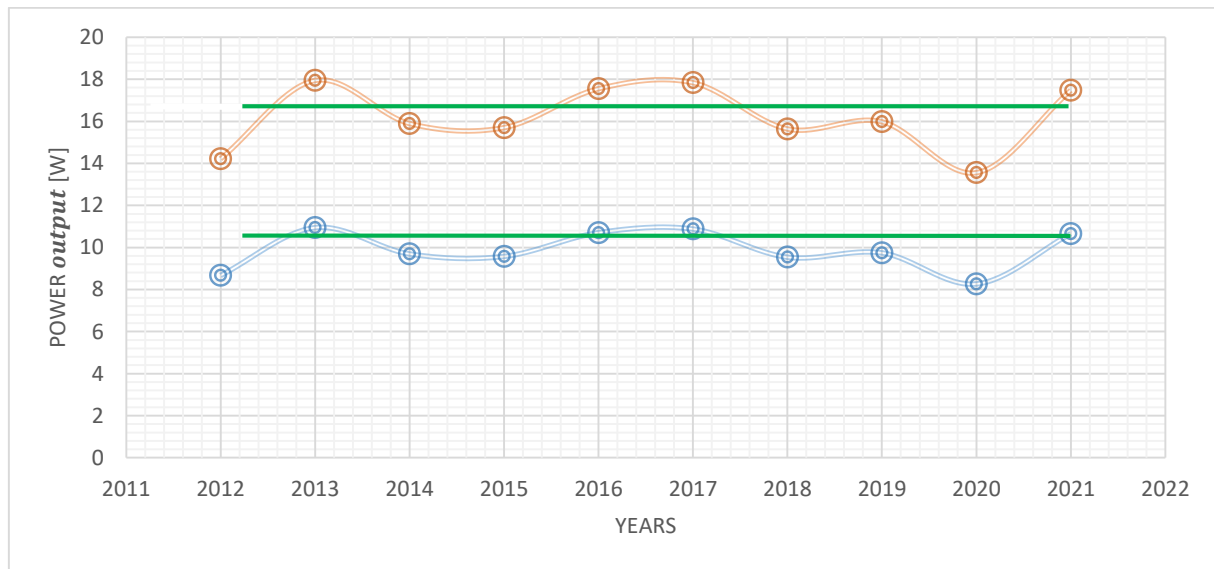


Figure 2.22: Variation in useful power.

The difference between the two values of useful power is as follows: the first value ranges from 8.27 W to 10.94 W, while the second value is limited to 13.56 W to 17.94 W.

The average value of useful power is 10.03 W when the machine efficiency is 0.3, and 16.45W when the machine efficiency is 0.5.

Conclusion

This section presents a numerical analysis of windmills for the Ouargla region, which includes the calculation of the mean useful force and its range. This information can be used to select suitable wind turbines and achieve high yields from cultivated fields. The section also determines the expected nominal speed for the region, which can assist in negotiating with factories. The use of scientific and technical analysis is highlighted as a valuable tool for making informed decisions and achieving desired outcomes.

Chapter III:

Estimation of wind energy potential and
vertical extrapolation of the Weibull
parameter

3.1 introduction:

In this chapter, we will study the possibility of the winds in each zone, the dynamic energy power of the winds with transformation of dynamic energy of the winds to a rotary dynamic energy of wind turbine; it finds a range of losses in the latter. Also we try to choose and specify the wind turbine specific to each zone, with a test of calculation the maximum useful power, even of a form.

3.2.The geographical location of the selected places



Figure 3.1: picture showing the study areas in the state of Ouargla [24]

In this study, we selected four areas in the desert of Ouargla with different heights ranging between 48 and 173 meters above the height of the meteorological station that measured the wind speed. These areas are located in places that are far from each other and have different ground characteristics.

Area coordinates and altitudes:

Zoon1: 32°00'26"N5°16'00"E height 72m

Zoon2: 31°56'04"N4°35'31"E height 114m

Zoon3: 31°48'48"N5°16'02"E height 48m

Zoon4: 31°52'35"N4°17'18"E height 173m

3.2.1. WIND ENERGY POTENTIAL: Modeling the power of the wind:

In the wind turbine we are forced to transform the dynamic energy of the winds to another rotating dynamic energy of the wings all this by the method of pushing the wind to the wings, and after this transformation of energy, we have too many losses (Betz limit, Machine thresholds and conversion losses). [1]

Moreover, that what we see in **figures (3-1)** which shows the power available at a useful power, with presentation of the losses found.

3.2.1.1 Theoretical mean incident wind power:

This is what the energy power available to us looks for; we calculate the average kinetic energy at each special site, during a unit of time and unit of surface, at the expense of the speed, which is at home with the following law (58):

$$P_{the} = \frac{1}{2} \rho V^3$$

The speed used in this law is the speed that we extracted from WIEBULL's law, also the cubic mean of this speed. Namely that $\rho = 1.25 \text{ m}^3/\text{kg}$.

These results have the converted to the curves shown which represents in the figure (3.2) is

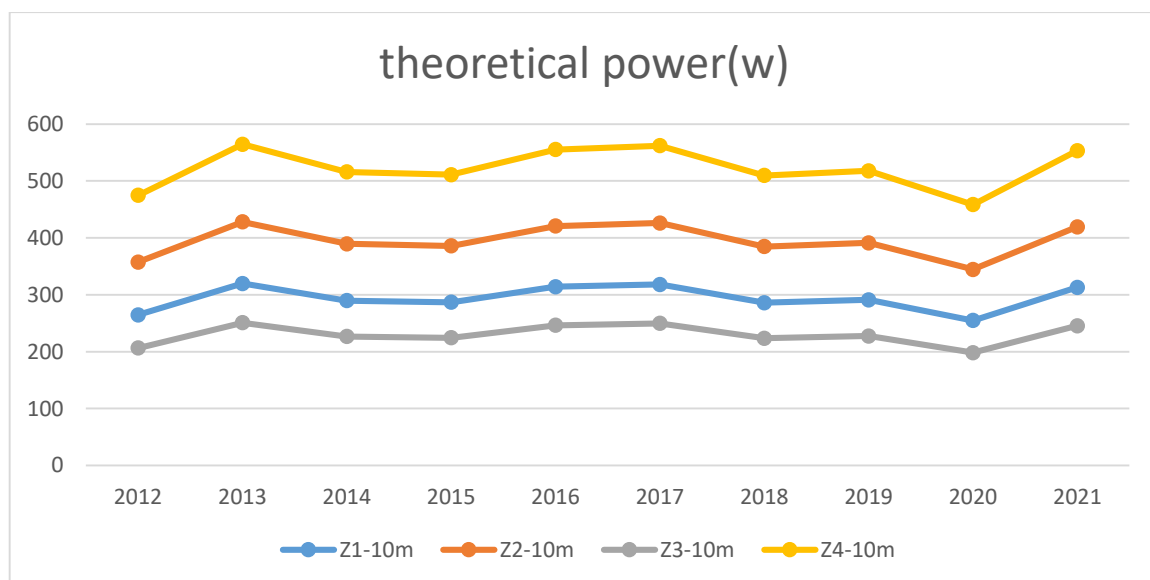


Figure 3.3: theoretical mean incident wind power for each station [2012 to 2021]

What is remarkable here is that the average theoretical (available) power at zoon4 is greater than that of the other zones. It is about 290 watts higher than the nearest zoon, which is zoon2, over the period from 2012 to 2021. Then comes zone01, then zoon3 with a power between

(254.61W-319.68W) watts and (198.18W-564.39W) watts respectively, over the period 2012-2021

The following histogram is a general explanation of the average energy power available at 10 years

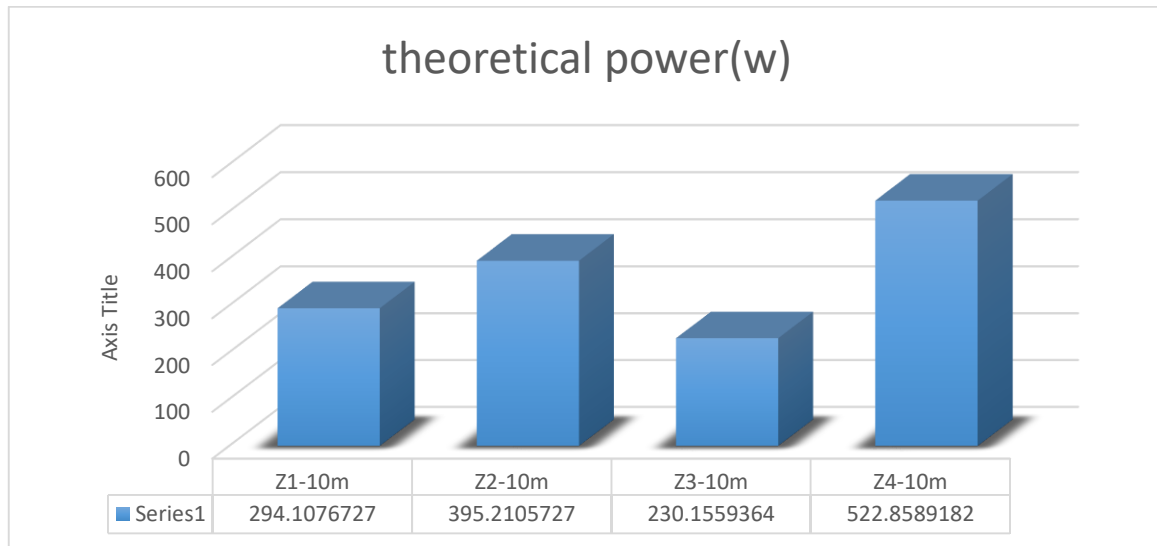


Figure 3.4: The histogram of average energy power available at 10 years.

What is remarkable here is that the average theoretical (available) power at zoon4 is greater than that of the other zones. It is about 290 watts higher than the nearest zone, which is zoon2, over the period from 2012 to 2021. Then comes zoon1, then zoon3 with a power between (254.61-319.68) watts and (198.18-564.39) watts respectively, over the period 2012-2021

3.2.2 The theoretical maximum recoverable power (Betz limit):

The figurative form below gives us an idea of (Betz's theorem) which we have already explained in the 2nd chapter.

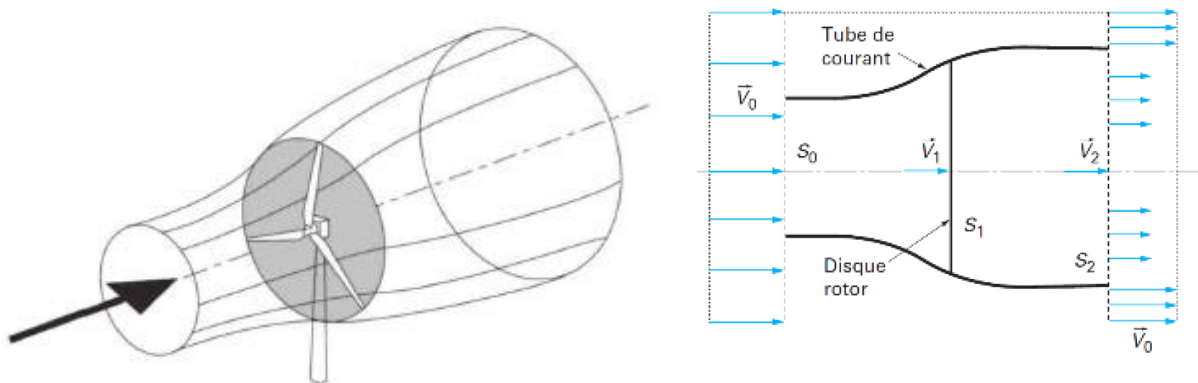


Figure 3.5: Representation of the current tube.[30]

V_0 : the wind speed upstream of the rotor (initial)
 V_1 : the wind speed in the plane of the rotor
 V_2 : wind speed downstream of the rotor
 S_0 : the upstream surface (at the entrance of the current tube)
 S_1 : the surface of the rotor
 S_2 : the surface downstream of the rotor
 Or: $V_0 > V_1 > V_2$

It means:
$$V_2 = \frac{V_0}{3} \quad \text{with} \quad V_1 = V_0 + \frac{V_2}{2}$$

$$\begin{cases} 0.66 V_0 \\ 0.33 V_0 \end{cases}$$

A) The power absorbed by the rotor per unit area:

Here the surface A is assumed equal to 1 [m²], while the relation will be:

$$P_{abs} = \rho V_1^2 (V_0 - V_2)$$

I report these results on the curves below, these curves represent the power absorbed by the rotor per unit area for all the stations concerning all the years over a period of 10 years, and that between 201 to 2021 and that is the result of these curves:

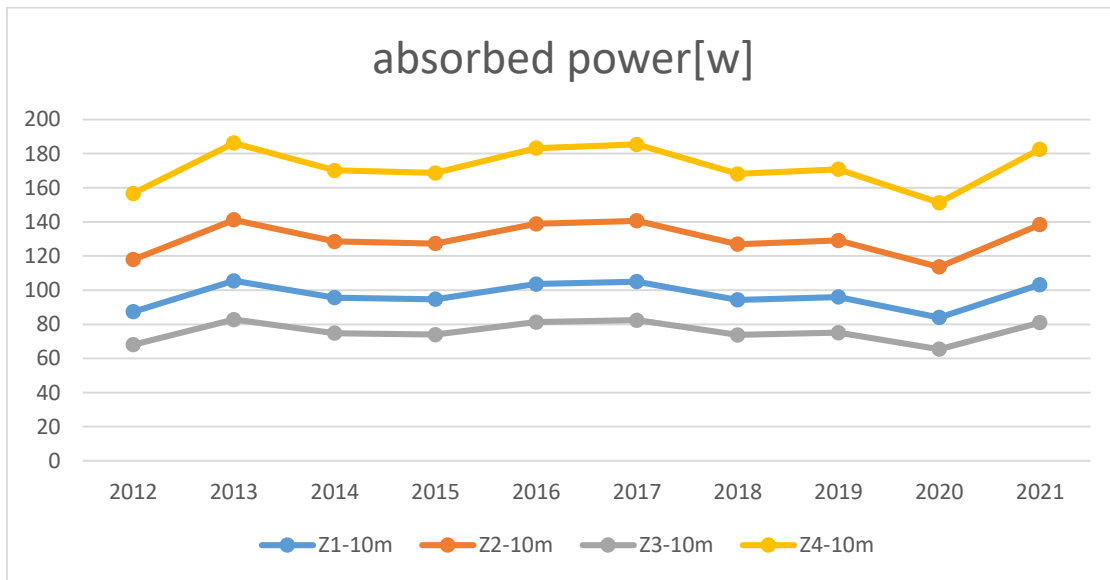


Figure 3.6: power absorbed by the rotor per unit area for all stations [2012 to 2021].

As the present case shows, the observation is almost identical in terms of available energy capacity. Zoon4 regularly exceeds an annual capacity of 150 watts, and in some cases even reaches 170 watts. For instance, in 2013 the power was 186.25 watts, then it was 183.20 watts in 2016 and 182.6269 watts in 2021. Then comes zoon2, where its maximum capacity was

141.25 watts in 2013, and its minimum capacity was 113.63 watts. Then there is zoon1, which registered its highest capacity in 2013 with 105.49 watts, and its minimum capacity was 84.022W in 2020. Finally, zoon3 had a maximum capacity of 82.80 watts in 2013 and a minimum capacity of 65.40 watts in 2020.

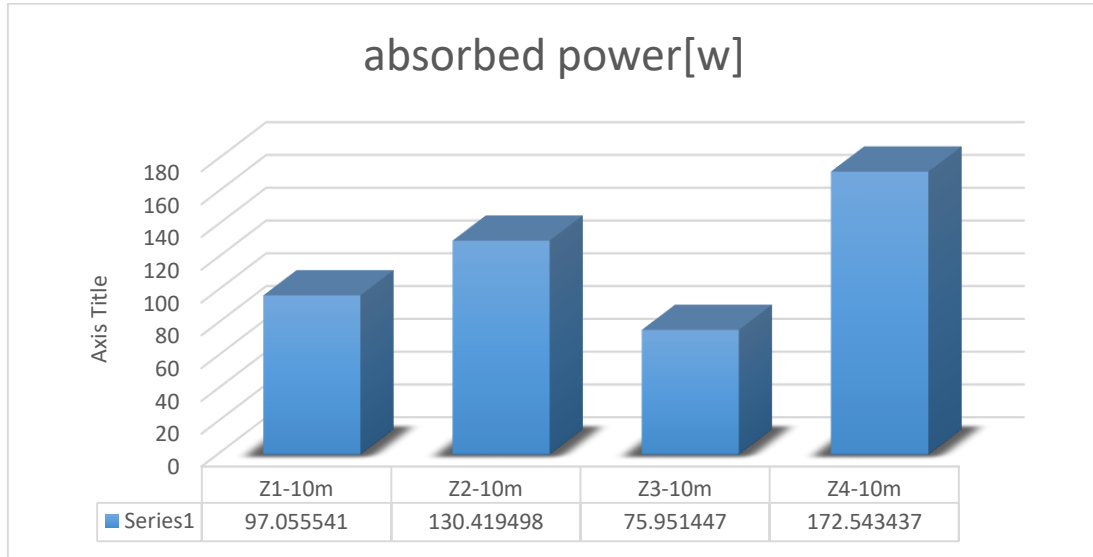


Figure 3.7: The histogram of the power absorbed by the rotor per unit area (mean) a10 years.

In this figure, the general explanation of all stations over a period of 10 years is presented it is the power absorbed by the rotor per unit area.

The average power output for zoon4 is 172.54 watts. In zoon 2, the average power exceeds 130 watts, followed by zoon1 and zoon3 with an estimated average power of 97.05 watts and 75.95 watts respectively.

B) Average maximum recoverable power:

The average power during a unit time and in the surface A, depending on the speeds V_0 , V_1 , V_2 on (Betz's theorem) finds with us with the following law

$$P = \frac{1}{2} \rho A V_1 (V_0^2 - V_2^2)$$

While $V = V_0 + \frac{V_2}{2}$ while the relation stern:

$$P = \frac{1}{2} \rho A (V_0^2 - V_2^2) (V_0 + \frac{V_2}{2})$$

And $V_2 = V_0 + \frac{V_0}{3}$ while we get on the maximum average power relation

Recoverable following:

$$P_{max} = \frac{1}{2} \rho A (V_0^2 - \frac{V_0}{3})^2 (\frac{V_0}{2} + \frac{V_0}{6})$$

Here the surface A is assumed to be equal to 1m², and namely that p = 1.25 m³/kg, while the relation will be:

$$P_{Max} = P_{the} \frac{16}{27}$$

16/27 equals 0.59 is the Betz limit, and we explain the results in this curve for all stations:

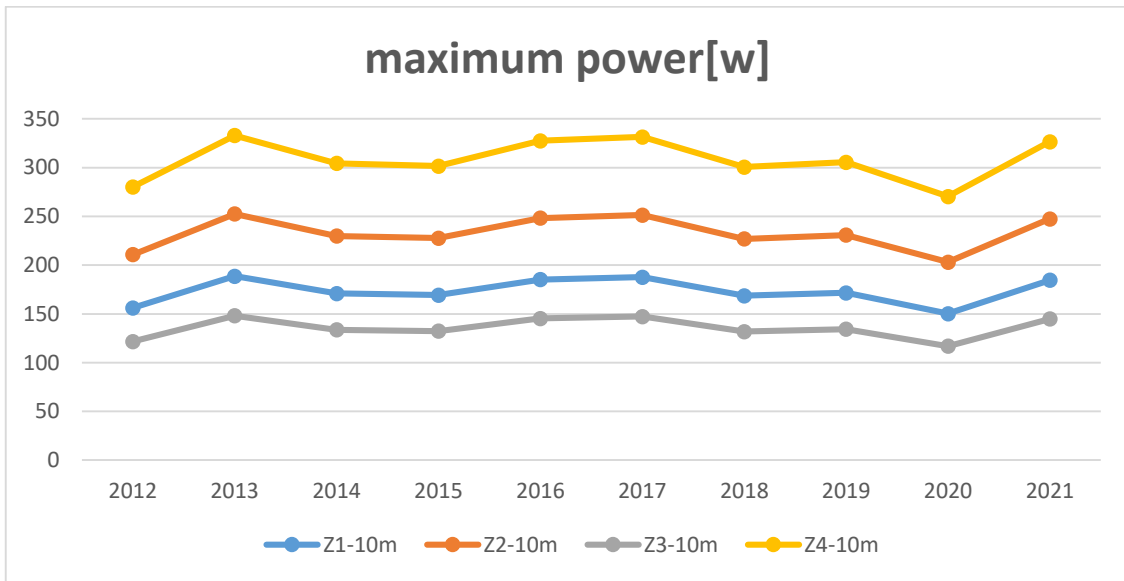


Figure 3.8: average maximum recoverable power for all stations [2012 to 2021]

What we notice here is that the average maximum recoverable power in zoon4 was between 270.43W and 332.99W. On the other hand, in zoon02, it has decreased to be between 1679.20 W and 252.55W. Then, the recoverable power in zoon1 continued to decrease, being between 188.61W and 150.22W. As for zoon3, it was less than 117W.

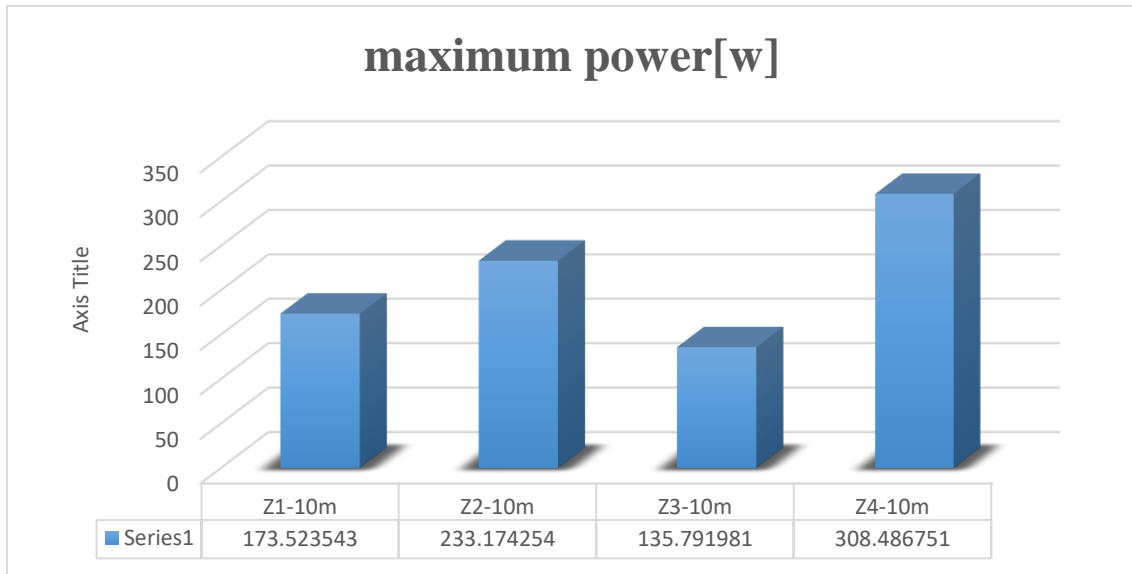


Figure 3.9: The histogram of the average maximum recoverable power at 10 years.

From the histogram, we see that Zoon 4 contained the 10-year average maximum recoverable power of 308.48 W, followed by Zone 2 with 233.17 W. In contrast, Zoon1 recorded power of 173.52W, and finally zoon3 recorded a power of 135.79 W

C) The average recoverable energy over a year:

The average recoverable power per unit area A equal to m² is given:

$$Pr=0.37.9V^3$$

On the other hand, the average recoverable energy density, which symbolized its E, write the relation in one year, is equal to [3]:

$$\bar{E}= P_r.d_t = 0,37.24 . 365. V^3 \text{ KWh.}$$

The results obtained, translate into the following two forms:

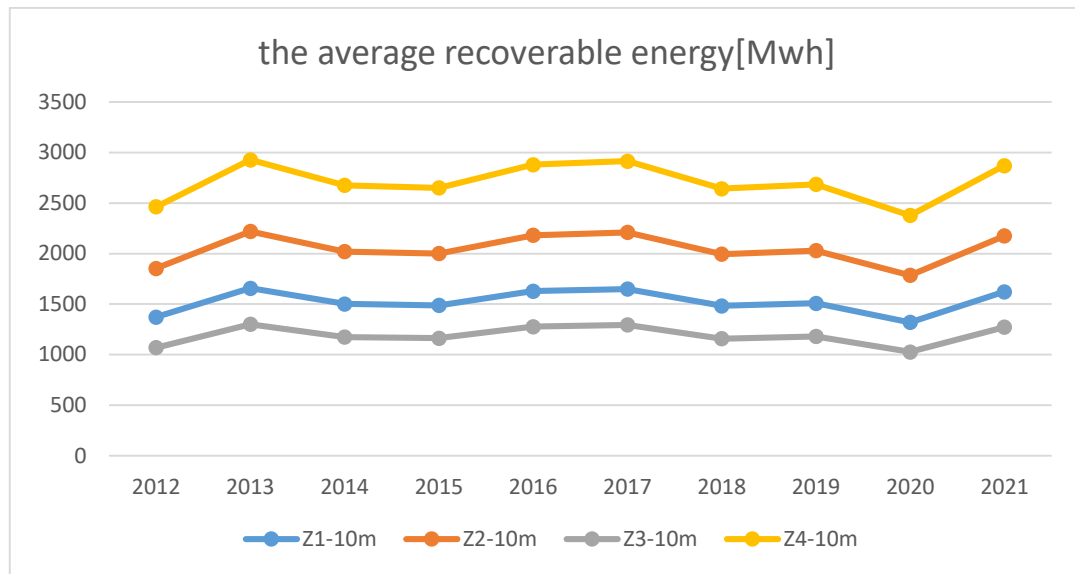


Figure 3.10: average recoverable energy over a year for all stations [2012 to 2021]

The first form, it is a curve, shows us the annual variation of this energy,

So in zoon4, there was energy exceeding **2300Mwh** in all years. In zoon2, it exceeded **1700Mwh** throughout all the years. Zoon1 recorded the highest value, estimated at **1657.86Mwh**. As for zoon3, it ranged between **102.78Mwh** and **1301.2Mwh**.

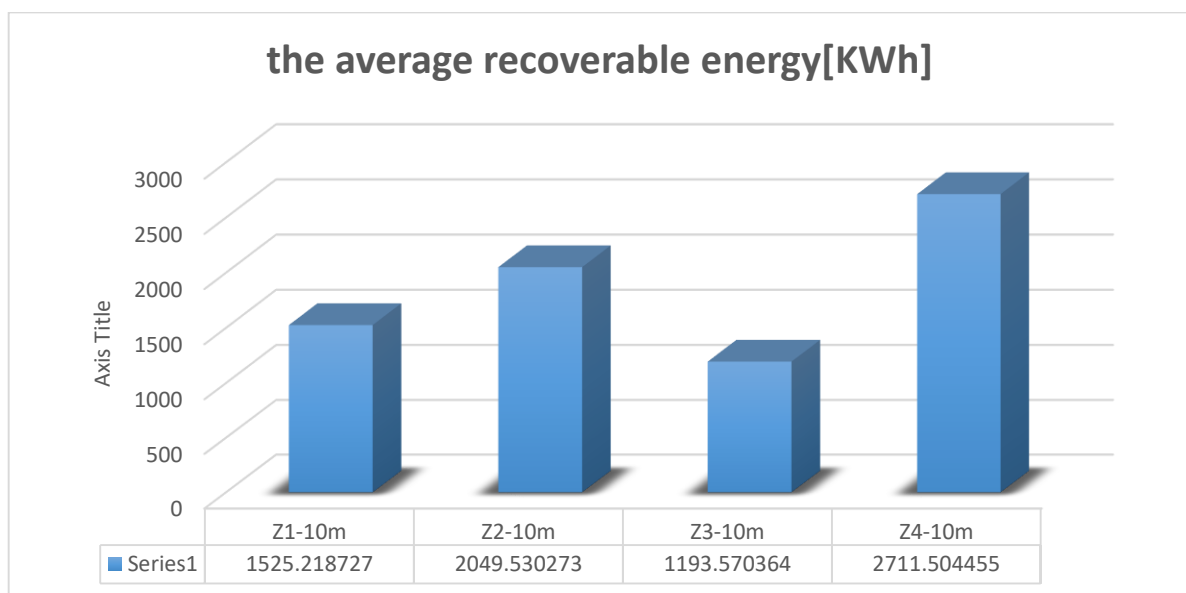


Figure 3.11: The average recoverable energy histogram over one year.

The second form is an average recoverable energy histogram over a year,

in terms of WIBULL's average speed for 10 years, this is an average recoverable energy over one year close to real ones.

As it is clear in the figure, in zoon 4, the recoverable energy was always the highest, reaching **2711.50Mwh**. The following is zoon, 2 with **2049.53Mwh**. In zoon 1, the recoverable energy was estimated at **1525.218Mwh**. On the other hand, zoon 3 recorded the lowest percentage, with **1193.57Mwh**

3.2.3 Useful Power by a wind turbine:

In each wind turbine unit, the factory gives us three technical parameters, this speed setting is required to operate and these speeds are:

- 1st speed of start of work V_D : it is a speed where the wind turbine starts to produce energy.
- 2nd nominal speed V_N : The wind turbines produce energy at this speed. Maximum.
- 3rd stop speed V_c : this is the speed at which the wind turbines stop producing energy.

As we were told that these speeds in reality it is the manufacturer who gives this, but in my studies for this project it is the search for an ideal area to plant a field of wind turbines, and to choose the special wind turbine for each zoon, and that speeds which is found, at least designates the device that we chose him.

Betz limit is 0.59, it is impossible for the yield to be more than 0.59 but as known or by experience before, the yield is between 0.3 to 0.5 [3].

And from this we find:

$$\eta = \frac{P_n}{P_{the}}$$

$$P_n = \frac{1}{2} \rho A V_n^3 \quad \text{and} \quad P_{the} = \frac{1}{2} \rho A \bar{V}^3$$

In

$$\eta = \frac{\frac{1}{2} \rho A V_n^3}{\frac{1}{2} \rho A \bar{V}^3} \quad \Longrightarrow \quad \eta = \frac{V_n^3}{\bar{V}^3} \quad \Longrightarrow \quad V_n = \sqrt[3]{\eta \bar{V}}$$

$$V_n = \begin{cases} 0.67\bar{V} \\ \vdots \\ 0.79\bar{V} \end{cases}$$

With that gives us this table, which shows the nominal speeds at station and in each year thereafter the yield [0.3 to 0.5]:

Table 3.1: Nominal velocities at all stations at 10 m height and machine performance interval [0.3 to 0.5], in each year

10m	Zoon1		Zoon2		Zoon3		Zoon4	
year	Vn1	Vn2	Vn1	Vn2	Vn1	Vn2	Vn1	Vn2
2012	4.063	4.791	4.491	5.295	3.739	4.409	4.937	5.822
2013	4.327	5.102	4.770	5.624	3.992	4.707	5.230	6.167
2014	4.188	4.938	4.622	5.450	3.858	4.549	5.075	5.985
2015	4.174	4.921	4.607	5.433	3.845	4.533	5.060	5.966
2016	4.301	5.072	4.742	5.592	3.967	4.677	5.201	6.133
2017	4.320	5.094	4.762	5.615	3.985	4.699	5.222	6.158
2018	4.169	4.916	4.603	5.427	3.840	4.528	5.055	5.960
2019	4.194	4.945	4.629	5.458	3.864	4.556	5.082	5.992
2020	4.011	4.730	4.436	5.230	3.690	4.351	4.880	5.754
2021	4.296	5.066	4.737	5.585	3.962	4.672	5.196	6.127
2012/2021	4.227	4.984	4.663	5.499	3.895	4.593	5.119	6.036

We have a useful average wind power:

$$P_u \begin{cases} 0 & \bar{V} < V_i \\ \frac{1}{2} \rho V^3 & V_i \leq \bar{V} \leq V_n \\ \frac{1}{2} \rho V_n^3 & V_n \leq \bar{V} \leq V_s \\ 0 & \bar{V} < V_s \end{cases}$$

While $V_n = [0.67V \text{ to } 0.79 V]$ i.e. $V_n < V$ that is why:

$$P_n = \frac{1}{2} \rho V_n^3$$

And by that we find of this table in a unit area:

Table 3.2: Variations of the useful powers in the stations with a height of 10 m and at the efficiency interval of the machine [0.3 to 0.5], in each year.

10m	Zoon1		Zoon2		Zoon3		Zoon4	
year	Pu ₁	Pu ₂	Pu ₁	Pu ₂	Pu ₁	Pu ₂	Pu ₁	Pu ₂
2012	93.426	110.15	126.13	148.73	72.82	85.86	167.61	197.65
2013	112.85	133.06	151.11	178.17	88.57	104.44	199.24	234.92
2014	102.27	120.58	137.53	162.16	79.98	94.30	182.08	214.69
2015	101.24	119.38	136.21	160.61	79.15	93.33	180.42	212.73
2016	110.83	130.69	148.52	175.13	86.936	102.50	195.98	231.08
2017	112.30	132.42	150.41	177.35	88.131	103.91	198.35	233.88
2018	100.92	119.005	135.80	160.13	78.89	93.02	179.89	212.11
2019	102.71	121.11	138.1036	162.83	80.34	94.73	182.80	215.54
2020	89.884	105.98	121.564	143.33	69.96	82.495	161.81	190.79
2021	110.45	130.23	148.0312	174.54	86.62	102.13	195.35	230.34
2012/2021	105.16	123.99	141.2476	166.54	82.32	97.07	186.78	220.24

While the nominal speed V_n varied from one year to another and in all stations, it was impossible to choose the wind turbine at a unit area $A=1 \text{ m}^2$, ie . Their diameter equals 1.127 m, and a nominal speed V_n limited in the efficiency interval [0.3 to 0.5] during the average speeds of 10 years, this table shows the nominal speed:

Table 3.3: Rated speed at all stations at 10 m height and machine performance interval [0.3 to 0.5].

station	Vn1	Vn2
Zoon1	4.20	4.96
Zoon2	4.64	5.47
Zoon3	3.87	4.57
Zoon4	5.09	6.01

Here we conclude that the wind turbine that we will have chosen for each station has a unit of Surface at an equal diameter of 1.127 m and height of 10 m per- up port - the-land, the nominal speed of each station is as follows:

In Station 4, the nominal speed ranges from **[6.009 to 5.096] m/s**. In Station 2, the nominal speed ranges from **[4.642 to 5.473] m/s**. In Station 1, the nominal speed ranges from **[4.206 to 4.960] m/s** . On the other hand, the nominal speed in Station 3 ranges from **[3.876 to 4.570] m/s**.

From here we conclude the average useful wind power of each plant as indicated in the following table:

With: $p=1.25 \text{ kg/m}^3$, $A=1 \text{ m}^2$

Table 3.4: Variations of the useful power in the Stations with a height of 10 m and at the efficiency interval of the machine [0.3 to 0.5].

Station	Pu1	Pu2
Zoon1	103.82	122.42
Zoon2	139.58	164.50
Zoon3	81.25	95.80
Zoon4	184.58	217.64

This means that the average useful wind power provided with a height of 10 m and a diameter of 1.127 m (or their surface area 1 m^2) and nominal speed which is shown above, at Station 4,

the average supplied wind power ranges from [184,58 to 217,64] watts. At Station 2, it ranges from [139,518 to 164,506] watts. Station 1 has an expected average power ranging from [103,82 to 122,42] watts, while the expected average at Station 3 falls between [81,25 to 95,80] watts.

Table 3.5: Wind parameters at all stations at two altitudes.

	Z=25m				Z=50m			
Stations	K	C	V	\bar{V}^3	K	C	V	\bar{V}^3
Zoon1	3.36	7.37	6.53	530.42	3.45	7.79	6.90	625.00
Zoon2	3.50	8.03	7.12	686.35	3.57	8.36	7.40	773.04
Zoon3	3.26	6.89	6.10	433.27	3.37	7.39	6.55	534.32
Zoon4	3.65	8.74	7.75	885.48	3.70	9.00	7.97	964.84

And from there we collected the following figures

Table 3.6: Variations of the useful powers in the stations with a height of 25 m-50 m and at the efficiency interval of the machine [0.3 to 0.5], in each year.

	Z=25m			Z=50m		
Stations	P_{the}	P_{u1}	P_{u2}	P_{the}	P_{u1}	P_{u2}
Zoon1	331.51	99.45	165.75	390.62	117.18	195.31
Zoon2	428.96	128.69	214.48	483.15	144.94	241.57
Zoon3	270.79	81.23	135.39	333.95	100.18	166.9
Zoon4	553.42	166.02	276.71	603.02	180.90	301.51

Here, station 4 always remains the best because the average useful wind power in zoon4 is limited between [166.02W to 276.71W] at a height of 25 meters. On the other hand, at a height of 50 meters, the average power is limited between [180.90W to 301.51W]. Similarly, in zoon2 at a height of 25 meters, the expected average power is limited between [128.69W to 214.48W], and at 50 meters, it is limited between [144.94W to 241.57W]. Then it passes through station 1

at a height of 25 meters, which is limited between [99.45W to 165.75W], and at 50 meters, the expected average power is limited between [117.18W to 195.31W]. On the other hand, in zoon3, the average useful wind power at these locations will be approximately 10 W. At a height of 25 meters, the average useful wind power is limited between [81.23W to 135.39W], and at 50 meters, it is expected to be limited between [100.18W to 166.90W].

3.3. Study of turbine surface change:

In this study, we will change the value of the turbine surface A using the law:

$$P = \frac{1}{2} \rho AV^3$$

These curves were generated using EXCEL software and CAMVA software:

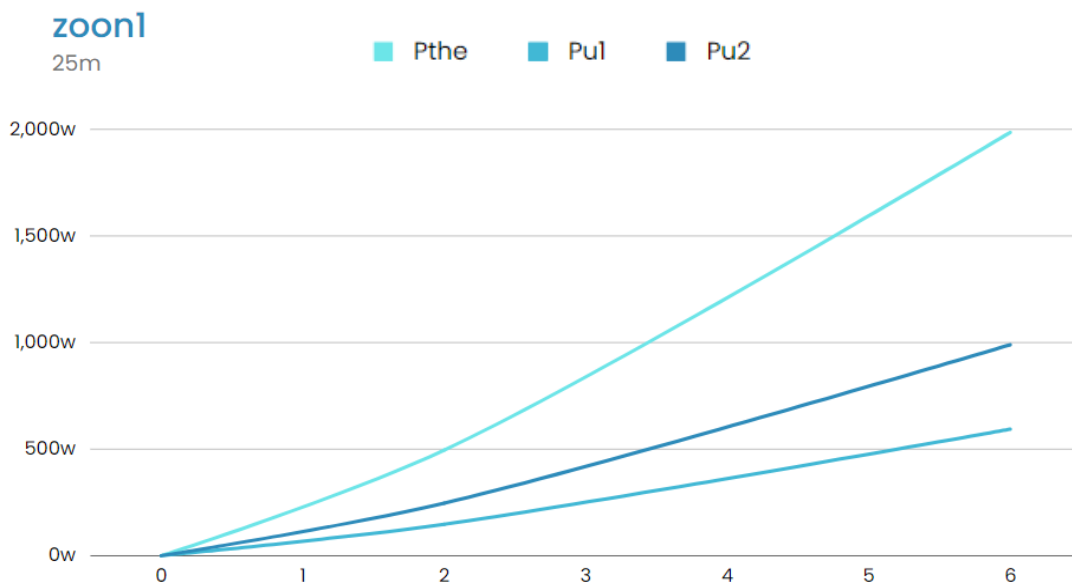


Figure 3.12: Useful power curves P_{u1} , P_{u2} and the theoretical power at station 11

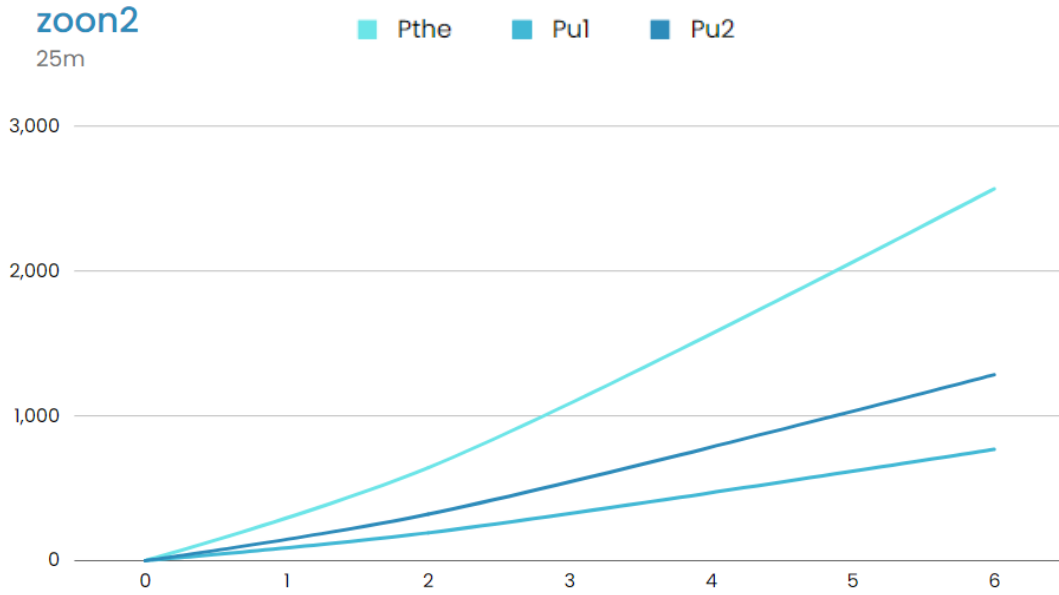


Figure 3.13: Useful power curves P_{u1} , P_{u2} and the theoretical power at station 2

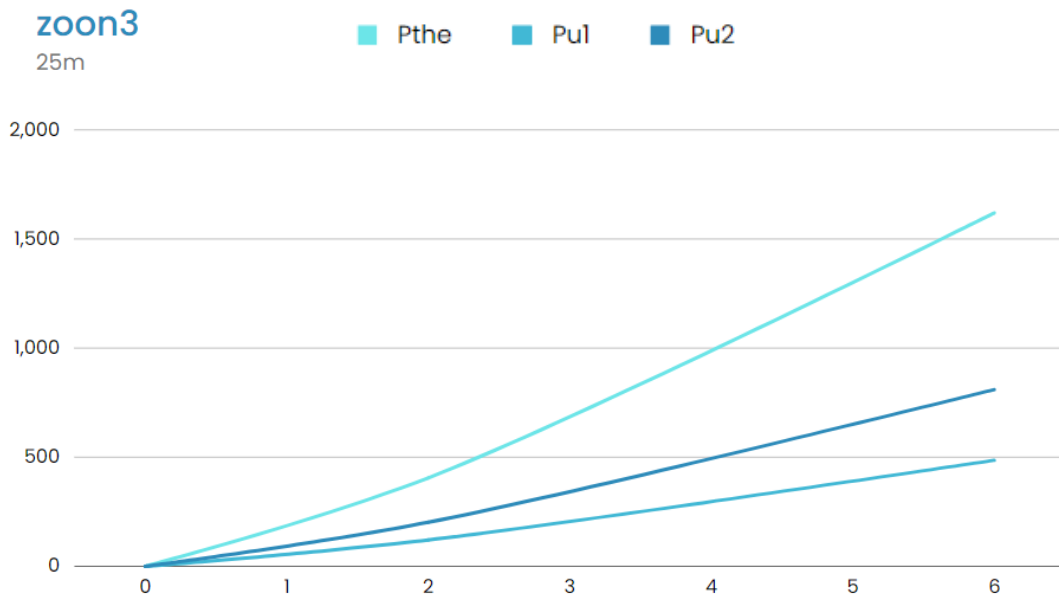


Figure 3.14: Useful power curves P_{u1} , P_{u2} and the theoretical power at station 3

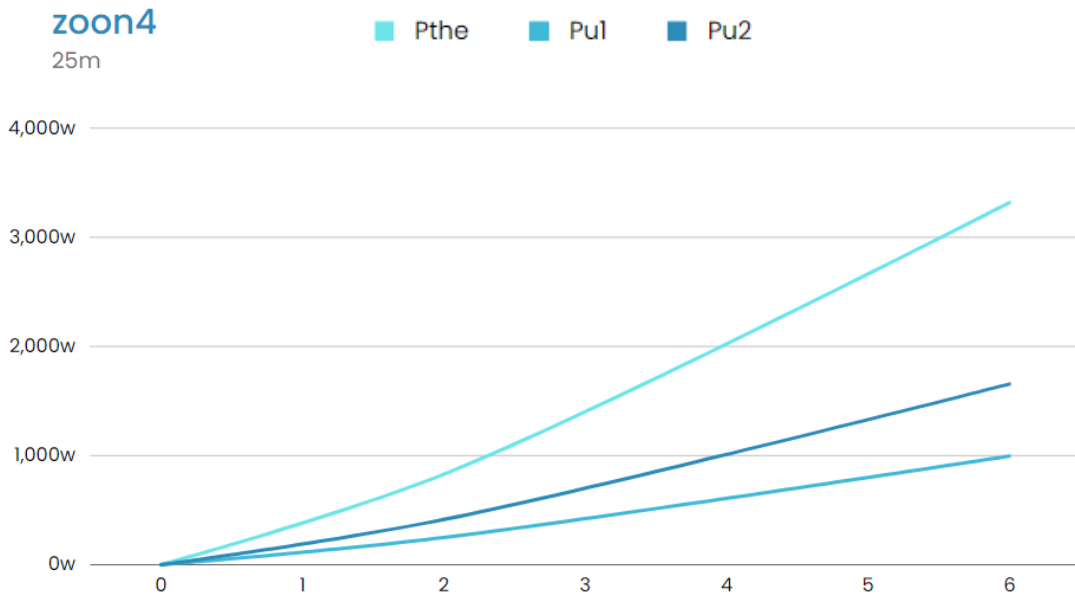


Figure 3.15: Useful power curves P_{u1} , P_{u2} and the theoretical power at station 4

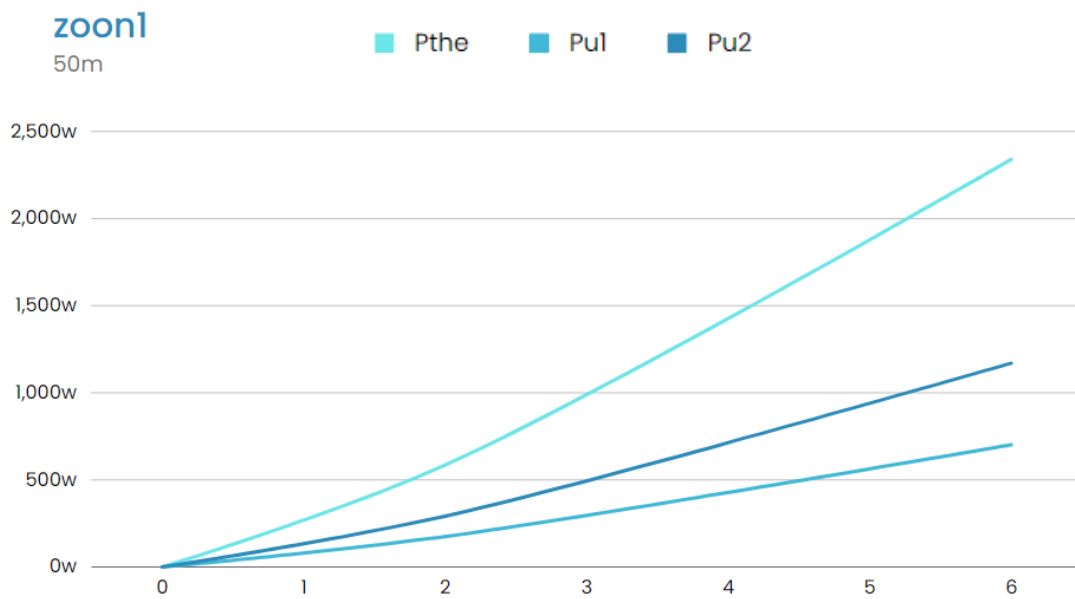


Figure 3.16: Useful power curves P_{u1} , P_{u2} and the theoretical power at station 1

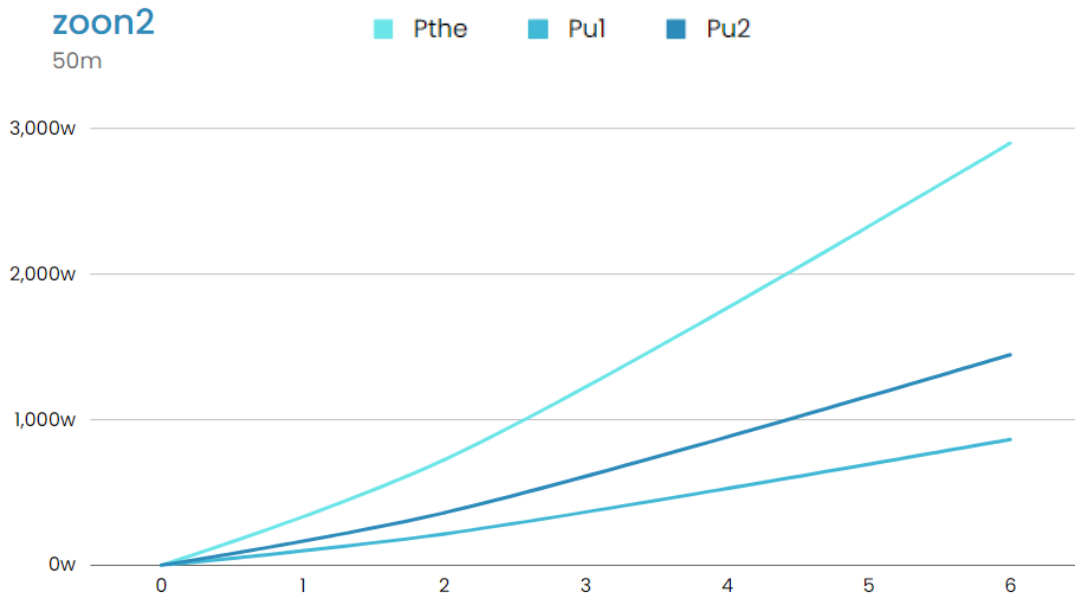


Figure 3.17: Useful power curves P_{u1} , P_{u2} and the theoretical power at station 2

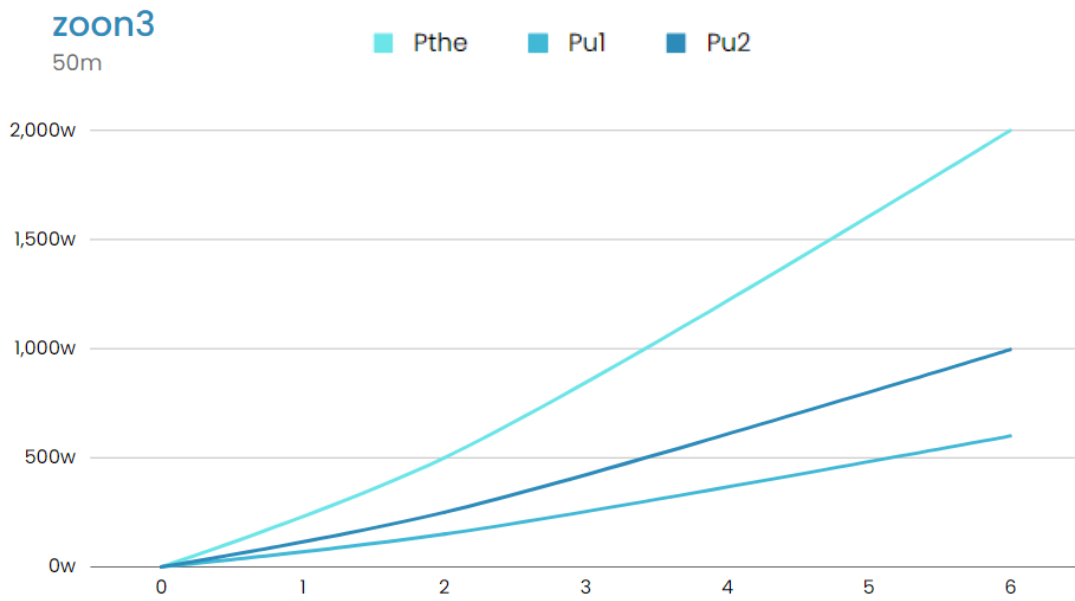


Figure 3.18: Useful power curves P_{u1} , P_{u2} and the theoretical power at station 3

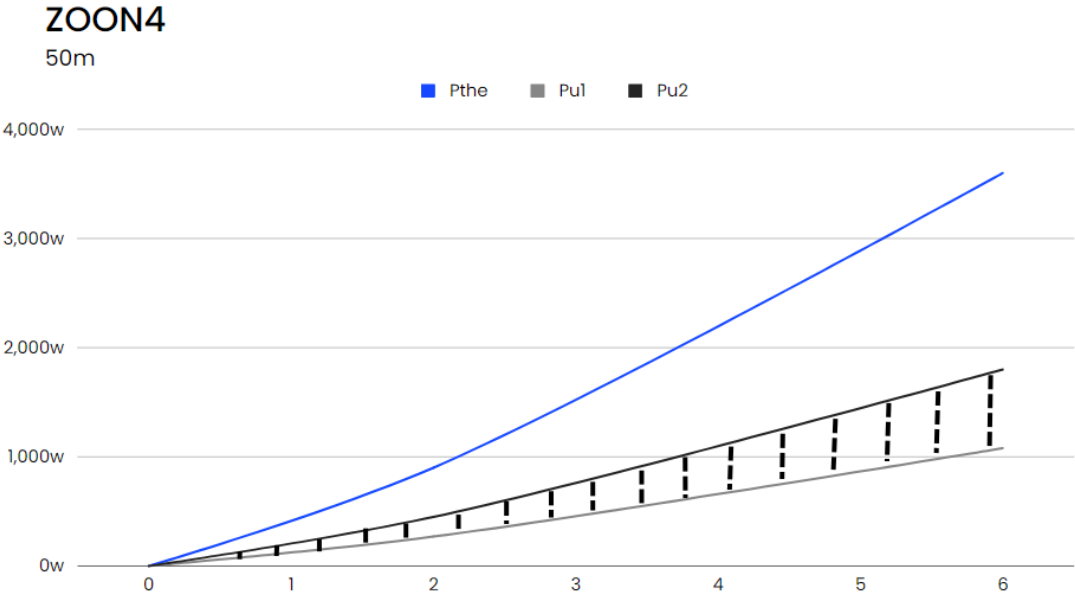


Figure 3.19: Useful power curves P_{u1} , P_{u2} and the theoretical power at station 4

The remark in these figures when we increase the diameter of the wind turbine the power will be more, also when we increase the height of the wind turbine with the change of the diameter, there is a large addition of the average power useful, for example at the station4 when the diameter equals

4 meter. the surface that the rotor creates equals $12.56m^2$ at a height of 25 m, the useful power limited between [512.94 W to 965.10 W], but at a height of 50 m we see that the power limited between [800.13W to 1289.29W], we see a variation in the altitude of the wind turbine, the interval where the expected average useful power will be is not the same in the two heights of 25 m and 50 m , with a big difference raising.

But when we say the diameter of the fins at 6 meter. The area of the circle will be $28.26 m^2$, the interval will be at a height of 25 m [1025.02 W to 1853.47 W], and at a height of 50 m will be [1297.21 W to 1869.96 W], the remark here that the difference increases with a large deviation.

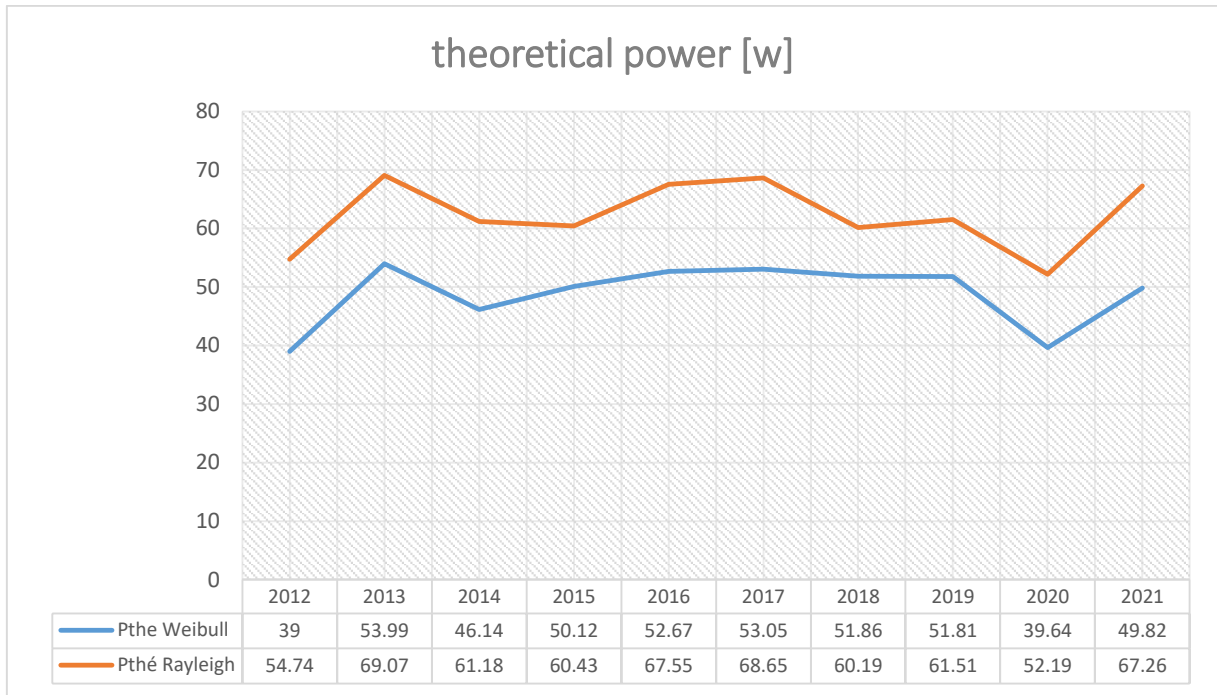


Figure 3.20: Mean incident theoretical wind power for 10 years

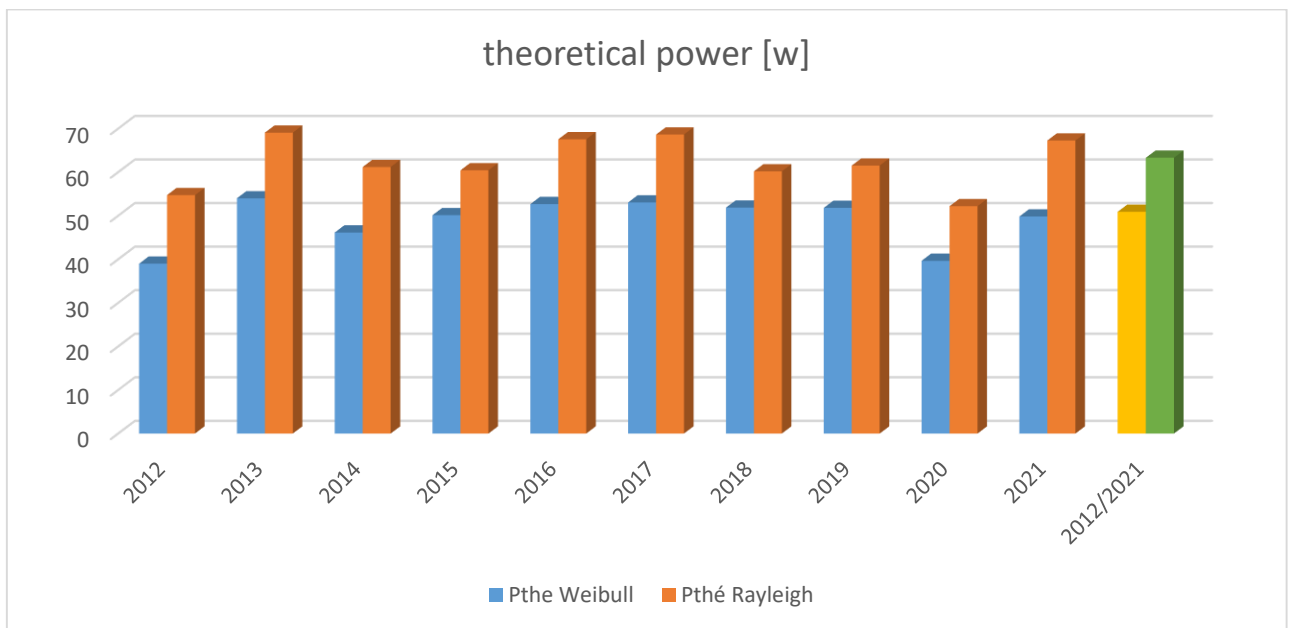


Figure 3.21: Histogram of mean incident theoretical wind power for each year and for 10 years.

Based on the data, using the Rayleigh law, the highest value of theoretical power was 69.07 w in 2013, while the lowest value was 52.19w in 2020. However, when using the Weibull law, the highest value of theoretical power was 53.99w in 2013, and the lowest value was 39.64w in 2020. The Rayleigh law outperformed the Weibull law by 19.63% over ten years.

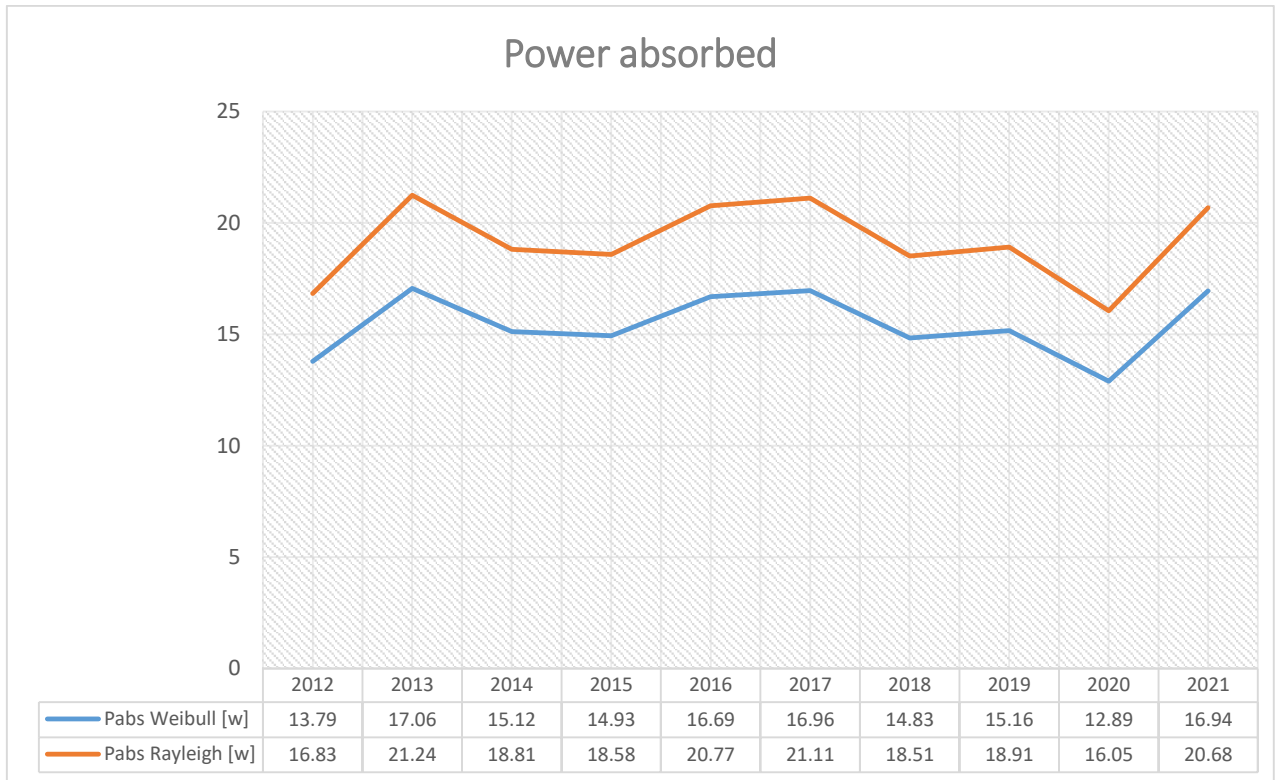


Figure 3.22: Power absorbed by the rotor for each year and at 10 years.

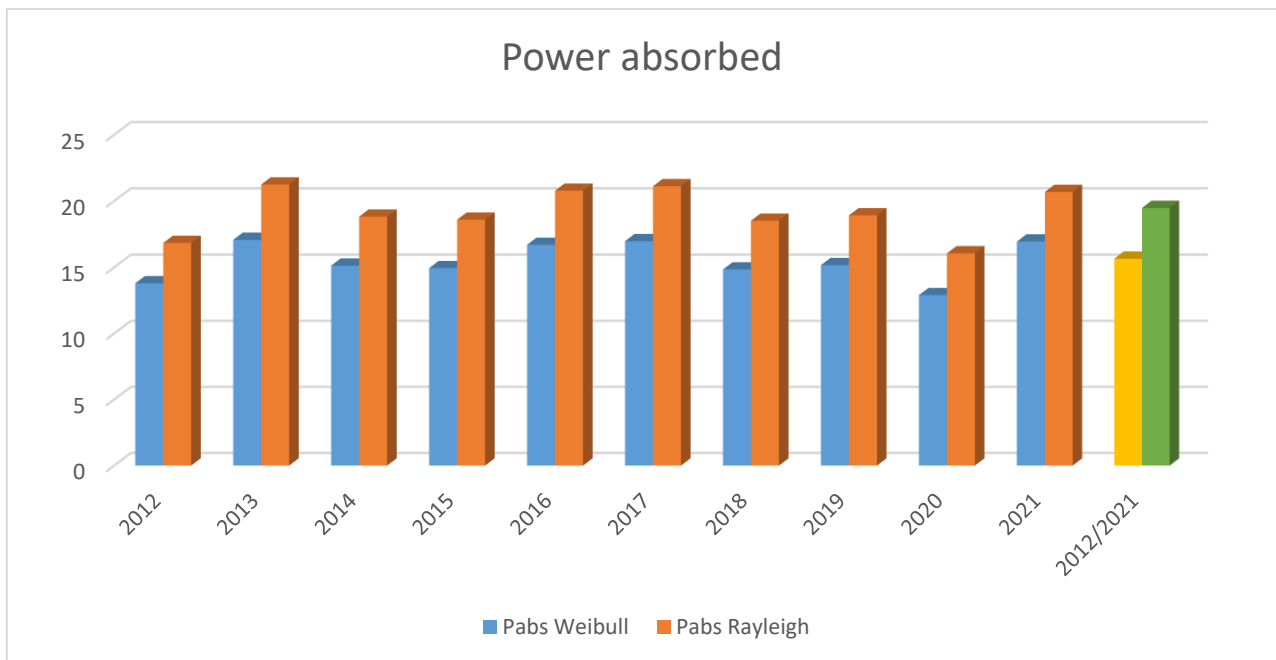


Figure 3.23: Histogram of power absorbed by the rotor for each year and at 10 years.

The absorbed power was 21.243 W as the highest value in 2013, and reached its minimum value in 2020 estimated at 16.053 W according to Rayleigh’s law. However, when using Weibull law, we find that the highest value of absorbed power reached 17.06954w in 2013, and the lowest value was 12.89951w in 2021. The Rayleigh method outperformed the Weibull method by 19.65% over 10 years.

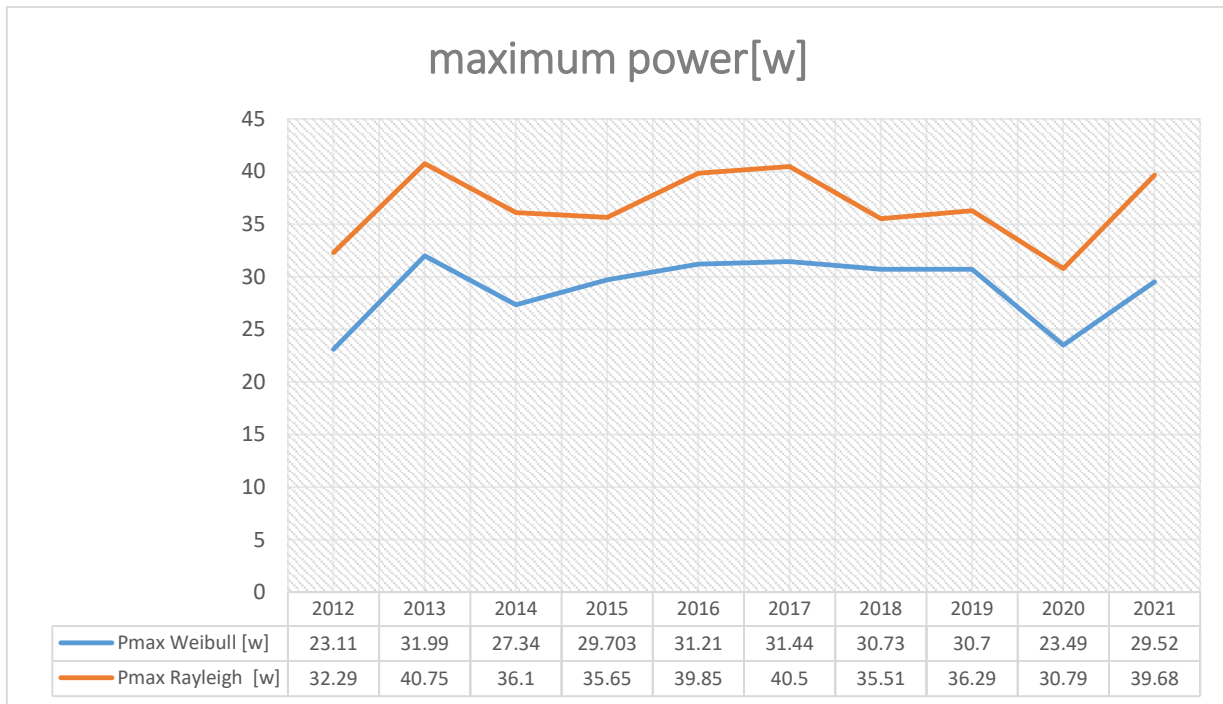


Figure 3.24: Average maximum recoverable wind power for each year and over 10 years.

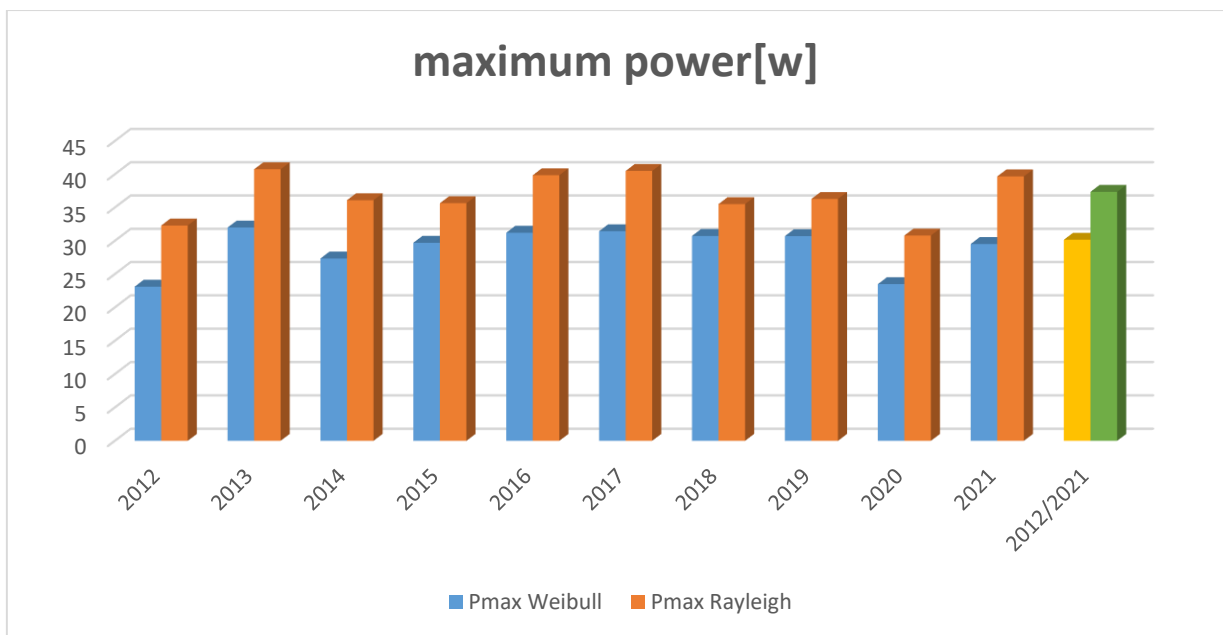


Figure3.25: Histogram of maximum recoverable wind power for each year and over 10 years.

According to Rayleigh's law, the maximum power reached its highest value of 40.7524 watts in 2013, while its lowest value was 30.7967 watts in 2020. On the other hand, when applying the Weibull law, the maximum power had its peak at 31.99768 watts in 2013, and the lowest value was 39.64556 watts in 2020. Over a span of 10 years, the Rayleigh method demonstrated superior performance compared to the Weibull method, achieving a 19.27% higher power output.

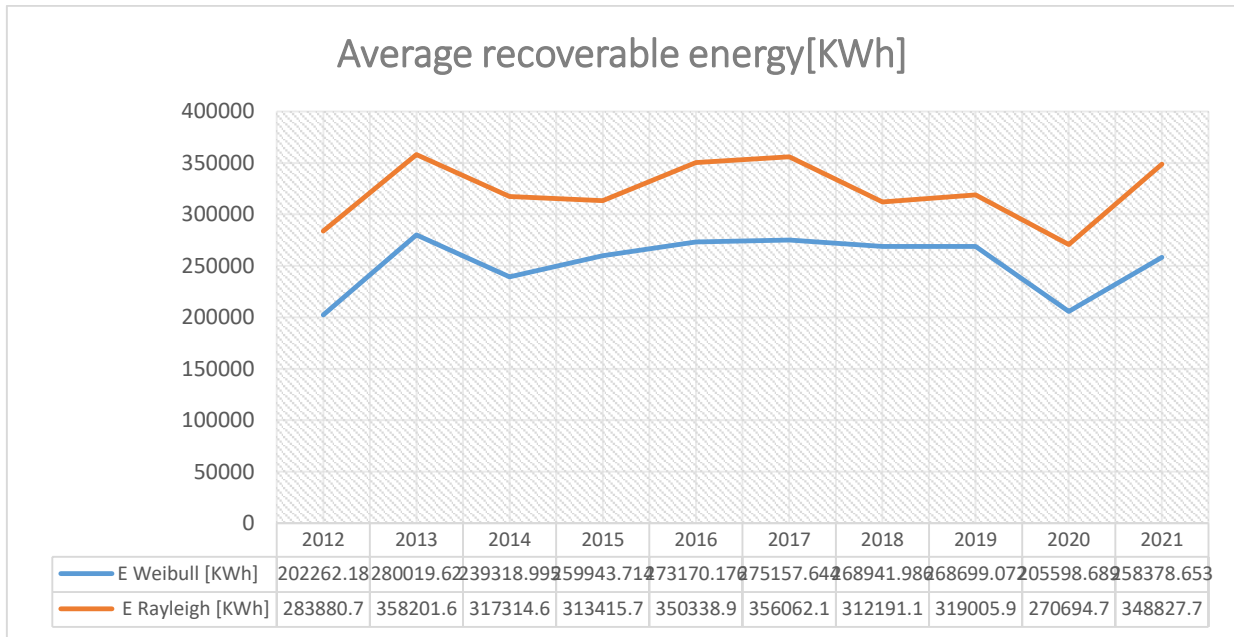


Figure 3.26: Average recoverable energy for each year and over 10 years.

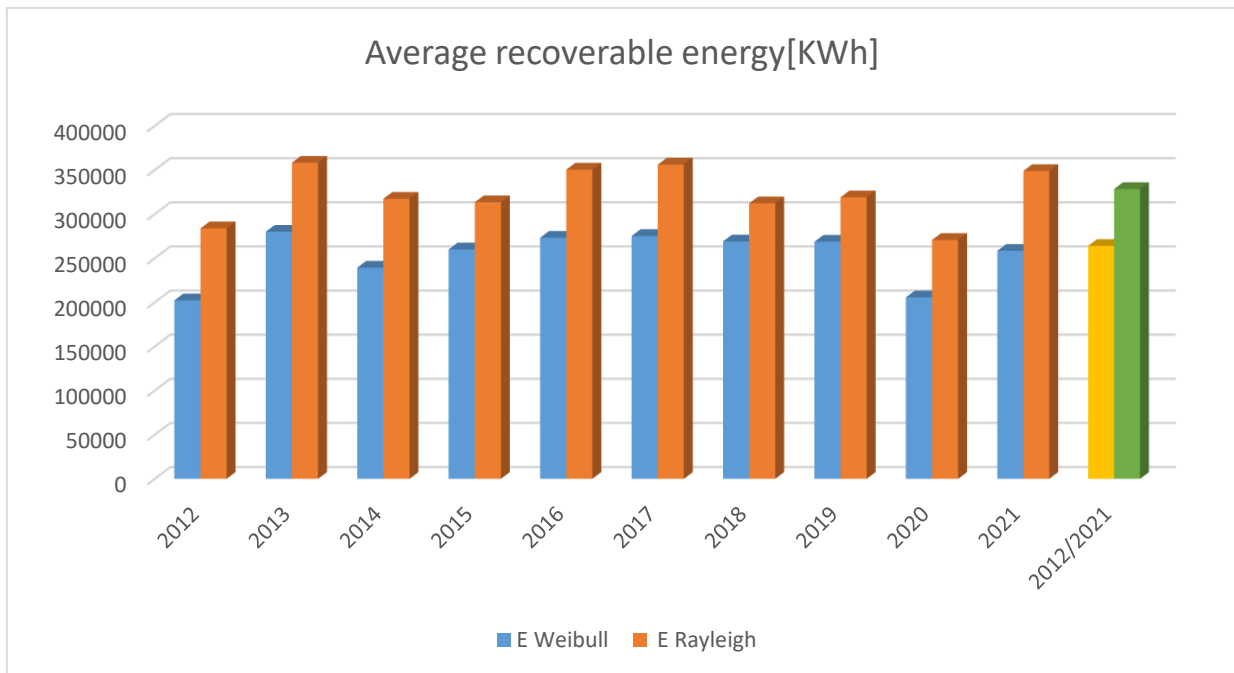


Figure 3.27: Histogram of Average Recoverable Energy per Year over 10 Years

Based on Rayleigh's law, the average recoverable power reached its peak at 358201.6536 kWh in 2013, while its lowest value was 270694.0747 kWh in 2020. Conversely, when utilizing the Weibull law, the highest value for average recoverable energy was 280019.6196 kWh in 2013, and the lowest value was 205598.6892 kWh in 2020. Over the course of 10 years, the Rayleigh method exhibited superior performance compared to the Weibull method, achieving a 19.62% higher average recoverable power.

Conclusion :

This chapter focuses on conducting a numerical analysis of wind power. We also make an effort to calculate the average useful power and its range, enabling us to effectively select the suitable wind turbine for each station. Additionally, within this chapter, we are able to ascertain the expected nominal velocity for each station. These findings facilitate the establishment of scientifically and technically sound agreements with factories, ensuring optimal productivity from the intended field cultivation.

General conclusion

In conclusion, of this study, summarizing everything that has been examined here and the results of this research, firstly, we conducted an analysis of the erratic velocities obtained from the national meteorological office using a scientific method and statistical analysis to identify areas where wind turbine farms can be established. The outcome of all this analysis indicates that the zoon4 is the best, followed by zoon2, zoon1, zoon3

This classification is not arbitrary, as we analyzed the irregular velocities over a 10-year period. The extensive duration of this study provides a high level of confidence in this ranking. We also neglected the topographic cadaster of each zone, except for the areas surrounding the velocity measurement stations. Analyzing the entire topographic zone would require significant time and resources.

On the other hand, selecting wind turbines suitable for each zone posed a challenge. The typical efficiency is determined by the manufacturer, as well as the technical velocities represented by the nominal velocity. Through these factors, we can calculate the useful power. However, we attempted to determine, within a limited range between [0.3 and 0.5], the closest match for wind turbines in each zone, as we have previously observed. Based on past experiments, we concluded this interval, which allows us to determine the nominal velocity interval for each intended machine selection in the respective zone, as well as the expected renewable power output.

The choice of the turbine's diameter remains crucial, as it is related to the length of the mast and the wind speed. Considering that these zones have relatively lower wind strength, it is evident that smaller to medium-sized wind turbines are preferable.

In any case, we conduct studies under various scenarios and different diameters at different altitudes to gain a comprehensive understanding of the appropriate wind turbine selection.

Bibliographical references

- [1]. https://en.wikipedia.org/wiki/Weibull_distribution, accessed on 29 September 2021.
- [2]. A. Parajuli, "A Statistical Analysis of Wind Speed and Power Density Based on Weibull and Rayleigh Models of Jumla, Nepal," *Energy and Power Engineering*, vol. 8, pp. 271-282, 2016.
- [3]. N. Eskin, H. Artar and S.Tolun, "Wind energy potential of Gökçeada Island in Turkey," *Renewable and Sustainable Energy Reviews*, vol. 12, no. 3, pp. 839-851, 2008.
- [4] Seyit AA, Onder G. Alternative moment method for wind energy potential and turbine energy output estimation. *Journal of Renewable Energy* 2018;120:69-77.
- [5]. Manwell, J.F.; McGowan, J.G.; Rogers, A.L. *Wind Energy Explained: Theory, Design and Application*, 1st ed.; John Wiley & Sons, Inc.: Chichester, UK, 2002; pp. 46–62. ISBN 978-0-470-01500-1.
- [6]. Jain, P. *Wind Energy Engineering*; McGraw-Hill Companies, Inc.: New York, NY, USA, 2011; pp. 26–37, ISBN 978-0071714778.
- [7]Costa Rocha, P.A.; de Sousa, R.C.; de Andrade, C.F.; da Silva, M.E.V. Comparison of seven numerical methods for determining Weibull parameters for wind energy generation in the northeast region of Brazil. *Appl. Energy* **2012**, 89, 395–400. [[CrossRef](#)]
- [8]. Seguro, J.V.; Lambert, T.W. Modern estimation of the parameters of the Weibull wind speed distribution for wind energy analysis. *J. Wind Eng. Ind. Aerodyn.* **2000**, 85, 75–84. [[CrossRef](#)]
- [9]. Chang, T.P. Performance comparison of six numerical methods in estimating Weibull parameters for wind energy application. *Appl. Energy* **2011**, 88, 272–282. [[CrossRef](#)]
- [10] J.A. Businger, J.C. Wyngaard, Y. Izumi, E.F. Bradley, Flux-profile relationships in the atmospheric surface layer, *J. Atmos. Sci.* 28 (1971) 181-189]:
- [11] Monin A.S. et A.M. Obukov, « Basic Regularity in Turbulent Mixing Surfaces Layer of the Atmospheric », *Akad. Nauk. S.S.S.R., Trud Geof. Inst*, 24, 151, 1954 .
- [12] [Poje S. et B. Cividini, « Assessment of Wind Energy Potential in Croatia » *Solar Energy* vol.41 N°6 pp 543 554, 1988
- [13] *Nachida KASBADJI MERZOUK -Thèse De Doctorat* « Evaluation Du Gisement

Energétique Eolien Contribution A La Détermination Profil Vertical De La Vitesse Du Vent En Algerie ».

[14] KHANTOUT Abdelkader –thèse de magister << établissement d'un gisement éolien des zones côtières algériennes en raison d'implantation des aérogénérateurs à petite puissance >> [2011/2012)

[15] Justus C.G. et A. Mikhail, « Height Variation of Wind speed and Wind Distributions Statistics ». Geophysical Research Letters, vol. 3, N° 5, 1976//// Peterson E., « On the Use of Power Laws Estimates of Wind Power Potential » J. of Applied Meteorology, vol. 17, pp 390:394, 1978].

[16] Saidou Madougou-Thèse << Etude du potentiel éolien du jet nocturne dans la zone sahélienne à partir des observations de radars profileurs de vent >>

[17] [Http : //www. lyc-richelieu-rueil.ac-versailles.fr/arch](http://www.lyc-richelieu-rueil.ac-versailles.fr/arch)

[18] M. Ben medjahed, « Gisement éolien de la région côtière de Béni Saf Et son impact sur

[19] DELORD Jean - David, ROGER Emmanuel, , Étude d'un aérogénérateur Analyse fonctionnelle et comportementale ,France

[21] <https://www.windpowerengineering.com/cant-buy-turbine-can-buy-power/>

[22] DELORD Jean - David, ROGER Emmanuel, Lycée Maximilien Perret – Alfortville

Académie de Créteil / Étud d'un aérogénérateur Analyse fonctionnelle et comportementale

[23] SAYID MANSOUR " L'énergie éolienne et ses diverses applications: Exploitation, maintenance et installation d'éoliennes" 2018, p 101 , <https://www.noor-book.com/>

[24]<https://earth.google.com/web/@31.91685634,5.28712507,135.47170281a,9728.56926369d,34.99999998y,0.00000001h,20.07110017t,0r>

[25],A. L. Neumann, La energía eólica: principios básicos y tecnología, 2002. Available: http://www.agenergia.org/files/resourcesmodule/@random49917eec3c3bd/1234272455_eolica_ALecuona.pdf.

[26] Wais P. Two and three-parameter weibull distribution in available wind power

analysis. *Journal of Renewable Energy* 2017;(103):15-29.

[27] Kantar YM, Usta I. Analysis of the upper-truncated weibull distribution for wind speed. *Journal of Energy Conversion and Management* 2015;96:81-88.

[28] G. L. Johnson, *Wind Energy Systems*. Manhattan, KS, USA: Kansas State University, 2006.

[29] ÉNERGIES ÉOLIENNE, ÉNERGIES SOLAIRE THERMIQUE, ÉNERGIES PHOTOVOLTAÏQUE , ÉNERGIE ÉOLIENNE , Génie énergétique et environnement (GEE)
Notes de cours 2017/18 Pr. B. KHARBOUCH

[30] T. Burton, D. Sharp, N. Jenkins, and E. Bossanyi. *Wind Energy Handbook*, 2012.

[31] Akda, S. a., & Dinler, A. (2009). A new method to estimate Weibull parameters for wind energy applications. *Energy Conversion and Management*, 50(7), 1761–1766. <https://doi.org/10.1016/j.enconman.2009.03.020>